MÁSTER EN INGENIERÍA DE SISTEMAS Y CONTROL

Ship Resistance Estimation using Artificial Neural Networks

Author: Daniel Marón Blanco

Supervisor: Matilde Santos Peñas

September 2018

Máster:	Ingeniería de Sistemas y Control
Título:	Ship Resistance Estimation using Artificial Neural Networks
Proyecto:	Trabajo Fin de Máster
Tipo:	Proyecto específico propuesto por el alumno
Autor:	Daniel Marón Blanco
Directora:	Matilde Santos Peñas

Autorización

Autorizamos a la Universidad Complutense y a la UNED a difundir y utilizar con fines académicos, no comerciales y mencionando expresamente a sus autores, la memoria de este Trabajo Fin de Máster.

Firmado:

Firma del alumno

Abstract

The ship resistance estimation is one of the most important problems to be solve by naval architects in the early stages of the project. An accurate estimation of the ship resistance will enable a good design regarding such important aspects as the propulsive system, the power system and the fuel consumption, among others.

In this report a new tool for ship resistance prediction is presented, using artificial intelligence techniques such as Neural Networks (ANN). This tool is presented as an alternative to traditional empirical methods based on regression analysis, such as the Holtrop and Mennen method.

This master thesis is a continuation of a previous research where the applicability of ANN to the ship resistance problem was analysed (Marón and Santos, 2017). ANN are easy to implement, could be re-trained with future data and can identify non-linear behaviours such as the relationship between the wave resistance and the ship speed.

The ANN have been trained with a data base composed by model tests performed in CEHIPAR (INTA-CEHIPAR, 2018), where the ship models are towed, and the force needed to achieve a certain speed (resistance) was measured.

The pre-processing carried out to adequate the data base to the training algorithm is also explained. Since the behaviour of the ship resistance is different depending on the type of ship, it is important to highlight the filtering that has been made to divide the data base in groups of ships.

Different ANNs have been trained to estimate the two main components of the ship resistance; the viscous and the wave resistance. The first one has been calculated by means of the form factor.

The results show a good agreement with the data base. In addition, the ANN performance has been compared against the Holtrop and Mennen method, showing in general better estimations.

Finally, a tool has been developed where, applying the ANN trained with empirical data, the ship resistance is estimated as a function of simple parameters defining the hull geometry. Other less relevant components of the resistance have been also included, such as the resistance of appendages, tunnel thrusters and the model-ship correlation resistance.

Keywords

Artificial Neural Networks, Feedforward network, Ship Resistance, Holtrop and Mennen method, CEHIPAR, ship design.

Resumen

La predicción de la resistencia al avance es uno de los problemas más importantes a los que se enfrentan los ingenieros navales en las etapas iniciales de diseño de un nuevo buque. Una estimación precisa de dicha resistencia permitirá diseñar correctamente aspectos tan importantes como el sistema propulsivo, la planta eléctrica o la capacidad de combustible entre otros.

En este trabajo fin de máster se presenta una nueva herramienta para la predicción de la resistencia al avance de buques aplicando técnicas de inteligencia artificial como son las redes neuronales artificiales. Esta herramienta se concibe como una alternativa a los métodos tradicionales basados en análisis de estadísticos de regresión como por ejemplo el método de Holtrop y Mennen (1978).

Este trabajo es una continuación de una investigación previa donde se analizó la aplicación de las redes neuronales artificiales al problema de la predicción de la resistencia al avance (Marón y Santos, 2017). De este trabajo previo se sacaron conclusiones interesantes como la fácil implementación de las redes neuronales artificiales, la posibilidad que tiene de ser reentrenadas con datos de futuros ensayos y la habilidad que tienen de identificar comportamientos no-lineales como es la relación que existe entre el número de Froude y la resistencia al avance.

Para entrenar las redes neuronales se ha utilizado una base de datos de ensayos con modelos a escala realizados en los últimos 60 años en el CEHIPAR (INTA-CEHIPAR, 2018). En estos ensayos los modelos son remolcados midiéndose la fuerza necesaria para remolcarlos a una cierta velocidad.

En el informe primero se resume el trabajo realizado para preprocesar la base de datos con el fin de adecuarla para poder ser utilizada por el algoritmo de aprendizaje. Además, como las componentes de la resistencia al avance tienen un comportamiento diferente dependiendo del tipo de buque, se ha incluido un filtro para generar grupos de buques.

Las diferentes redes artificiales generadas se han entrenado para estimar las dos componentes principales de la resistencia, la resistencia viscosa y la resistencia por formación de olas. La primera se ha calculado a partir del factor de forma siguiendo la teoría generalmente aplicada en la industria naval.

Los resultados muestran una buena correlación con la base de datos. Por otro lado, las redes neuronales generadas presentan en general una precisión superior al método de Holtrop y Mennen.

Finalmente se define la herramienta desarrollada que estima los componentes más importantes de la resistencia aplicando redes neuronales, a partir de los principales parámetros que definen la geometría del casco de un buque. Otras componentes menos importantes, como la resistencia debida a los apéndices, se calculan aplicando métodos basados en regresiones empíricas.

Palabras Clave

Redes neuronales artificiales, red multicapa, resistencia al avance de buques, método de Holtrop y Mennen, CEHIPAR, diseño de buques.

Contents

List of Figures

List of Tables

List of Abbreviations

ANN	Artificial Neural Networks
CEHIPAR	Canal de Experiencias Hidrodinámicas del Pardo
INTA	Instituto Nacional de Técnica Aeroespacial
RANN	Resistance Artificial Neural Networks tool
RORO	Roll-on Roll-off cargo vessels.

Nomenclature

A_{MS}	Mid-ship section area
A_{WP}	Waterplane area
B	Ship Beam
C_A	Ship-model correlation resistance coefficient
C_B	Block coefficient of ship hull
C_F	Skin friction resistance coefficient
C_M	Mid-ship section coefficient
C_P	Prismatic coefficient of ship hull
C_T	Total resistance coefficient
C_V	Viscous resistance coefficient
C_W	Wave making resistance coefficient
C_{WP}	Waterplane are coefficient of ship hull
C_{Fm}	Model scale skin friction resistance coefficient
C_{Tm}	Model scale total resistance coefficient
F_n	Froude Number
k_s	Full-scale hull average rugosity
L_{wl}	Hull waterline length
r	Form factor
rms	Root mean squared error
R_A	Ship-model correlation resistance
R_{APP}	Resistance of the hull appendages and tunnel thrusters
R_F	Skin friction resistance
R_R	Residual resistance
R_T	Total resistance
R_V	Viscous resistance
R_W	Wave making resistance
S_W	Hull wetted surface
T	Ship´s draft
V	Ship´s velocity
v_m	Ship model velocity
α	Hull semi angle of entrance
λ	Model scale
v_f	Fresh water kinematic viscosity
v_{sw}	Sea water kinematic viscosity
ρ_f	Fresh water density
ρ_{sw}	Sea water density
∇	Hull volume of displacement

1 Introduction

One of the main problems to be solved by naval architects is the estimation of the hull resistance of a new vessel design already at very early stages of the project. An accurate estimation of the ship resistance will enable a good design regarding such important aspects as the propulsive system, the power system and the fuel consumption, among others.

Nowadays, there is a hard competition on the global markets between shipyards to get contracts for the construction of new ships. Usually shipyards have their technical design office of confidence or even their own one. These technical offices are ordered to design new projects of ships to comply with a set of specifications defined by the owner, such as the cargo capacity, deck area or the vessel speed. The latter is one of the most important factors to be considered, as it is strongly dependent on the hull resistance.

1.1 Motivation

The vessel contract speed is defined in the design specifications to be achieved in the sea trials after the construction. This contract speed is in general the key factor for the design of the propulsive and the power systems.

The ship design must be good enough to win the contract against competitors. To achieve a specified contract speed, a slightly higher demanding power could mean that your design is not selected by the owner. On the other hand, a low estimation of the hull resistance could mean that the contract speed will not be achieved during sea trials. In this case, the shipyard usually is entitled to pay a penalty to the owner, or even to lose the contract.

In addition, in respect to economic matters, the world trend is to minimise the fuel consumption, without penalizing the vessel speed. From an environmental point of view, the International Maritime Organisation [29] and the European Union regulations are demanding a decrease in the emissions [32].

An inaccurate prediction of the ship resistance could lead to important changes in later phases to meet the owner specifications or even the international or environmental obligations.

There are different methods to estimate the vessel resistance during the design; namely: empirical methods, computational fluid dynamics (CFD) and model test.

For very early design phases empirical methods are used. In these phases the designer defines the main hull dimensions and main shape characteristics such as the length, the beam or the displacement. For this objective, empirical methods are the best option to obtain a good prediction and can be used to optimize the vessel resistance focusing on global hull parameters.

CFD simulation is more time consuming and at least preliminary hull forms must be defined before. These techniques are usually applied to optimize local shapes such as the bulbous bow or the flow at the vessel stern.

To obtain more reliable estimations, model test campaigns are usually performed at towing tank facilities. These are specialised scientific research centres where scaled replicas of the hull shape are modelled and towed at different speeds and drafts. From these tests, the force done to tow the model are measured and the different components of the ship resistance are obtained.

1.2 Objective

The main object of this master thesis is to obtain a preliminary estimation of the ship resistance in the early stages of the design project by applying artificial intelligence techniques, such as Artificial Neural Networks (ANN). The analysis described in this work is focused on mono-hull vessels.

There are well-known empirical methods in the industry to estimate the resistance of a ship as a function of some basic parameters related to the hull forms. These empirical methods are based on regression analysis of a series of model tests performed in towing tanks. The most common used method in the naval architecture for quick estimates is the one proposed by Holtrop and Mennen (1978), who used a set of model tests with 334 hulls.

Although this method is widely used in the industry, the advantages of the application of ANN to solve this problem are various. Some important ones are the possibility to adapt to different types of ships, the ability to represent the non-linearities of the ship resistance behaviour, and the possibility of the continuous learning of the network. Re-training with new data a defined ANN is much easier and faster than re-fitting a statistical regression. This is an important advantage due to the continuous model test campaigns that are performed in the research centres.

The data regarding the model test campaigns performed in towing tanks are of strong importance for these research centres as it represents their cumulated know-who during years. Unfortunately, this is a sensible information and in most cases is confidential.

The study presented in this master thesis is a continuation of a previous academic research that was presented in the XXXVIII Jornadas de Automática (Marón and Santos, 2017).

Due to the difficulties to obtain model test data, in this paper a data base of different hull shapes is created and the Holtrop method is used to estimate the ship resistance as a function of the speed. This “synthetic” data base is used to train the networks and analyse the applicability of ANN to estimate the different components of the ship resistance. The results given in this article show a god agreement with the data base and suggest that ANN could be a proper method for the estimation of the hull resistance.

After the publication of the mentioned paper (Marón and Santos, 2017), a confidentiality agreement was signed with INTA-CEHIPAR in which the research centre allowed me to use the database of all the calm water resistance tests performed in their facilities since they started.

The available data from scaled model tests has been used now to develop a tool based on ANN for the estimation of the ship resistance. This tool is supposed to be used in the early stages of a vessel design, therefore the information needed should not be very detailed. The inputs of the program are the main particulars of a hull shape such as the waterline length, the beam or the block coefficient.

A friendly user tool has been created in MATLAB to estimate the different components of the ship resistance for a given hull and several speeds. The performance of the tool is calculated against the scale model tests and has been compared with the performance achieved when applying the Holtrop method.

It is important to note that the work performed in this master thesis is focused on mono-hull vessels, leaving other special vessels for future researches.

1.3 Report structure

This report is outlined as follows:

- An introduction is made where the different components of the ship resistance are described. A brief introduction to the state of the art is given, where the different traditional and future techniques for the estimation of the ship resistance are explained.
- Then are described the materials and the tools used to develop and train the ANN. The materials in this case is the huge amount of data of model test campaigns. It is explained how this data base is pre-processed and the methodology used to train the ANN to estimate the different considered outputs.
- A summary and a discussion of the results is given in section 5.
- The developed tool is described in section 6, where the program inputs are defined. It is also explained the way the different components of the ship resistance are estimated by the tool, and some examples of results are shown.
- Finally, some conclusions and possible future works are presented.

1.4 Acknowledgments

I want to acknowledge Emilio Fajardo, subdirector of INTA-CEHIPAR, the confidence placed on me giving the access to the confidential data of model tests performed over the last 80 years.

My particular gratitude to Juan José Pelayo, responsible for database provided, with his caring assistance helping me to understand the content.

2 Ship Resistance

2.1 Introduction to ship resistance

The ship resistance represents all the forces that act against the straight movement of a vessel in calm water. The definition of the resistance is therefore the force required to tow a ship at a certain speed in calm water.

The required power to counteract this resistance is called effective power (EHP), and it is a very important input for the design of the propulsive and power systems.

The work developed for this master thesis is focused on the resistance of mono-hull vessels, therefore this chapter is dedicated only to this type of ships.

According to Hughes hypothesis (Baquero, 2011), the ship resistance, R_T, can be divided into two components: viscous, R_V, and the wave resistance, R_W.

$$R_T = R_V + R_W \tag{1}$$

The ship resistance is usually made non-dimensional as:

$$C_T = \frac{R_T}{\frac{1}{2}\rho S_W v^2} \tag{2}$$

Where:

- ρ is the fluid density, in this case fresh water or sea water (t/m^3).
- S_W is the hull wetted surface (m^2).
- v is the ship speed (m/s).

This is applied to all the components of the ship resistance. The resistance coefficients are useful for extrapolating measurements from model scale to full-scale.

2.2 Viscous resistance

The viscous resistance is due to the fluid viscosity involving the hull friction and the pressure changes as a result of the hull shape.

This viscous resistance is composed of frictional and residual components arising from pressure gradients along the hull. The first one is assumed to be related to frictional resistance that a flat plate with an equivalent wetted surface can suffer. The second one is the remaining viscous resistance associated with the flow deviation by hull shape.

The frictional resistance due to a flat plate towed in water is dependent on the Reynolds number:

$$\mathrm{Re} = \frac{vL_{wl}}{\upsilon} \tag{3}$$

Where:

- υ is the fluid kinematic viscosity (m^2/s).
- L_{wl} is the hull waterline length (m).

There are several methods to estimate the frictional resistance coefficient. These methods are based in measurements performed in towing tanks along the last century. For each method there is a "frictional line" defining the frictional coefficient as a function of the Reynolds number.

In 1957 in Madrid, the ITTC decided to define a new line to be used by all the research centres, this is called the ITTC-57 line and is defined as follows:

$$C_F = \frac{0.075}{\left(\log_{10} R_n - 2\right)^2} \tag{4}$$

As stated before, the viscous resistance is composed by the frictional resistance and a component arising due to the pressure gradients along the hull.

It is usually assumed that the residual part of the viscous resistance is proportional to the frictional resistance by a coefficient called form factor (r). This factor depends on the hull shape and indicates how different is the hull shape of a ship when compared to a flat plate.

The viscous resistance is then defined as:

$$R_V = r\, R_F \tag{5}$$

The value of the form factor is always positive and higher than one. For most ships it takes values ranging from 1.1 to 1.6.

2.3 Wave making resistance

When a body is floating in a free surface between two fluids (water-air), pressure fields due to its surroundings generate a wave pattern that accompanies the body in its movement.

The wave pattern modifies the pressure field in such a way that in certain points can be increased or decreased. A new force shows up when integrating the pressure field, this one opposes to movement and it is named as wave making resistance, R_W.

The Froude number relates the effect of the inertial forces and the forces due to gravity, which are essential when studying the wave making resistance. Therefore, model tests are performed at the same Froude number as full-scale ship. This number is defined as:

$$F_n = \frac{v}{\sqrt{gL_{wl}}} \tag{6}$$

The wave resistance is strongly dependent on the vessel speed, the hull shape and the dimensions.

2.4 Model-Ship correlation

Model-ship correlation methods are the hypothesis used to extrapolate the model scale measurements to full-scale results. This is one of the most important problems to be solved by research centres.

Following the above definitions, the hull resistance coefficients measured in a towing tank can be defined as:

$$C_{Tm} = C_{Vm} + C_{Wm} = r_m C_{Fm} + C_{Wm} \tag{7}$$

Where the sub-index "m" represents the model, C_V is the viscous resistance coefficient, r is the form factor and C_W is the wave resistance coefficient.

The resistance coefficients for full-scale (sub-index "s") can be defined as:

$$C_{Ts} = C_{Vs} + C_{Ws} = r_s C_{Fs} + C_{Ws} \quad (8)$$

As explained before, model tests are performed at the same F_n, and thus the wave resistance coefficient is the same for the model and the ship.

$$C_{Wm} = C_{Ws} \quad (9)$$

So, the ship resistance coefficient can be obtained as:

$$C_{Ts} = C_{Tm} + r_s C_{Fs} - r_m C_{Fm} \quad (10)$$

Where:

- C_{Tm} is known from model test measurements.
- C_{Fs} and C_{Fm} are obtained applying the ITTC-57 line.
- The model form factor, r_m, is obtained from the model tests applying different methods. The most used is the one proposed by Prohaska (1966) (see 4.1.2.4).

The full-scale form factor, r_s, is unknown and depends on the hull shape, the dimensions, the flow, etc. The hypothesis presented by Hughes is that the form factor is the same for the model scale and full-scale (Baquero, 2011). Therefore, the resistance coefficient can be obtained, knowing the form factor, as:

$$C_{Ts} = C_{Tm} + rC_{Fs} - rC_{Fm} \quad (11)$$

The method presented by Hughes is recommended by the ITTC since 1978.

2.5 Additional resistance components

The total ship resistance at full-scale is usually increased to take into account other less important components such as the hull appendages, the hull rugosity, etc. These are usually added to the total resistance calculated as (1), when extrapolating to full-scale ship resistance.

2.5.1 Resistance of appendages

The resistance due to hull appendages is usually calculated applying empirical methods. In this thesis the method proposed by Holtrop and Mennen (1982) is considered.

The resistance of appendages is defined the sum of the resistance due to hull appendages and tunnel thrusters:

$$R_{APP} = R_{APP_{APP}} + R_{APP_{tunnel}} \quad (12)$$

The resistance of the hull appendages, such as rudders or bilge keels, is estimated as:

$$R_{APP_{APP}} = \frac{1}{2} \rho_{sw} C_F S_{APP} r_{APP_{eq}} v^2 \quad (13)$$

Where:

- C_F is again the ship frictional resistance.
- S_{APP} is the area of the appendages (m^2).
- r_{APPeq} is the equivalent appendages resistance factor.
- v is the ship speed (m/s).

Holtrop and Mennen (1982) give some approximate appendages resistance factors for different types of hull appendages:

Table 2.1. Approximate hull appendages resistance factors (Holtrop and Mennen, 1982).

Approximate appendage resistance factors	
Rudder behind skeg	1.5-2.0
Rudder behind stern	1.3-1.5
Twin-screw balance rudders	2.8
Shaft brackets	3.0
Skeg	1.5-2.0
Strut bossings	3.0
Hull bossings	2.0
Shafts	2.0-4.0
Stabilizer fins	2.8
Dome	2.7
Bilge keels	1.4

The equivalent appendage resistance factor is obtained as:

$$r_{APP_{eq}} = \frac{\sum r_{APP} S_{APP}}{\sum S_{APP}} \tag{14}$$

The resistance increment due to tunnel thrusters is estimated as:

$$R_{APP_{TUNNEL}} = \rho_{sw} \pi d^2 C_{BTO} v^2 \tag{15}$$

Where:

- d is tunnel diameter.
- C_{BTO} is a coefficient that ranges from 0.003 and 0.012 depending on the tunnel geometry and the location along the vessel.
- v is again the ship speed (m/s).

2.5.2 Model-ship correlation resistance: hull rugosity

An additional resistance component often included in the total resistance is the model-ship correlation due to the hull rugosity. This rugosity is larger in the full-scale ship than in the model.

To this end the ITTC recommend a value for this coefficient (Baquero, 2011):

$$C_A = \left(105 \left(\frac{k_s}{L_{wl}} \right)^{\frac{1}{3}} - 0.64 \right) 10^{-3} \tag{16}$$

Where k_s is the average rugosity. Usually this value is taken as 1.5 E-04 m.

The model-ship correlation resistance is then calculated as:

$$R_A = \frac{1}{2} \rho_{sw} C_A S_W v^2 \tag{17}$$

2.6 Influence of hull shape on the resistance

In this chapter is given an overview of how the different hull geometrical characteristics affects the ship resistance. This behaviour is deeply analysed in Baquero (2011).

2.6.1 Hull dimensions

The main dimensions defining the wetted part of a ship hull are the length, the beam and the draft.

As the ship length increase, the wetted surface does too and therefore the frictional resistance become greater. On the other hand, the Froude number decreases and the wave resistance in general decreases.

The beam influence highly the ship resistance. In general, it can be said that when the beam increases all the components of the resistance rise, frictional, viscous and wave resistance.

The frictional and wave resistance components increase with the vessel draft. This is due to the rise in the wetted surface and volume. The ship is bigger and therefore disturbs more the free surface.

2.6.2 Shape coefficients

There are several coefficients that relates some hull magnitudes, as for example the volume, with the main dimensions.

The block coefficient is ratio between the hull volume and the three main dimensions. So, it defines how different is a hull than a paralepidid with the same main dimensions. It is defined as:

$$C_B = \frac{\nabla}{L_{wl} B T} \tag{18}$$

The prismatic coefficient relates the volume with the mid-ship section area and the length:

$$C_P = \frac{\nabla}{L_{wl} A_{MS}} \tag{19}$$

The Mid-ship section coefficient defines how different is the section than a rectangle:

$$C_{Ts} = \frac{A_{MS}}{BT} \tag{20}$$

And the waterplane coefficient is the ratio between the waterplane surface and the rectangular plane with the same length and beam:

$$C_{WP} = \frac{A_{MS}}{L_{wl} B} \tag{21}$$

A larger block and prismatic coefficient mean full hull shapes and therefore it disturbs more the free surface increasing significantly the viscous and the wave making resistance. A lower value of C_B should be corresponded with a low value of C_M and C_{WP}, trying to avoid large flow pressure gradients along the hull shape.

3 State of the art

3.1 Ship resistance estimation

As stated previously, in the early stages of the ship design process the hull resistance estimation is one of the main concerns, since the optimization of this characteristic results in a reduction in the power system and therefore also in the fuel consumption. This is one of the reasons why naval architects have been studying for years how to best estimate the ship resistance.

There are three main current methods to estimate the ship resistance: model testing, empirical methods and CFD (Larsson and Hoyte, 2010).

Model testing was the first method to be investigated. It dates from the 15th century, when Leonardo Da Vinci carried out some ship model tests. The first step is to build the hull models, usually made by wood, at a proper scale, and then to tow it on a towing tank measuring the force needed to achieve this movement. An example of a towing test is shown in Figure 3.1.

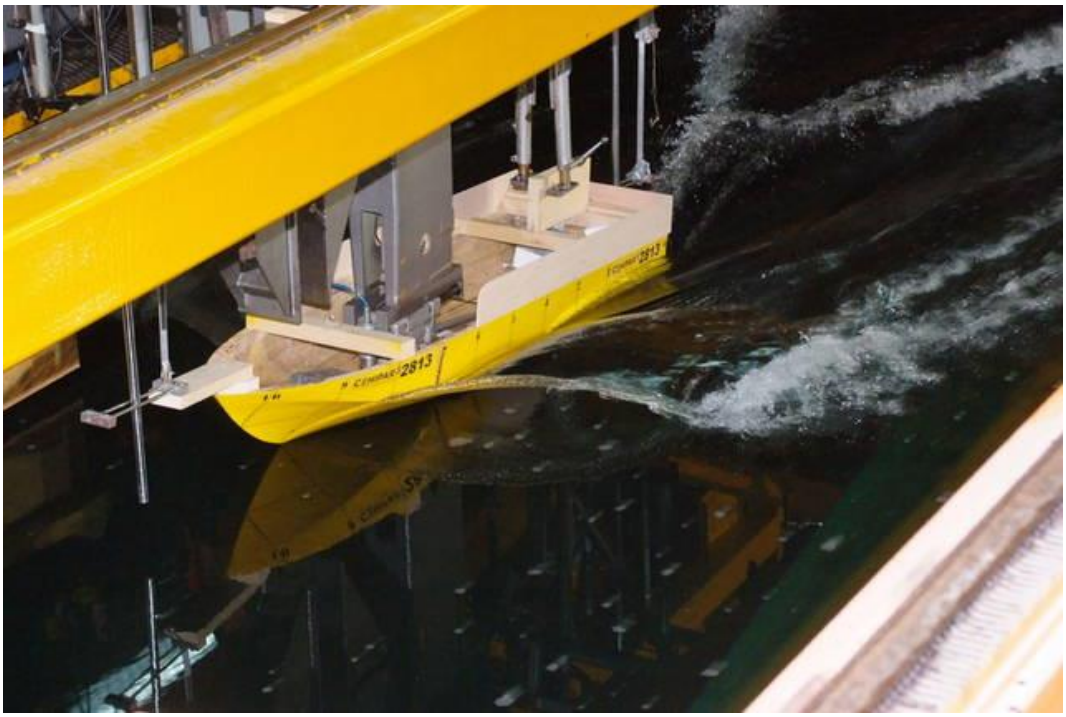

Figure 3.1. Example of towing test. Calm Water Towing Tank at INTA-CEHIPAR.

The major problem is the scaling of the results to a full-scale ship. The problem is not only how to extrapolate the measured towing force but also how to define the speed at which the model should be towed.

It was not until the 19th century when this problem was solved by Froude (1955), who postulates that: “The (residuary) resistance of geometrically similar ships is in the ratio of the cube of their linear dimensions if their speeds are in the ratio of the square roots of their linear dimensions.”. This residuary resistance is the total resistance minus that of an equivalent flat plate with the same area and length moving at the same speed as the hull (R_F as defined in section 2).

The equivalent plate resistance is defined as the resistance due to friction, and the residuary is the resistance due to wave generation. The first one can be easily obtained towing flat plates that do not generate waves, but the residuary, once the equivalent plate resistance has been

obtained from the total resistance, must be scaled in proportion to the hull displacement from the model to the ship.

A prerequisite for this scaling is that the ratio of the speeds at the two scales must be equal to the square root of the length ratios, or, in other words, the speed divided by the square root of the length should be the same at both scales. This is the well-known Froude number defined in section 2.

Reynolds found a scaling parameter for the viscous components of the resistance, and the correct way of scaling this component was defined and adopted as recommendation by the ITTC (International Towing Tank Conference).

Nowadays, there are not only simple towing tanks to measure the resistance, but also research centres that generate waves to study the movements of the ships in a seaway (Figure 3.2).

Figure 3.2. Ships Dynamics Laboratory at INTA-CEHIPAR.

The main problem of this model testing is the elevated time and economic cost of making several different models for the first phases of the design. Therefore, empirical models are often used. These are not as accurate as towing tests, but it is faster and easier to carry out a preliminary ship resistance estimation and define the hull main dimensions.

There are two different types of empirical methods: systematic series and statistical formulas based on unsystematic data.

The series are based on the results of several ship model tests with realistic hulls analysed in a towing tank and with main characteristics varied in a systematic way covering a range of possible hull forms.

There are some statistical formulas developed by different authors that used values of model test measurements from different vessels. As stated before, the most known is the Holtrop and Mennen method (1978), that used a theoretical expression for the wave resistance of two travelling pressure disturbances (the bow and the stern) in their regression formula, where the coefficients were determined from tests with 334 hulls.

The most recent method to estimate the ship resistance are the Computational Fluids Dynamics (CFD), which have been developed mainly during the last century thanks to the rapid computer development (Larsson and Hoyte, 2010).

This CFD defines the ship hull as finite element panels and simulate the flow field around the ship hull and the wave pattern. The pressure distribution is then calculated for each panel and integrated along the hull the total resistance can be obtained.

There are different types of CFD depending whether they are based on inviscid flows (potential flow) around the hull or implement viscous flows computational techniques. The latter enables the analysis of detailed hull areas, especially the stern flow, but are much more time consuming.

The CFD techniques are commonly used nowadays in ship design offices for second phases where the hull dimensions have been preliminary defined using empirical methods. The purpose of CFD application is normally to minimise the wave making resistance. In Figure 3.3 and Figure 3.4 are presented the wave pattern and the pressure distribution on a ship hull calculated suing potential CFD.

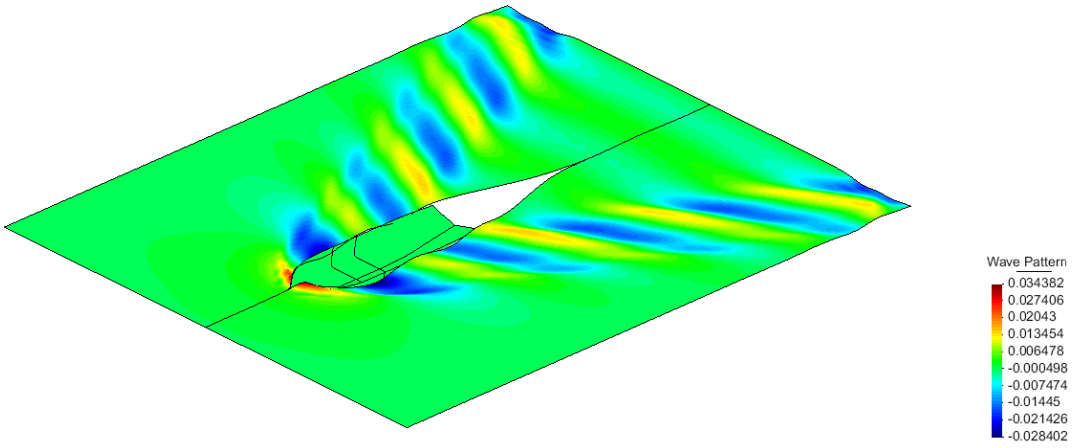

Figure 3.3. Example of potential flow CFD simulation. Wave pattern.

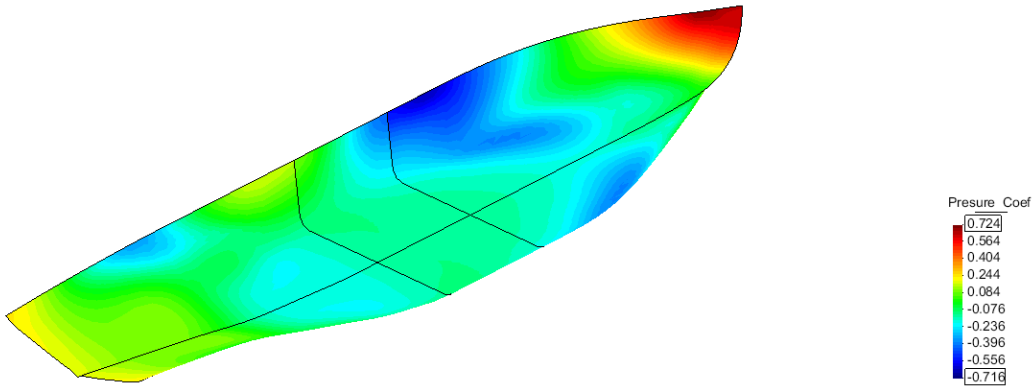

Figure 3.4. Example of potential flow CFD simulation. Pressure distribution.

3.2 ANN for the estimation of ship resistance

3.2.1 Artificial Neural Networks and their advantages

Artificial neural networks are artificial intelligent techniques that can be applied to the identification of complex systems. It is a type of computation tool inspired by biological systems, especially the human brain structure. These networks are systems made of a great number of simple processors organised in layers and highly interconnected. Each simple neuron process information as a response to external inputs and generate simple outputs that act as new inputs for the next neurons (Hilera and Martínez, 1995).

Biological neural networks are composed of thousands of hundreds of neurons and an even greater number of connections. These large number of connections enables the system to process a huge amount of information using simple processors. ANN have a larger number of connections than neurons.

Each neuron receives information from other connected neurons. This information is processed, and a specific weight is applied to each received input. In this way, the output of each neuron is the sum of each individual weighted input. Each neuron has a transfer function that defines if its activated or not, depending on the received input.

The way an ANN learns is by modifying the weights associated to each input for every neuron of the network. They can learn from examples adjusting the outputs. This learning can modify, disable or even create new connections. When the values of the network weights become stationary, the learning process ends. This process is known as training the neural network.

These characteristics makes the ANN to have a similar behaviour as a human brain. The main advantages of this behaviour for the objective of this study can be summarised as:

- Learning: This characteristic of ANN is of great importance, as it gives the possibility to obtain results of a system without the need to develop a model for it. On the other hand, the training of the network needs a proper algorithm for the correct learning.
  For this master thesis, this characteristic gives the ANN the ability to be applied to different types of vessels and hull shapes.

- Non-linear behaviour: they can adapt to non-linear systems. Given the strong non-linear relation between the Froude Number and the wave resistance, this is an important advantage for the estimation of the ship resistance.
- Easy implementation: although it is important to have a proper data base for the training, nowadays is quite easy to develop the architecture of a neural network with available commercial software. As a disadvantage, it is sometimes difficult to obtain a proper data base.
- Continuous learning: a developed and trained network can be easily retrained with new data. For instance, the tool developed here for the estimation of ship resistance could be retrained in the future with the experiments carried out in the coming years in CEHIPAR. Or even retrained with new data from other towing tanks.

All these advantages make the ANN suitable for the estimation of the ship resistance, training it with a data base made up of empirical information.

3.2.2 Ship resistance estimation using neural networks

Although during early project phases, ship design offices still use empirical methods based on regression analysis, some advances in the use of artificial neural networks for ship resistance prediction have been done.

As an alternative to traditional empirical methods, Couser et al. (2004) study the applicability of artificial neural networks to the problem of ship resistance prediction. In this article, the authors present an analysis of the use of ANN as an interpolation tool to predict the residual resistance of a systematic series of catamaran forms.

The resistance data used for this investigation was a series of model tests of a total of ten hulls, most of them tested for F_n between 0.2 and 1.0. The results of this article (Couser et al., 2004) show that ANN can provide good approximations to hull resistance data.

One of the main conclusions from this analysis is the difficulty to predict the high non-linear relationship between the ship resistance and the Froude number. This behaviour can be better handled by artificial neural networks than traditional regression methods.

The same authors continue this research and analyse the influence of the number of layers in the ANN outcome (Mason et al., 2005). They found that the performance of the networks increases with the number of hidden layers and neurons. On the other hand, neural networks trained with large numbers of hidden layers tend to suffer from overfitting.

Other authors have applied neural networks for the estimation of ship resistance using systematic series´ hull forms (Chen et al., 2009; Margari et al., 2018). Margari et al. also suggested that CFD calculations could be used as training data bases. On the other hand, Radojcic et al. applied NN to a data base composed by systematic series of simple hard chine hulls and conclude that regression analysis is more convenient for simpler relations.

More recent researches analyse the application of artificial neural networks to the problem of ship resistance by using a “synthetic” database made by applying the Holtrop method to a wide range of hull shapes and dimensions (Ortigosa et al., 2009; Marón and Santos, 2017).

As stated before, the research presented in this master thesis is a continuation of Marón and Santos (2017). In this article a synthetic data base of 12000 cases was generated using the Holtrop method. This data base was used to train two different ANN for the estimation of the form factor and the wave resistance, separately.

The results of this paper showed a good agreement between the estimated parameters and the synthetic data base, making a good first step for the possible application of ANN to the ship resistance problem.

Figure 3.5 shows the regression plot of the estimation of the wave resistance presented in Marón and Santos (2017), showing a good agreement.

In the present work, ANN are trained with a data base made up of thousands of data measured in model test campaigns carried out in CEHIPAR.

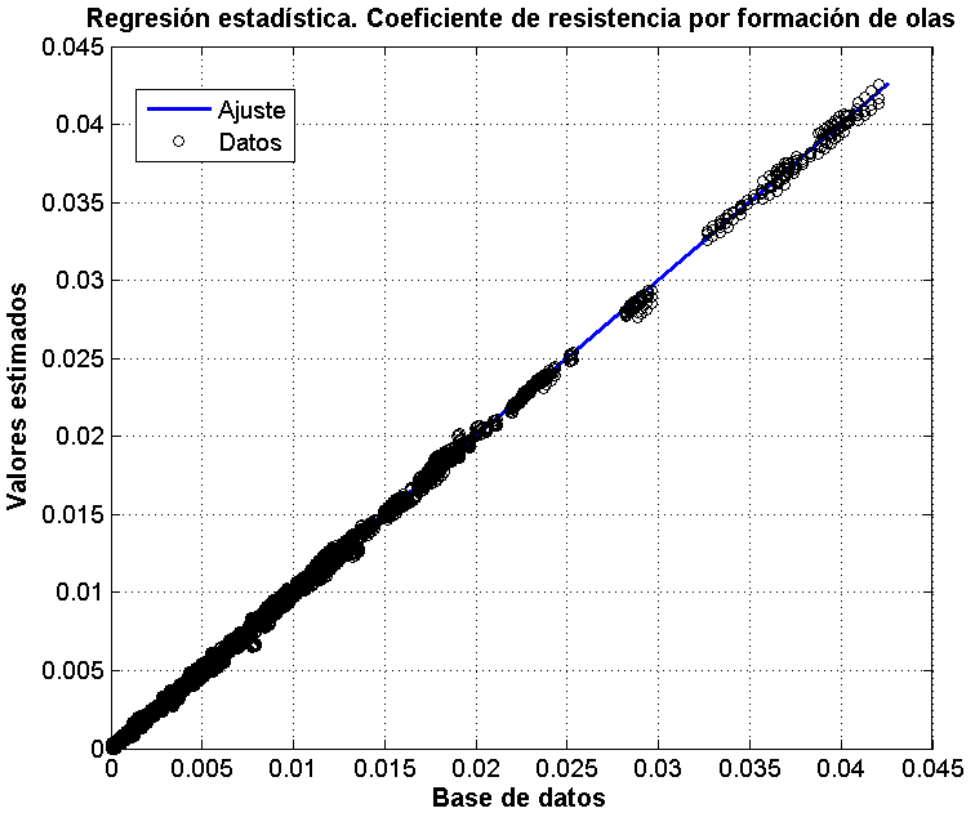

Figure 3.5. Wave resistance estimation regression (Marón and Santos, 2017).

4 Materials and methods

In this section an overview of the developed ANN for ship resistance estimation is presented.

The code developed has been written using MATLAB, and the "Neural Network Toolbox" within MATLAB suite (Hudson et al., 2018).

The units are given in the International System of Units except the following:

- Ship speed is presented in knots (kn), as is usually done in the naval field.
- Hull resistance is defined in kN, due to the huge magnitudes of the related variables.
- Water density is defined in t/m^3, to be consistent with the above mentioned variables.

4.1 Materials: Data base

After signing a confidentiality agreement with INTA-CEHIPAR, the research centre gave access to some data regarding the calm towing tank tests. This data base contains information of model test campaigns for more than a thousand hull shapes.

The information contains the following "text files":

- Carenas: contains information regarding the main dimensions of each scaled model, such as the length, beam, or the block coefficient. It also identifies the type of ship been tested.
- Sit: contains data of the loading conditions for each test performed such as the waterline length or the wetted surface. This data is of great importance for the hull resistance estimation.
- Remolques: this text file gives information of the model tests performed for a specific hull and a specific loading condition. It contains important data as the number of velocities tested, the model scale, the estimation of the form factor (not always) and temperature of the tank water at the moment when the test was done.
- Tab_remol: for each hull model and loading condition specified in "Remolques", this file gives the velocities and the measured total resistance in model scale. From these data the velocities and the different resistance components for full-scale hulls can be obtained.

The data base contains more than two thousand model tests performed and more than thirty thousand velocities measured. All this information has been pre-processed manually to delete unnecessary data and correct duplicated data.

A "cell array" has been created containing the type of ship. This is done to have a set of pre-defined ship types, trying to uniform the "strings" that define these types. All the vessels have been defined as one of the following types:

- Barge
- Bulkcarrier
- Classic
- Container
- Cruise
- Fishing vessel
- General cargo
- Offshore
- RORO

- Small Craft
- Special Purpose vessel
- Tanker
- Tug
- Warship

After this manual pre-processing, a binary MATLAB file has been created with the "matrices" and the "cell array" identifying the ship type for each scaled hull shape.

A script called "parse_database" has been written to parse the data in a proper way and obtain the information needed to train the neural networks. This script is explained in the following sub-sections. A flow diagram showing the different steps of the code is presented in Appendix B.

4.1.1 Parse data base variables

The script "parse_database" first performs a loop for each measured case in the towing tank (velocity for each hull model and loading condition) and obtains the indexes that identify to which hull model and loading condition each case belongs.

With this information a parse of the variables of interest is done, such as the main hull dimensions, the hull shape coefficients, the type of ship, the model scale, the water temperature, the velocity of the test and the measured resistance. When the form factor is given in the data base, this value is also saved. Some other variables are calculated at this time such as the Froude number and the Reynolds number.

The fresh water density and kinematic viscosity are obtained interpolating the temperature measured during the tests (see Table 4.1). These values are given in the ITTC recommended procedures (see [14]).

Table 4.1. Fresh water properties.

Temperature (ºC)	Density (t/m^3)	Kin. Visc. (m^2/s)
10	0.9997	1.3063 E+06
12	0.9995	1.2347 E+06
14	0.9992	1.1692 E+06
16	0.9989	1.1093 E+06
18	0.9986	1.0542 E+06
20	0.9982	1.0034 E+06
22	0.9978	0.9565 E+06
24	0.9973	0.9131 E+06
26	0.9968	0.8729 E+06
28	0.9962	0.8355 E+06
30	0.9956	0.8007 E+06

After all the variables have been sorted, the total resistance coefficient (in the model scale) can be obtained for each measured velocity:

$$C_{Tm} = \frac{R_{Tm}}{\frac{1}{2}\rho_f S_{wm} v_m^2} \qquad (22)$$

Where the sub-index “m” refers to the model scale. This coefficient is used to estimate the form factor when it is needed.

4.1.2 Form factor empirical estimation

Unfortunately, the form factor is not always given in the CEHIPAR data base. This lack of information affects more than half of the recorded tests.

To enable the use of all the data, the form factor has been estimated by several methods and a MATLAB function called “get_r” have been created to estimate it.

After this function was developed, the estimation of the form factor by different methods have been compared with the test data where this value is given by CEHIPAR. The most suitable method has been selected based on an error analysis and the recommended procedures of the ITTC.

4.1.2.1 Alaez method

This method is presented in Aláez Zazurca (1972). The form factor is estimated as:

$$r = 1 + 18.7\left(C_B \frac{B}{L_{wl}} \right)^2 \tag{23}$$

This method could be applied for full ships that meet the following relation:

$$0 < C_B \frac{B}{L_{wl}} < 0.11 \tag{24}$$

4.1.2.2 Sasajima and Tanaka method

This method of Sasajima and Tanaka (1963) is also applicable to full ships such as tankers, containerships, or bulkcarriers. The form factor is estimated as:

$$r = 1 + \sqrt{\frac{\nabla}{L_{wl}{}^3}} \left(2.2 C_B + \frac{P}{C_B} \right) \tag{25}$$

Where P is a coefficient given by a function of the ratio between the beam and the length of the run L_r (Figure 4.1).

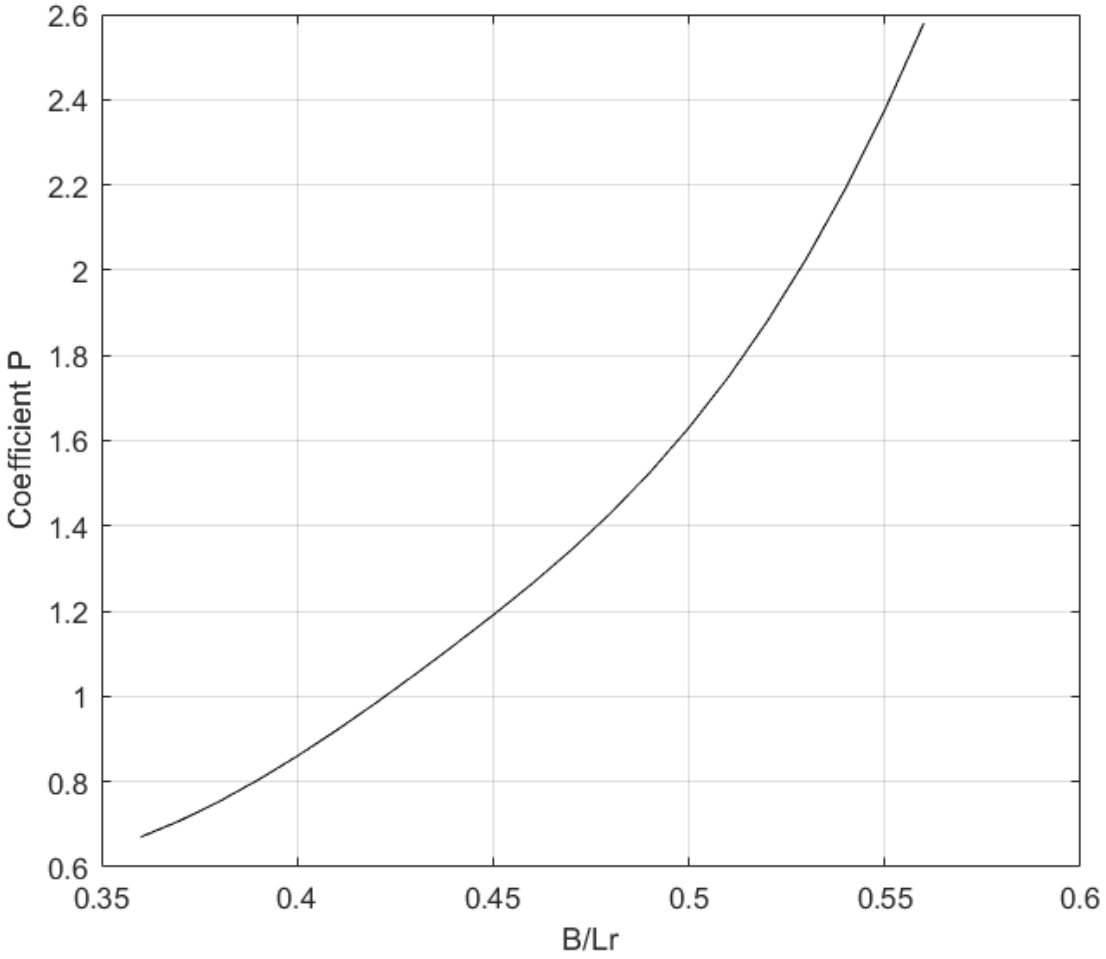

Figure 4.1. P coefficient. Sasajima and Tanaka (1963).

4.1.2.3 Holtrop and Mennen method

Holtrop and Mennen (1982) presents a formulation for the estimation of the form factor, r, as a function of the waterline length, L_{wl}, beam, B, draft, T, prismatic coefficient, C_P, the longitudinal position of the centre of gravity, lcb, and the length of the run, L_r [10]:

$$r = c_{13}\left(0.93 + c_{12}\left(B/L_r\right)^{0.92497}\left(0.95 - C_P\right)^{-0.521448}\left(1 - C_P + 0.0225\,lcb\right)^{0.6906}\right) \quad (26)$$

The length of the run can be estimated as:

$$L_r = L_{wl}\left(1 - C_P + 0.06\frac{C_P\,lcb}{4C_P - 1}\right) \quad (27)$$

The coefficient c_{12} are defined as:

$$c_{12} \begin{cases} c_{12} = \left(T/L_{wl} \right)^{0.2228446} & \text{when } T/L_{wl} > 0.05 \\ c_{12} = 48.2\left(T/l_{wl} - 0.02 \right)^{2.078} + 0.479948 & \text{when } 0.02 < T/L_{wl} < 0.05 \\ c_{12} = 0.479948 & \text{when } T/L_{wl} < 0.02 \end{cases} \quad (28)$$

The coefficient c_{13} accounts for the specific shape of the afterbody. It takes values from 0.97 for V-shaped sections to 1.03 for U-shaped sections. In this case, it has been considered 1 for all hull shapes.

4.1.2.4 Prohaska method

Prohaska (1966) presented a method for the estimation of the form factor based on the wave and the total resistance coefficients. The main hypothesis is that the wave making coefficient, C_W, can be approximated as a constant, y, multiplied by F_n to the forth power:

$$C_w = y F_n^4 \quad (29)$$

Which is applicable for moderate ship speeds, with Froude numbers between 0.1 and 0.2.

The total resistance coefficient, which can be obtained from the model test, is defined as:

$$C_T = rC_F + y\frac{F_n^4}{C_F} \quad (30)$$

Dividing both sides by C_F:

$$\frac{C_T}{C_F} = r + y\frac{F_n^4}{C_F} \quad (31)$$

This equation represents a first-degree polynomial where the additive constant is the form factor.

From the measured resistance for different velocities within one model test, a least-squares fitting can be done to obtain the additive constant of the first-degree polynomial. In Figure 4.2 an example where the Prohaska method is applied to one of the model tests of the data base is shown. In the example, the form factor estimated by this method is 1.072.

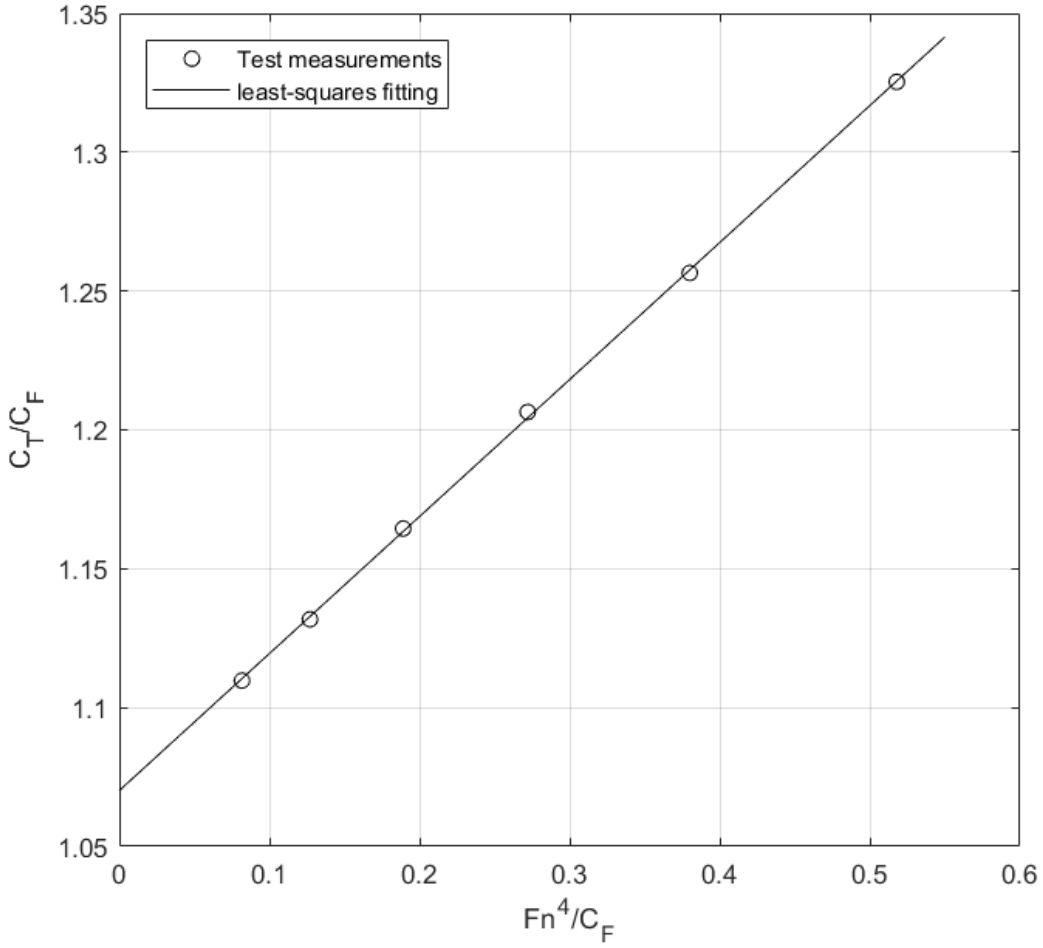

Figure 4.2. Example of the application of Prohaska method to obtain the form factor.

4.1.2.5 Selection of the estimation method

An error analysis has been carried out to select the method to be applied to the data base. The error is calculated as the difference between the estimated form factor and the given form factor in the data base (when available). The number of available form factor for the hull model tests is 650.

In Table 4.2 the results of the error analysis are. For each method, and depending on the range of application, the number of estimations is different.

The two simplest methods, Alaez and Sasajima, are applicable for less than 200 hull shapes. Regarding the mean square error, the Prohaska method is the one that gives the best performance.

Table 4.2. Form factor estimation by several methods. Error analysis.

Method	**Alaez**	**Sasajima and Tanaka**	**Holtrop and Mennen**	**Prohaska**
No. data	193	124	646	445
Mean square error	0.0216	0.0151	0.0273	0.0100
Max square error	0.0755	0.0385	0.0994	0.0460

Figure 4.3 to Figure 4.6 show error histograms for each analysed method, when comparing the estimation of the form factor with the one given in the data base. Figure 4.3 and Figure 4.4 shows smaller number of estimations, and the error ranges between -0.2 and 0.2. In Figure 4.5, the Holtrop method shows a larger number of estimations, with errors mainly between the same ranges. Prohaska method (Figure 4.6) show also many estimations within a smaller range, -0.1 to 01.

The histograms show that the method proposed by Holtrop and Mennen (1982), and Prohaska (1963) give a good performance within a wider range (a great number of estimations). The method proposed by Prohaska (1963) gives the best performance.

With these results and bearing in mind that the ITTC recommends the use of Prohaska method, this is the one considered for the estimation of the form factor to increase the number of points in the data base.

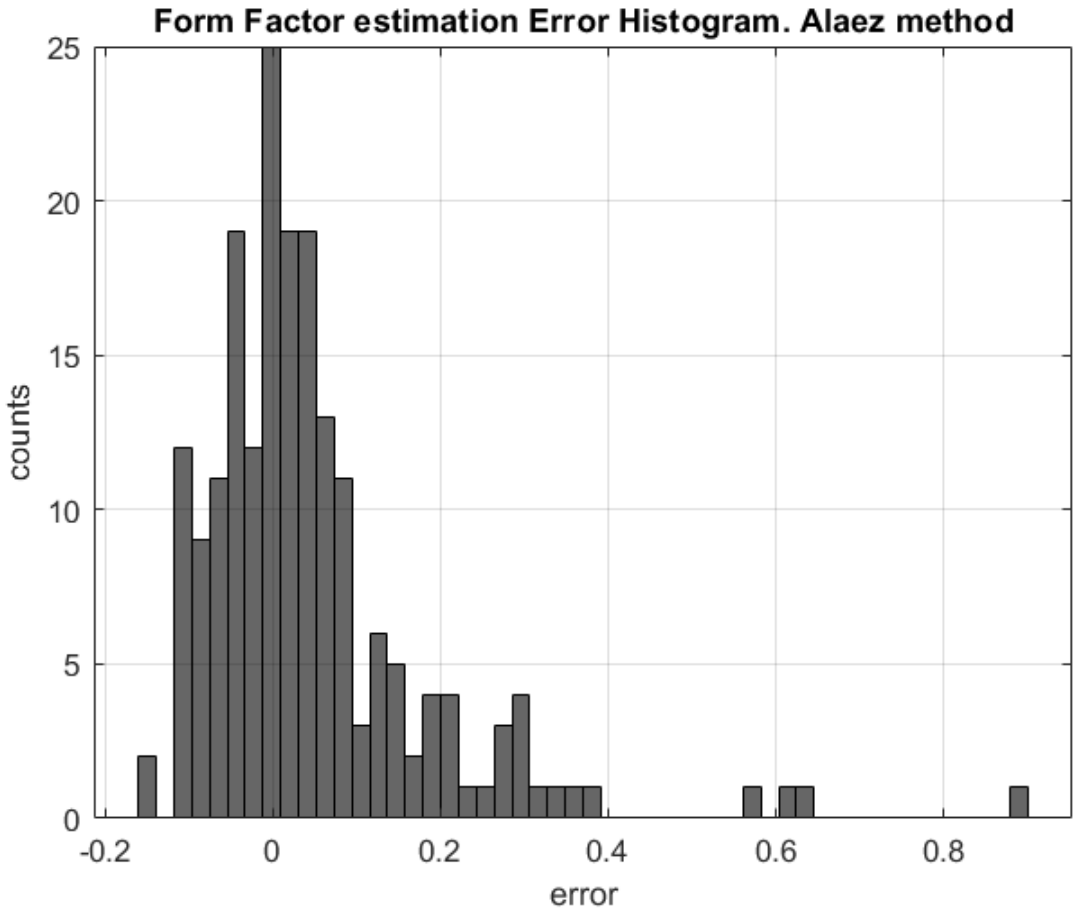

Figure 4.3. Form Factor estimation Error Histogram. Alaez method.

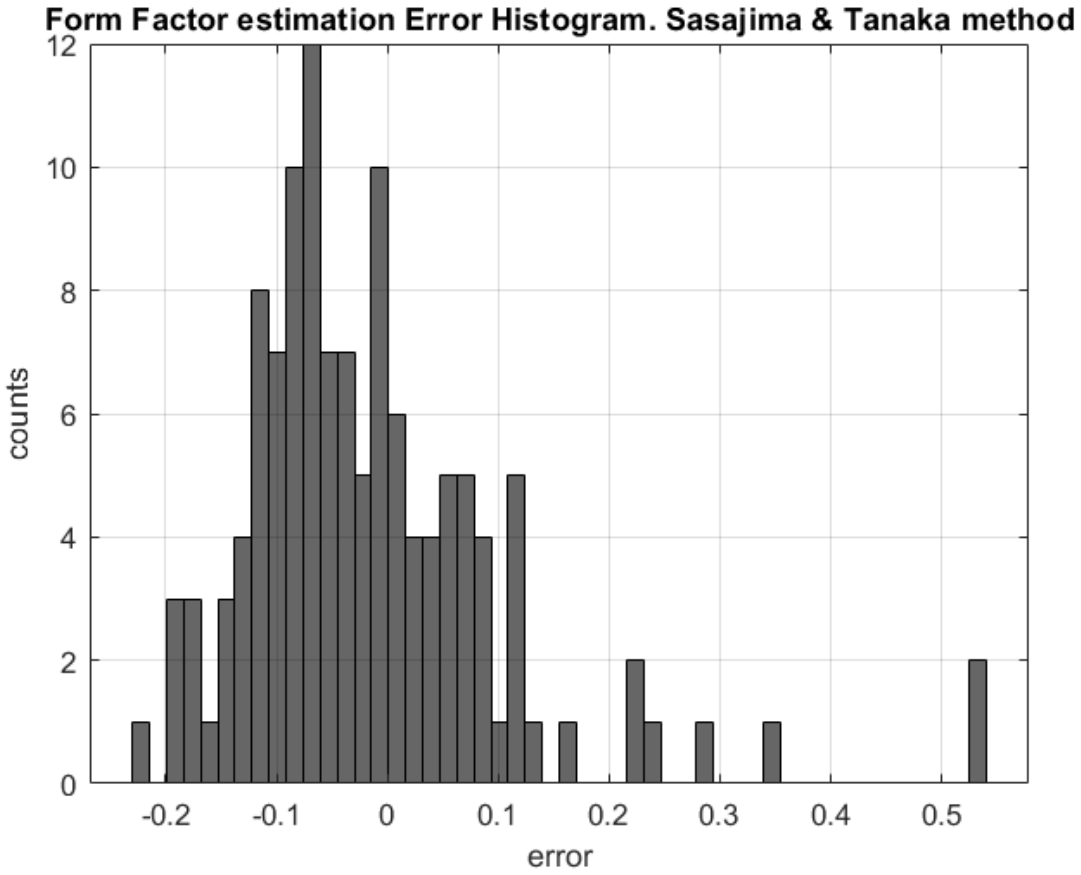

Figure 4.4. Form Factor estimation Error Histogram. Sasajima and Tanaka method.

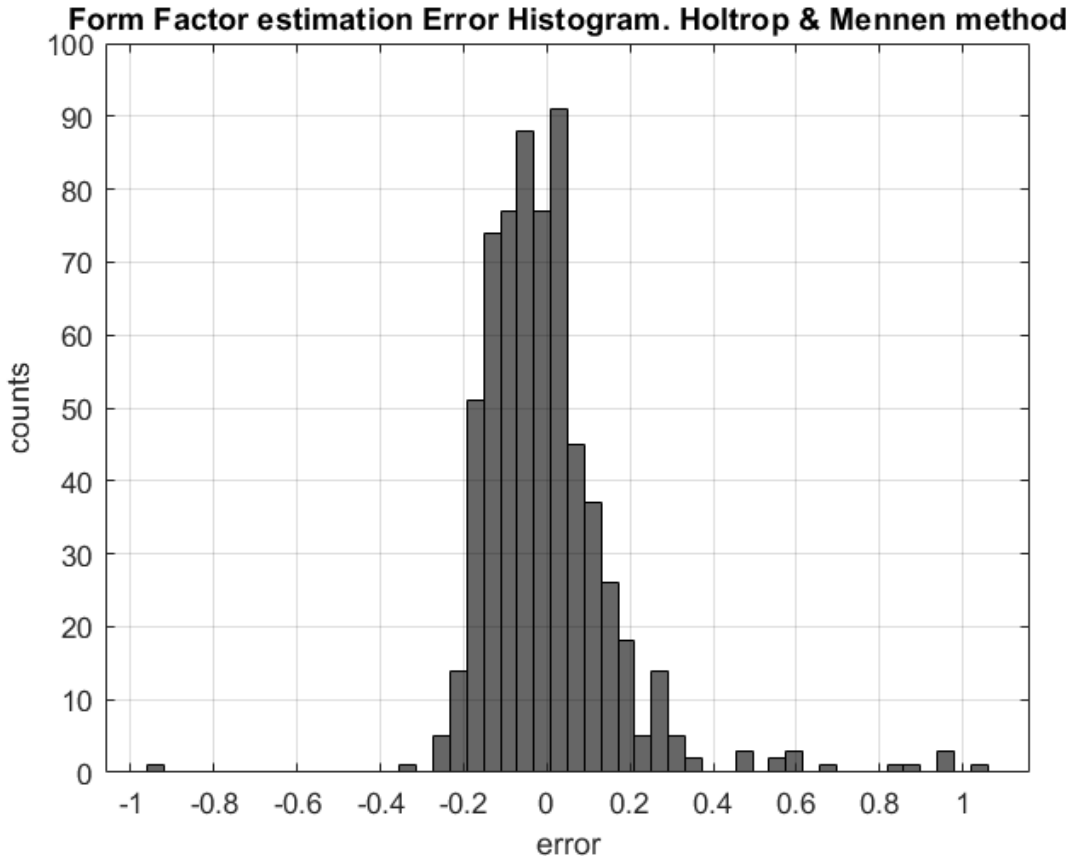

Figure 4.5. Form Factor estimation Error Histogram. Holtrop and Mennen method.

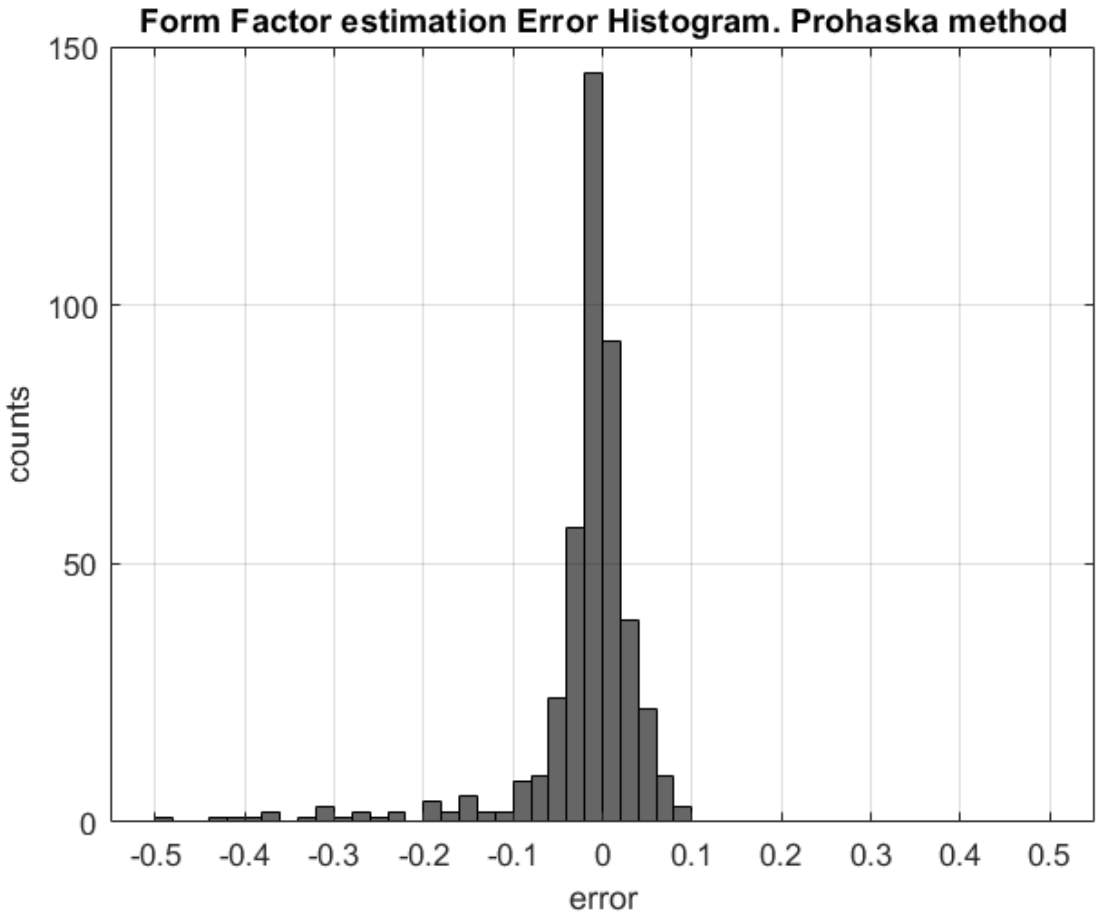

Figure 4.6. Form Factor estimation Error Histogram. Prohaska method.

4.1.3 Resistance coefficients

For each case, the resistance coefficients are calculated and saved in a new matrix of data.

The resistance coefficients can be directly calculated for the model as:

$$C_{Fm} = \frac{0.075}{\left(\log_{10}\left(\mathrm{Re}\right) - 2\right)^2} \tag{32}$$

$$C_{Tm} = \frac{R_{Tm}}{\frac{1}{2}\rho_{sw} S_w v^2} \tag{33}$$

Where the water density is obtained by interpolating in Table 4.1, for the temperature given in the data base for each test.

At this stage the form factor is available in the data base or it has been estimated applying the Prohaska method. Therefore, following the procedure defined in section 2.4, the resistance coefficients for the full-scale can be obtained.

4.1.4 Increasing number of velocities

The wave making resistance has a strong non-linear behaviour regarding the Froude number and therefore it is important to have enough data to learn this behaviour.

With the objective to have a better performance of the final tool, the number of data depending on the Froude number has been increased. A spline interpolation has been done to increase three times the number of velocities within one model test.

On the other hand, it is important for the ANN to learn that wave making resistance tends to zero when the ship´s velocity decreases. In order to reproduce this behaviour, a few points have been added from zero to the minimum velocity tested in each case. These points have been added interpolating a spline between zero and the first two velocities of the measured data.

In Figure 4.7, Figure 4.8 and Figure 4.9 some examples of the interpolation done to increase the number of velocities are presented. From zero to the first measured velocity two new points have been interpolated. In these figures is shown that, since the curves present a smooth behaviour, the interpolation is not introducing additional errors to the final estimation.

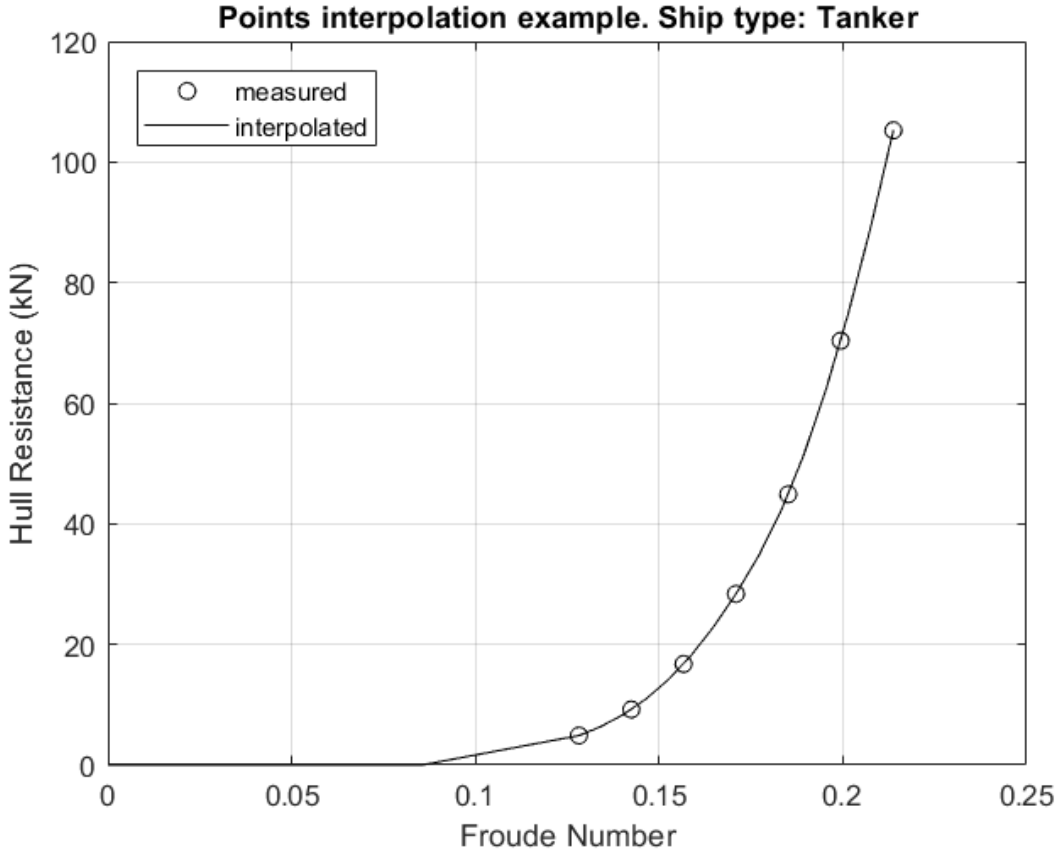

Figure 4.7. Increase of velocities. Points interpolation example. Ship type: tanker.

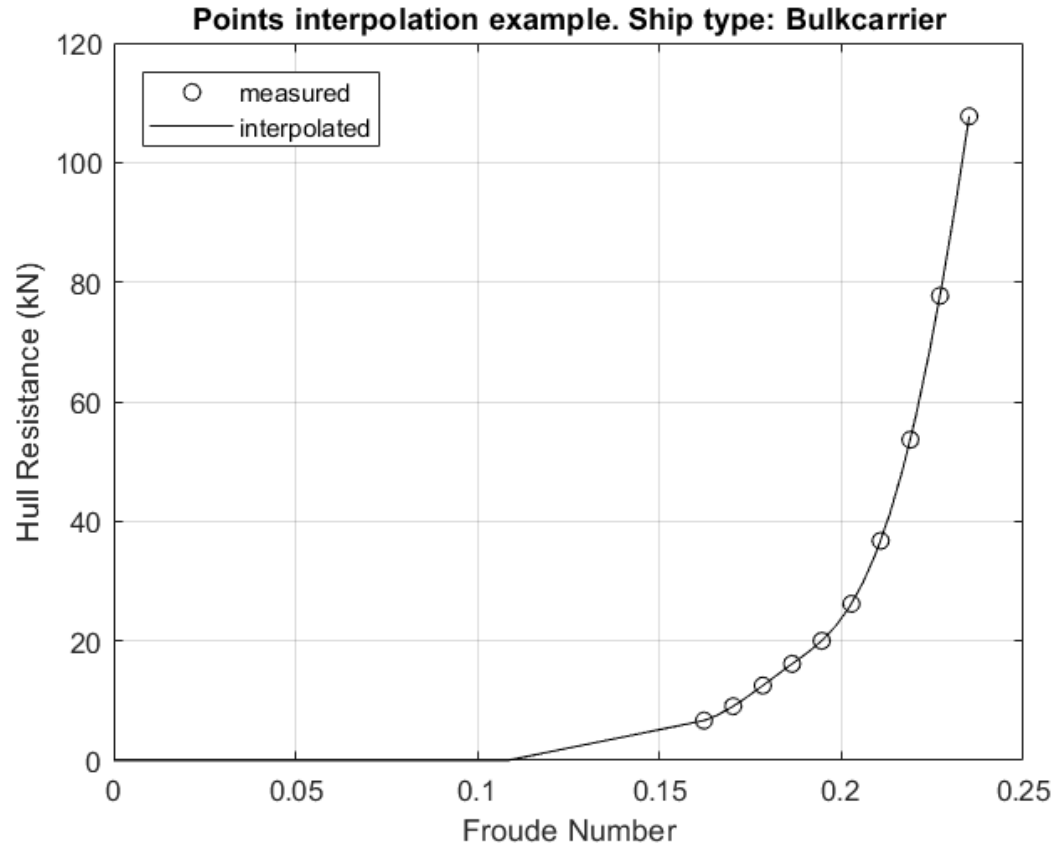

Figure 4.8. Increase of velocities. Points interpolation example. Ship type: bulkcarrier.

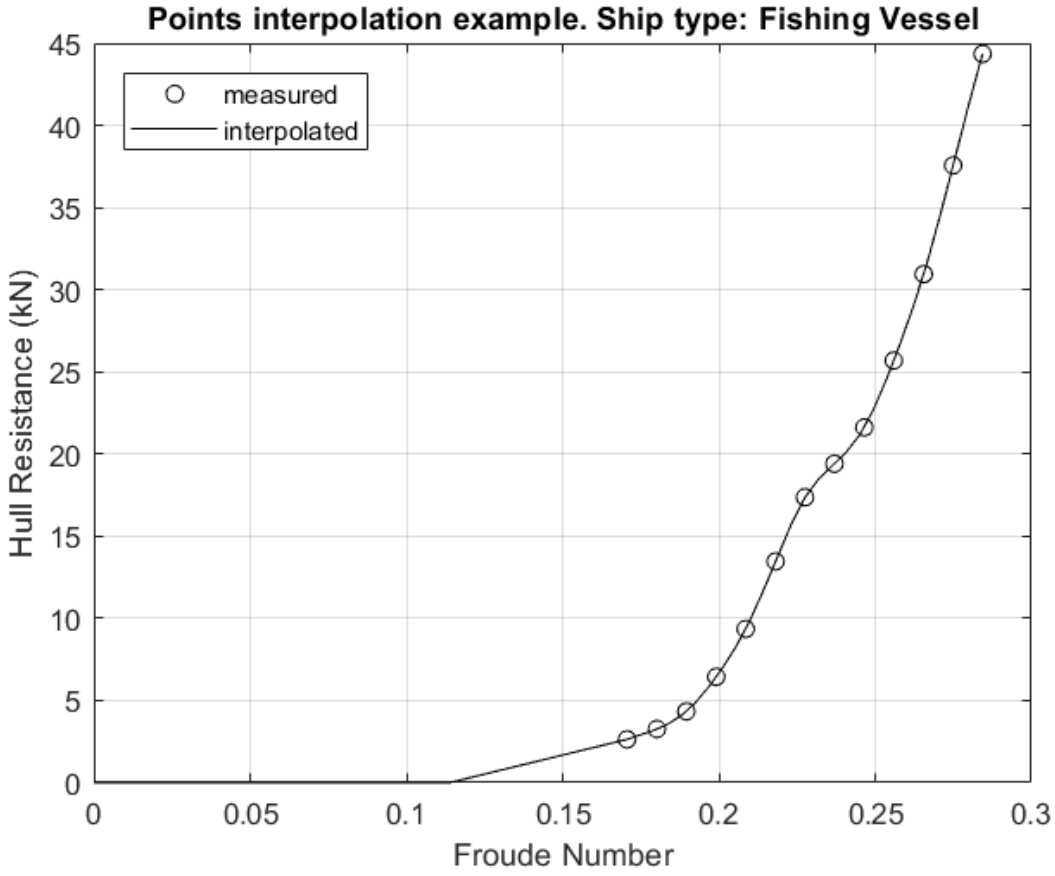

Figure 4.9. Increase of velocities. Points interpolation example. Ship type: fishing vessel.

4.1.5 Case filtering

After generating the data base to train the ANN, the cases were filtered, and different sets of training data bases were generated.

The procedure “parse_database” is as follows:

- First, the data base is filtered by type of ship (Figure 4.10). The user can specify one or more types of ships as defined in section 4.1.
- Then the filter is applied to delete those cases where the form factor is not available neither the Prohaska estimation method can be applied.
- Finally, if the user wants to use the semi-angle of entrance (α) as an input, the code deletes those cases where this parameter is not available.

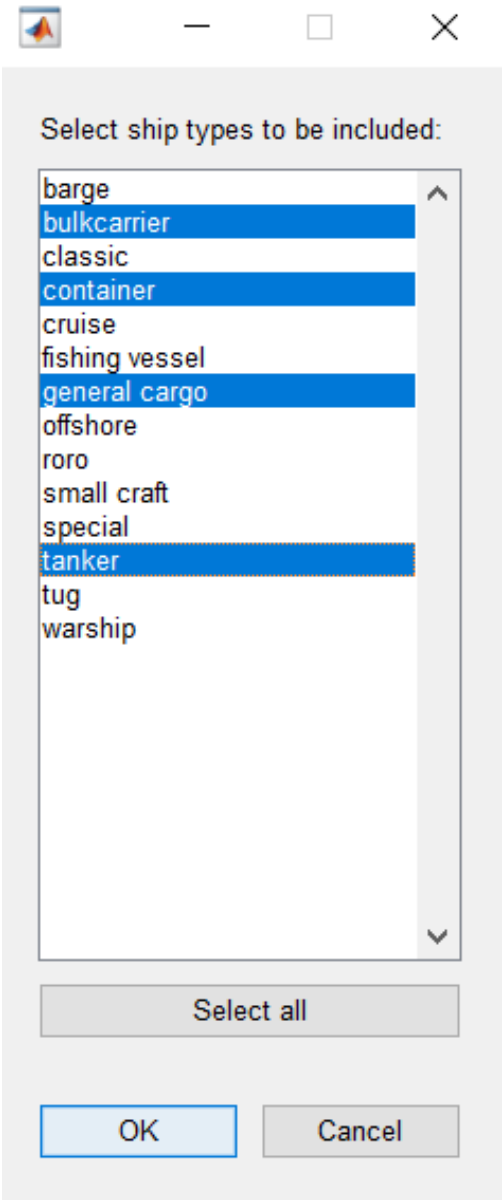

Figure 4.10. Pop-up menu to filter ship types.

4.1.6 Generated training data bases

Unfortunately, some of these ship type sets do not have enough data to be used as an independent data base.

Using the script "parse_database" the following training data bases have been generated:

- Cargo ships: bulkcarriers, general cargo vessels, tankers and container vessels.
- Fishing vessels.
- Warships.
- Small crafts.
- All ships: bulkcarriers, container vessels, cruise ships, fishing vessels, warships, general cargo vessels, offshore vessels, RORO vessels and tankers.

All these data bases have been analysed and used to train the ANN, although only some of them have been considered to develop the hull resistance estimation tool.

4.2 Neural Network

4.2.1 ANN Outputs

Although there are several components in the resistance of a sailing vessel, the estimation via neural networks have been focused on the most important components: the viscous resistance and the wave making resistance. A different neural network has been designed for the estimation of each component.

The rest of the components such as the resistance generated by the appendages or the tunnel thrusters are of lower magnitude and depend on the specific vessel. These additional components of the resistance are introduced in the final tool (see section 6) as a user selection.

As explained in section 2.2, the viscous resistance is calculated as the frictional resistance multiplied by the form factor. The form factor does not depend on the ship speed, but only on the hull shape and dimensions, and this reduces a lot the number of data to be used as training sets.

To estimate the viscous resistance two procedures have been analysed:

- First an ANN have been developed to directly estimate the form factor. The frictional resistance coefficient is defined as the ITTC curve and, therefore, the viscous resistance is known. This first attempt had the disadvantage of the low number of available data for the training procedure.
- To improve it, a second procedure has been applied where the viscous resistance is directly estimated by the ANN. In this case the viscous resistance depends on the ship speed, and the number of data is larger. This method has the disadvantage that to follow the ship resistance theory (see section 2), the form factor must be obtained from the estimated viscous resistance. Once the form factor has been obtained, the viscous resistance must be re-calculated applying formula (5).

Regarding the estimation of the wave resistance, it strongly depends on the ship speed. Keeping in mind that the number of points was increased to include more ship speeds (see section 4.1.4), the training data base is large enough. The ANN is trained to give the wave resistance.

4.2.2 ANN Inputs

The selection of the ANN inputs is one of the key points to the proper development of an ANN as a fitting tool.

In the ship design phase, the hull shapes are not defined in detail and are still subject to changes. Consequently, the inputs should be basic hull dimensions and parameters defining the geometry.

A deep analysis of the ship resistance has been done and explained in section 2. This preliminary study was of great importance to understand correctly the different components of the resistance and the dependence of those components on different parameters of the ship, such as speed, the dimensions and the hull shape.

The inputs have been defined considering the direct or indirect influence on the ANN outputs. In this way, the number of inputs has been minimized as much as possible keeping a good general performance.

4.2.2.1 Inputs: form factor direct estimation

The following input parameters have been used for the direct estimation of the form factor:

i. Waterline length (L_{wl}).
ii. Beam (B).
iii. Mean draft (T).
iv. Wetted surface (S_w).
v. Block coefficient (C_B).
vi. Prismatic coefficient (C_P).
vii. Midship section coefficient (C_M).
viii. Waterplane coefficient (C_{WP}).

4.2.2.2 Inputs: viscous and wave making resistance

The input parameters used for the estimation of the viscous and the wave making resistance are the same as defined for the form factor, but including the Froude number:

ix. Froude number (F_n).

In addition, some analysis has been done including the semi-angle of entrance (α) and the longitudinal centre of buoyancy (lcb) as inputs, but the influence on the performance was unsatisfactory. Therefore, these were discarded and are not included as inputs in the developed tool (see section 6).

4.2.3 Neural Network Architecture

A feedforward network with two layers of neurons has been used to develop the computational tool to estimate the ship resistance. The networks are composed by two layers, a hidden layer and an output layer with a linear transfer function.

A NN has been developed for each output to be estimated: the viscous resistance and the wave making resistance. Therefore, the ANNs have multiple inputs and single output. The form factor is estimated using 8 input parameters, and the viscous and wave resistances are estimated with 9 outputs.

Several sensitivity analyses have been performed to select the number of neurons in the hidden layer. When increasing the number of neurons, the solution converges to a better general performance, but on the other hand the network becomes “unstable” and it may suffer

overfitting. For instance, it has been observed that for similar ships with very similar shapes, the resistance outputs could present large differences. Therefore, it is necessary to select a number of neurons enough to have a good general performance but giving reasonable results.

The number of neurons in the hidden layer was set to 15 for the neural estimation of the viscous resistance at full-scale, and 20 neurons to estimate the wave making resistance. This one has a strong non-linear behaviour regarding the Froude Number, and a larger number of neurons is needed to identify it.

The "Levenberg-Marquardt" algorithm was selected to train the ANN. This algorithm is often used to solve non-linear least squares problems, and it is recommended to be used for non-linear regressions problems [12]. Other training algorithms have been tried, such as the "Scaled Conjugate Gradient", without obtaining significant differences.

The statistical value used to measure the network´s performance during the training was the mean squared error.

The data bases have been divided in the following sets:

- Training set: it is used to train the neural network adjusting the weights according to its error. It has been defined as the 70% of the data base.
- Validation set: it is used to evaluate whether the training must continue or should be stopped depending on the performance and how this performance is changing in each iteration. It has been defined as the 15% of the data base.
- Evaluation set: it is used to evaluate the performance of the ANN. It does not have any effect on the network training and only provides an independent measure of the ANN performance. It has been defined as the 15% of the data base.

In the following table a summary of the ANN characteristics is presented.

Table 4.3. Summary of the Neural Networks Architecture.

Network output	Form Factor	Viscous Res.	Wave Making Res.
No. hidden neurons	10	15	20
Transfer Functions	Symmetric sigmoid		
Training set	70 %		
Validation set	15%		
Test set	15%		
Learning algorithm	Levenberg-Marquardt		
Performance function	Mean squared error		

4.3 Evaluation of the Tool performance

As explained before, the mean squared error have been used to measure the performance during the ANN training and to halt training when the performance stops improving.

Once the ANN have been created, the global performance has been analysed against the performance of Holtrop and Mennen method, the most widely used in the industry for early stages of the ship design projects.

To perform this comparison the following steps have been followed:

- The generated ANNs are used to compute the viscous and the wave making resistance with the inputs included in the data base.
- The absolute errors with respect to the model tests data base have been calculated. The root mean squared errors have been also used as the comparable statistical parameter. The relative error is presented as error histograms.
- Then the Holtrop and Mennen method is applied to estimate the resistance for the same cases, and the error is calculated again with respect to the model tests data.
- The comparison is made using only the cases included in the "evaluation data set".

As an example, in Figure 4.11 the histogram of the relative error when estimating the viscous resistance for the data base of cargo ships is presented, where "rann" refers to the ANN tool (resistance artificial neural network) and "Holtrop" is the Holtrop and Mennen method.

These error histograms give relevant information. In this example, the histogram for the Holtrop method has a wider range and therefore the accuracy of the ANN is better in most cases.

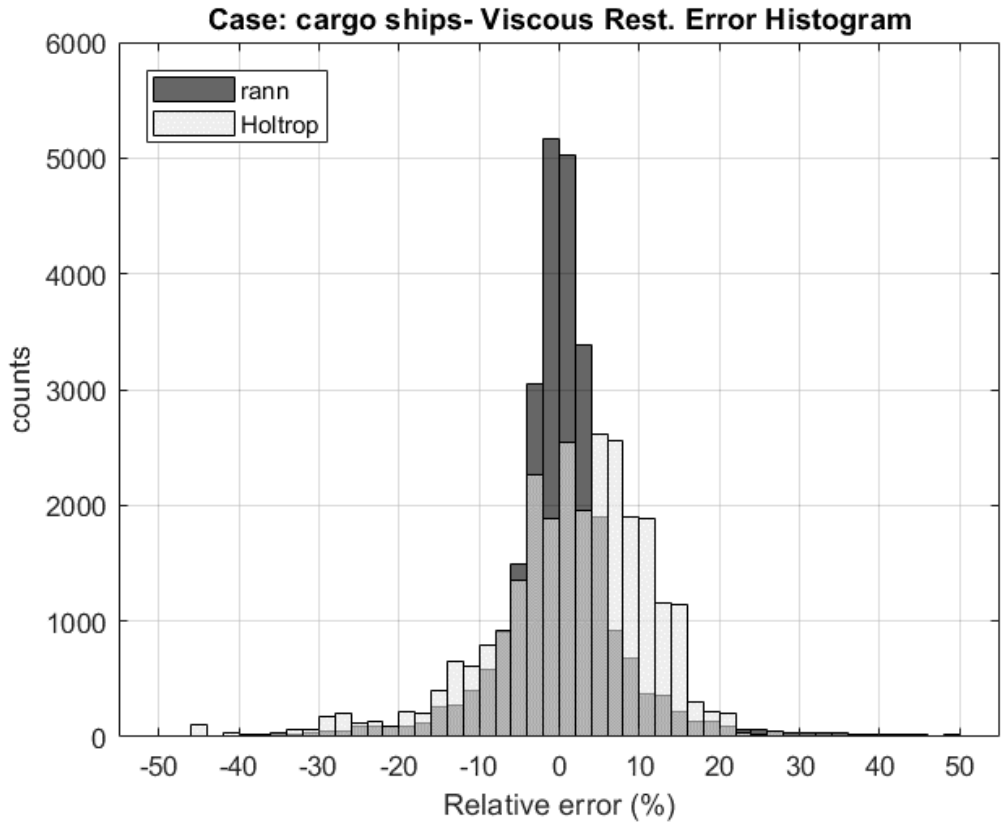

Figure 4.11. Example of error histogram. "rann" vs "Holtrop".

In addition, another statistical figure has been used to measure the tool performance. The regression factor "R" has been calculated and compared against the Holtrop method.

5 Discussion of the results

A summary of the results obtained in the analysis cases is discussed here.

Some results regarding preliminary analysis of the influence of the number of neurons and whether to include some other inputs such as the semi-angle of entrance and the longitudinal centre of buoyancy are also presented.

Then the form factor is estimated, and the results are shown in section 5.2. This estimation has been obtained by two different methods, directly predicting the form factor or estimating first the viscous resistance and then applying the theory to obtain the corresponding form factor.

Finally, the wave making resistance is estimated directly using the developed ANNs and the total resistance is obtained.

5.1 Preliminary analyses

5.1.1 Analysis of the number of hidden neurons

A sensitivity analysis has been done to select the proper number of neurons in the hidden layer. The form factor and the wave making resistance have been calculated for several configurations. The statistical performance for several number of neurons is given in Table 5.1.

Table 5.1. Sensitivity analysis: number of hidden neurons.

Form Factor			**Wave Resistance**		
no. h.n.	R corr.	rms	no. h.n.	R corr.	rms
5	0.611	0.096	10	0.954	54.70
10	0.742	0.063	20	0.971	43.16
15	0.737	0.085	30	0.975	44.41
20	0.743	0.072	40	0.977	37.78

The performance slightly increases with the number of neurons in the hidden layer. On the other hand, it is important to keep a proper number to avoid undesirable behaviours. It has been observed that when the number is high, the ANN present overfitting and then being sensitive to changes in the inputs. For example, a small change in the ship length could lead to large variations of the resistance.

The final number of hidden neurons used to develop the ANNs are:

- 10 neurons for the direct estimation of the form factor.
- 15 neurons to predict the viscous resistance.
- 20 neurons to estimate the wave making resistance.

5.1.2 Including α and lcb as inputs

Marón and Santos (2017) developed a good first approximation of what parameters are of importance for the estimation of the form factor and the wave making resistance. In that article the inputs for the ANN were the ones presented in section 4.2.2 but including the semi-angle of entrance, α.

In addition, the influence of the longitudinal centre of buoyancy, lcb, in the ANN performance has been analysed.

A sensitivity analysis has been done including these inputs for training the ANN. A disadvantage is that some cases included in the data base do not include the semi-angle of entrance, and therefore, the number of available samples is reduced.

Table 5.2 presents a summary of the statistics of the performance of each ANN analysed in this sensitivity analysis. The number of hidden neurons considered is as defined in section 4.2.3.

Table 5.2. Sensitivity analysis: influence of α and lcb.

Case	Form Factor		Viscous Resistance			Wave Resistance		
	no. pts.	rms	no. pts.	R corr.	rms	no. pts.	R corr.	rms
Cargo ships	749	0.125	27684	0.9992	17.3	27684	0.9645	49.08
Cargo + alfa	545	0.119	19516	0.9989	15.7	19516	0.9646	35.19
Cargo + lcb	749	0.117	27684	0.9993	16.9	27684	0.9759	42.09
Cargo + alfa + lcb	545	0.120	19516	0.9992	13.4	19516	0.9659	36.06

The statistical results show that the ANN performance when including α and/or lcb does not improves significantly.

The longitudinal centre of gravity is a hull shape parameter that depends on the type of ship. Baquero (2011) explains the influence of lcb in the ship resistance of mono-hull vessels. Usually slow ships (full ships) with a large viscous resistance have a positive lcb (forward of midsection). Fast ships have a negative value and the wave making resistance component is more important.

Other parameters that are already included in the data base, such as the shape coefficients, depend on the type of ship in a similar way. It can be considered that the lcb is implicitly defined by this already considered parameters. This could be the reason why when including lcb as an input there is not a performance improvement.

Baquero (2011) also defines the semi-angle of entrance as an influent parameter on the ship resistance. There is a slightly better improvement when considering α.

Anyway, when developing the ship resistance estimation tool (rann) it has been decided not to include α nor lcb.

The semi-angle of entrance has been discarded with the objective to have only one ANN for each type of ship defined in section 4.1.6. With this decision the problem to have large differences for one ship when using one or the other ANN data base is solved.

5.2 Form factor estimation

The estimation of the form factor using ANN have been done applying two different methods.

These methods are described in section 4.2.1 and the obtained results are presented in this chapter. In Appendix C several relative error histograms of both methods considered to estimate the form factor are shown.

5.2.1 Direct estimation of the form factor

The form factor is directly estimated applying an ANN. The inputs considered to train this ANN are defined in section 4.2.2.1.

This method has an important disadvantage. As the form factor does not depend on the ship speed, but only on the hull shape, the number of data available for the network training is small.

Therefore, it is not applicable for some cases due to the reduced number of data, and the direct estimation of the form factor has been applied only for the data bases of all ships, cargo vessels and warships.

Table 5.3 presents a summary of the performance of the ANN when estimating directly the form factor.

Table 5.3. ANN performance. Direct estimation of the form factor.

Case	Form Factor	
	no. pts.	rms
All ships	973	0.144
Cargo ships	749	0.129
Warships	120	0.131

5.2.2 Estimation of the viscous resistance

With this second method, the form factor is obtained indirectly by applying ANN for the prediction of the viscous resistance. This component of the resistance depends on the ship speed and therefore the number of data is much higher.

The inputs considered to estimate the viscous resistance are defined in section 4.2.2.2.

Once the viscous resistance is estimated, the form factor can be obtained as (see section 2.2):

$$r = \frac{R_V}{R_F} \qquad (34)$$

Where R_F is defined by the ITTC frictional line (4).

The main disadvantage of this method is that the definition of the form factor is theoretical, and the reality is that it is not constant with ship speed (Baquero, 2011).

Therefore, when applying (34), the resulting form factor depends on F_n. For this reason, the form factor is estimated for moderate ship speeds, when the F_n is between 0.1 and 0.2 (Baquero, 2011). The resulting form factor would be the average value.

Finally, to follow the proposed theoretical decomposition of the ship resistance (see section 2), the viscous resistance must be re-calculated with the estimated value of the form factor.

Table 5.4 shows a summary of statistics of the performance of the ANN when estimating the form factor applying the ANN to obtain the viscous resistance. There are not significant differences between these results and the ones obtained by direct estimation (Table 5.3).

Table 5.4. ANN performance. Estimation of the form factor from R_V.

Case	Form Factor	
	no. pts.	rms
All ships	973	0.181
Cargo ships	749	0.125
Warships	120	0.215
Fishing vessels	57	0.098
Small crafts	38	0.353

This second way to estimate the form factor has been selected to be implemented in the ANN tool (see section 6.3). Table 5.5 shows a comparison of the root mean square error of this developed ANN and the Holtrop method. This performance comparison is presented graphically in Figure 5.1.

Results show a better general performance with significant reductions, especially in the data bases for cargo ships and in the fishing vessels. It is also noticeable that the small crafts characteristics are out of the applicability range of the Holtrop method.

Table 5.5. Root mean squared error. Form factor estimation. rann vs Holtrop.

Case	**Form Factor**	
	rann	Holtrop
All ships	0.181	0.192
Cargo ships	0.125	0.158
Warships	0.215	0.218
Fishing vessels	0.098	0.192
Small crafts	0.353	0.743

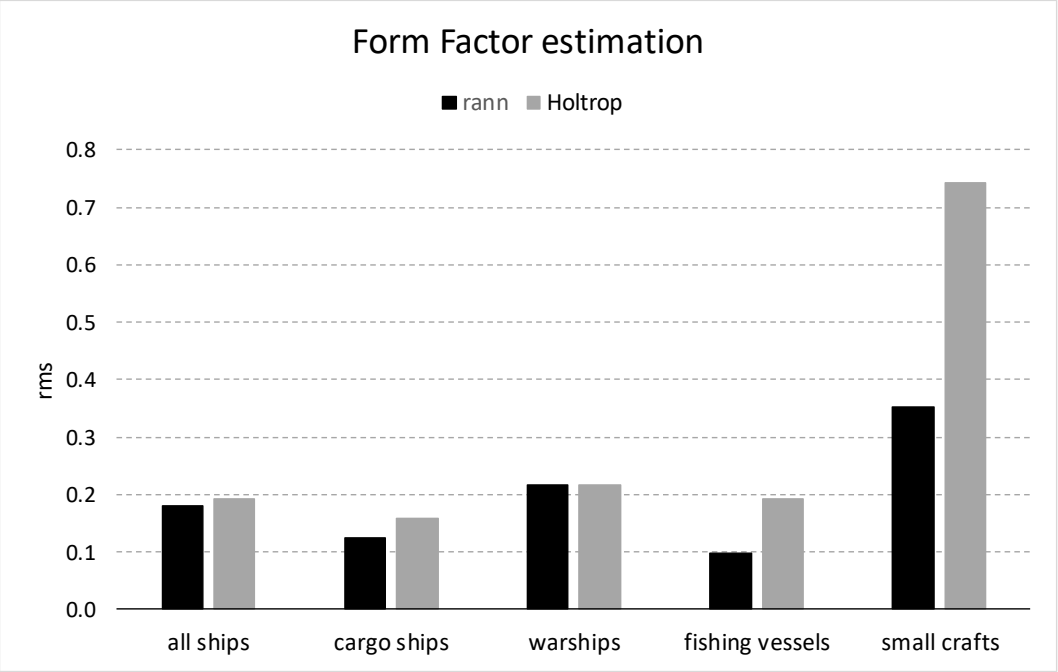

Figure 5.1. Root mean squared error. rann vs Holtrop. Form factor estimation.

In Appendix C the error histograms for the estimation of the form factor from the viscous resistance are presented. In these histograms it can be seen a slightly improvement in the performance of the tool against Holtrop method.

5.3 Wave resistance estimation

The wave resistance is directly estimated applying the developed ANN. The inputs considered for this component are the same as the ones used to estimate the viscous resistance and are defined in 4.2.2.2.

In Table 5.6 a summary of the performance of the ANN is presented for the estimation of the wave resistance component.

Table 5.6. ANN performance. Wave resistance estimation.

Case	Wave Resistance		
	no. pts.	R corr.	rms
All ships	39416	0.981	41.95
Cargo ships	27684	0.964	49.08
Warships	7322	0.999	17.21
Fishing vessels	2464	0.998	4.33
Small crafts	1946	0.985	71.37

Table 5.7 shows a comparison of the rms error of the ANN and the Holtrop method. The results show a reduction of the rms for all type of ships. It is also noticeable that the small crafts characteristics are out of the applicability range of the Holtrop method.

Table 5.7. Root mean squared error. Wave resistance estimation. rann vs Holtrop.

Case	Wave Resistance	
	rann	Holtrop
All ships	41.95	99.89
Cargo ships	49.08	108.87
Warships	17.21	141.61
Fishing vessels	4.33	28.23
Small crafts	71.37	1188.68

In Appendix D the error histograms for the estimation of the wave resistance for every ship type are shown.

The improvement of the performance against Holtrop method when estimating the wave resistance is important. The error histograms of the ANN prediction are centred around error 0% and presents a thinner band.

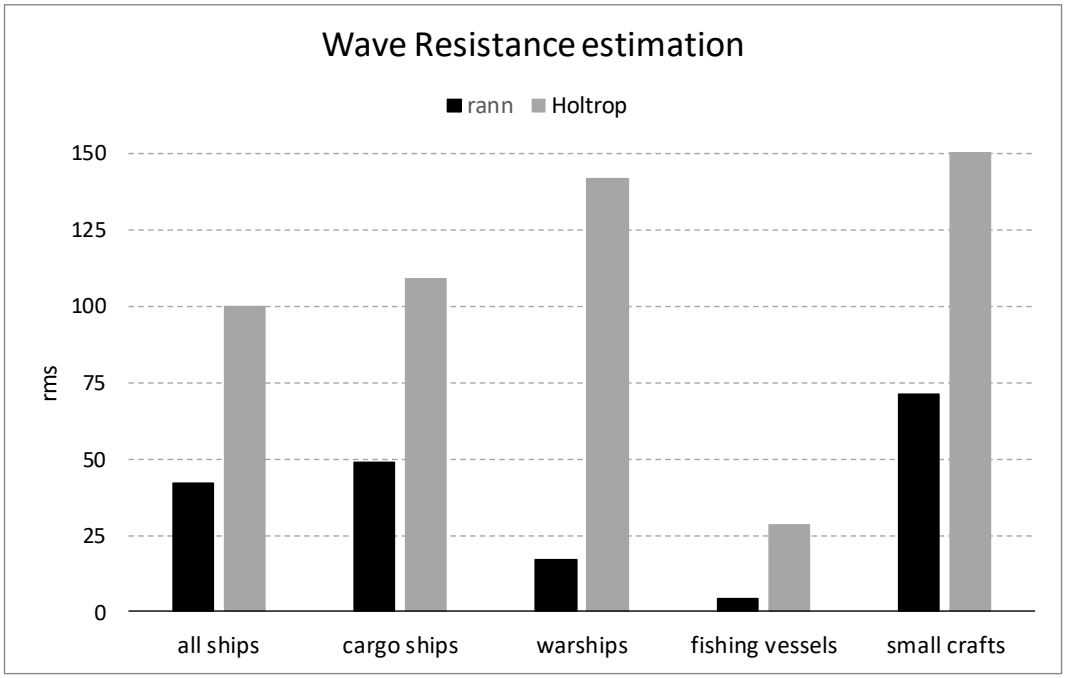

Figure 5.2. Root mean squared error. rann vs Holtrop. Wave resistance estimation.

5.4 Total resistance estimation

Table 5.8 shows a comparison of the rms error of the ANN and the Holtrop method. For this component the results also show a reduction of the rms for all type of ships.

In appendix E the histograms showing the relative error for both methods are presented.

Table 5.8. Root mean squared error. Total resistance estimation. rann vs Holtrop.

Case	**Total Resistance**	
	rann	Holtrop
All ships	43.22	104.61
Cargo ships	44.72	93.60
Warships	26.34	157.50
Fishing vessels	4.39	26.57
Small crafts	93.26	1418.50

6 Tool for ship resistance estimation

In this section an overview of the computational tool developed for ship resistance estimation is presented. This tool is called “rann” and it is written in MATLAB language.

Figure 6.1 shows a flow diagram of the process followed to estimate the ship resistance for a given hull shape and physical parameters. The following steps are followed:

- The user is asked to introduce the binary file containing the ship data. In addition, a pop-up menu, like the one shown in Figure 4.10, asks the user to select the type of ship ANN data base to be used.
- Depending on the user selection, the corresponding ANN data base is loaded, containing the networks architecture and neuron weights.
- The different components of the ship resistance are estimated, and the total resistance is calculated.

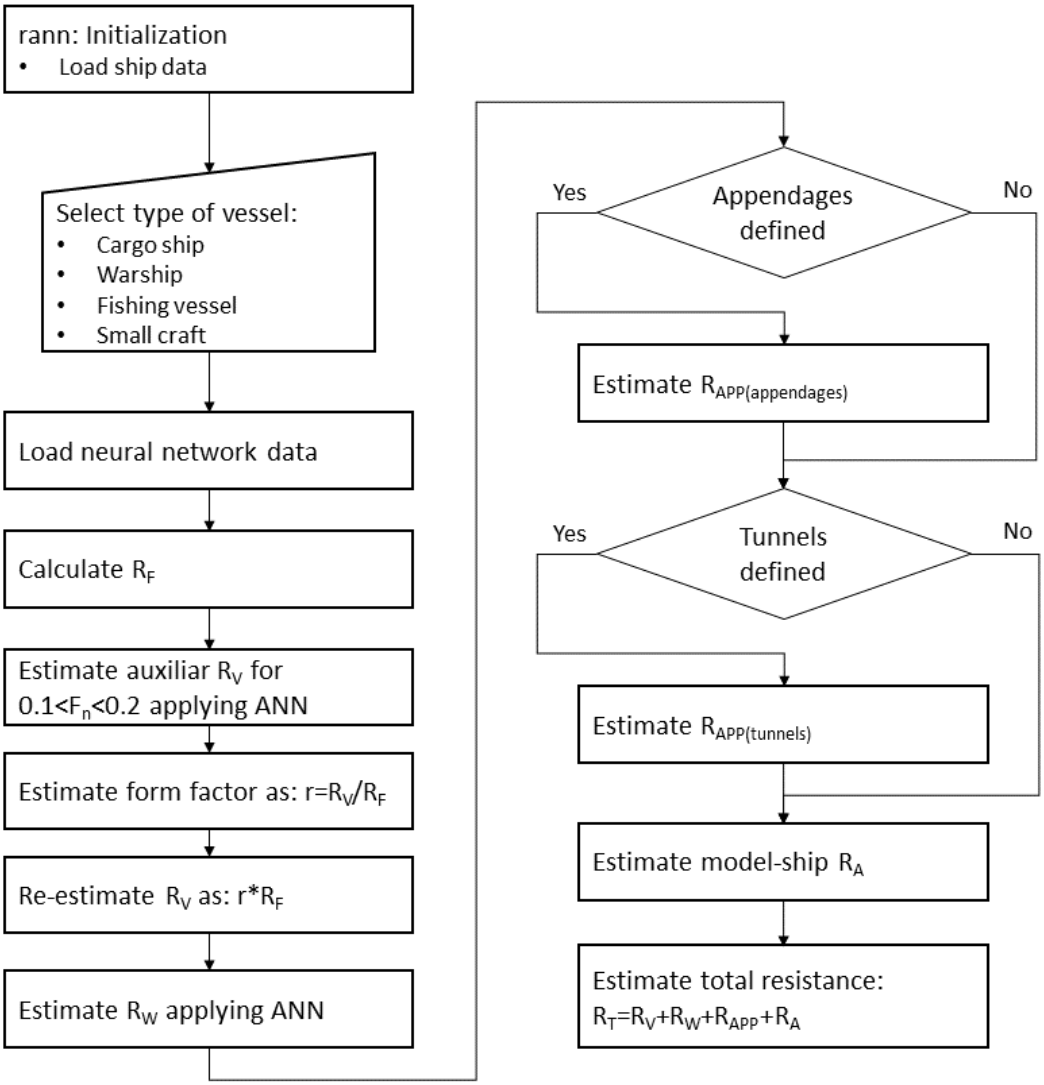

Figure 6.1. rann flow diagram.

6.1 Tool input and output data

6.1.1 rann input data

The following input data is to be defined to run the program:

- rho_sw: sea water density (t/m^3).
- visc_sw: sea water kinematic viscosity (m^2/s).
- vel: array of ship speeds (m/s).
- ship_data: array containing ship characteristics.
    1. L_{wl}: waterline length (m).
    2. B: beam (m).
    3. T: mean draft (m).
    4. S_w: wetted surface (m^2).
    5. C_B: block coefficient (-).
    6. C_P: prismatic coefficient (-).
    7. C_M: midship section coefficient (-).
    8. C_{WP}: waterplane coefficient (-).
- app_data: matrix containing appendages data (n_app x 2):
    1. appendage area (m_2).
    2. appendage resistance factor (-)
- tunnel_data: matrix containing tunnel thrusters data (n_tunn x 2):
    1. tunnel diameter (m).
    2. tunnel resistance coefficient (-).
- ks: average full-scale hull rugosity (m).

The matrices “app_data” and “tunnel_data” have several rows depending on the number of appendages/tunnels to be defined, and two columns. These matrices can be empty, in this case the program assume that no appendages nor tunnel thrusters are defined, and the corresponding resistance component is set to zero.

The value of “ks” can be also empty and the program defines the ship-model correlation resistance as zero.

6.1.2 rann output data

The following data compose the output of the program:

- type: ship type of the data base used.
- vel: array of ship speeds (m/s).
- r: estimated form factor (-).
- Resistance: estimated ship resistance (kN):
    1. R_F: frictional resistance component defined by the ITTC-57 curve.
    2. R_V: viscous resistance component.
    3. R_W: wave making resistance component.
    4. R_{APP}: appendages and tunnel thrusters resistance component.
    5. R_A: ship-model correlation resistance.
    6. R_T: total ship resistance.

6.2 Types of vessels

The following type of ships can be selected:

- Cargo ships.
- Fishing vessels.
- Warships.
- Small crafts.

In the following tables are given the ranges of application of the different inputs for each data base. These were defined depending on the data bases generated from CEHIPAR data and were used to train the different ANN.

Table 6.1. Ranges of application. Case: cargo ships.

	Cargo ships	
	Min value	Max value
F_n	0.00	0.30
L_{wl}/B	4.0	9.0
B/T	2.0	7.5
C_B	0.55	0.90
C_{WP}	0.65	0.95

Table 6.2. Ranges of application. Case: warships.

	Warships	
	Min value	Max value
F_n	0.00	0.70
L_{wl}/B	3.0	9.0
B/T	2.5	5.0
C_B	0.40	0.70
C_{WP}	0.60	0.95

Table 6.3. Ranges of application. Case: fishing vessels.

	Fishing vessels	
	Min value	Max value
F_n	0.00	0.40
L_{wl}/B	3.5	7.0
B/T	2.2	5.0
C_B	0.45	0.75
C_{WP}	0.70	0.95

Table 6.4. Ranges of application. Case: small crafts.

	Small crafts	
	Min value	Max value
F_n	0.00	1.00
L_{wl}/B	2.0	9.0
B/T	3.0	12.0
C_B	0.30	0.75
C_{WP}	0.40	0.90

6.3 Estimation of ship resistance components

The first step is to calculate Re and the frictional resistance coefficient applying the ITTC-57 frictional line (4). Then R_F is obtained.

The viscous resistance is calculated in the program as defined in section 5.2.2. An auxiliary viscous resistance is estimated applying the ANN for several F_n values between 0.1 and 0.2 (moderate ship speeds). This auxiliary R_V is used to estimate the form factor applying (34) and calculating the average value.

The viscous resistance is then calculated for the user defined ship speeds multiplying r and R_F.

The wave resistance is directly estimated applying the ANN developed for this component (see section 5.3).

The user can specify several appendages of the ship and tunnel thruster's characteristics. These additional resistance components are calculated following Holtrop and Mennen method (1982) described in section 2.5.1.

A model-ship correlation component is included in the code to account for full-scale hull roughness. To this end the ITTC recommended value for this coefficient is used (see section 2.5.2).

6.4 Ship resistance estimation examples

In this section some examples of different ship resistance estimated using "rann" are presented.

First, some comparisons for several ships showing the estimated curve are given. The comparison shows the obtained resistance applying the Holtrop method and the extrapolated curve from the model tests.

Then, the tool is applied to estimate the resistance components for two example ships. These results are shown in section 6.4.2.

6.4.1 Example of resistance results

In Appendix F some figures showing the comparison of some results for several ships selected randomly from the data bases are presented.

It must be noted that Holtrop method was not developed to be applied for the resistance estimation of small crafts or even warships. Some other empirical methods could present a better performance than Holtrop method.

The information regarding the type of data base used and the component of the resistance shown is given in the graph titles. Figure 6.2 is shown as an example.

The legend displays the following information:

- CEHIPAR: results extrapolated from model tests performed in towing tank.
- rann: results estimated with the tool developed.
- Holtrop: results estimated using Holtrop method.

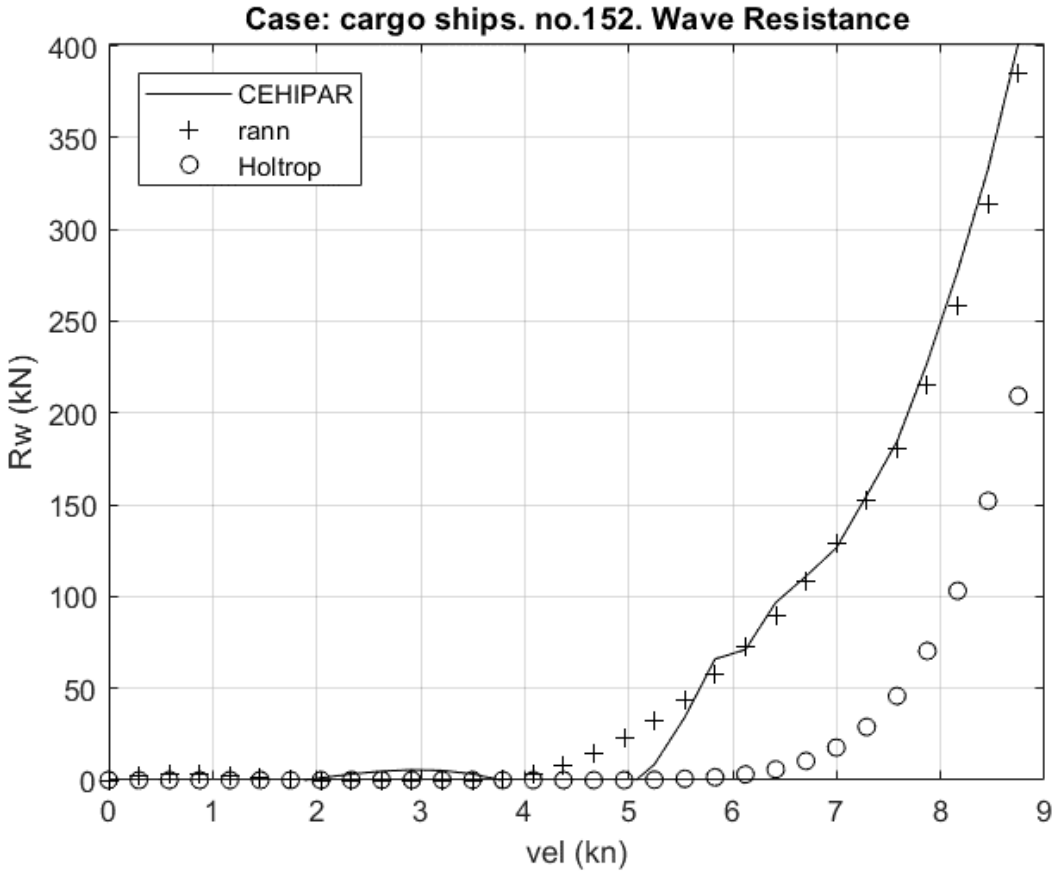

Figure 6.2. Example of resistance estimation.

6.4.2 Example using rann

The estimation of an example ship using "rann" is given in this section. This is a bulkcarrier and therefore it has been used the "cargo ships" data base.

The following input data is used to define the example ship.

- rho_sw: 1.025 t/m^3.
- visc_sw: 1.1 E-06 m^2/s.
- vel: from 0 to 10 m/s.
- ship_data:
  - L_{wl}: 177.2 m.
  - B: 29.0 m.
  - T: 9.75 m.
  - S_w: 7150 m^2.
  - C_B: 0.771.
  - C_P: 0.773.
  - C_M: 0.997.
  - C_{WP}: 0.828.

- app_data: included bilge keels resistance.
  - appendage area: 80 m_2.
  - appendage resistance factor: 1.40.
- tunnel_data:
  - tunnel diameter: 2.5 m.
  - tunnel resistance coefficient: 0.005.
- ks: 1.5 E+04 m.

The results for the example ship are shown in Figure 6.3 and Table 6.5. These results show a typical behaviour of the ship resistance. The viscous resistance and resistance due to rugosity is increasing proportional to ship velocity and shows up at low Froude numbers. On the other hand, the wave resistance starts to be of importance for moderate Froude numbers and increases exponentially. The resistance due to appendages is negligible in this specific case.

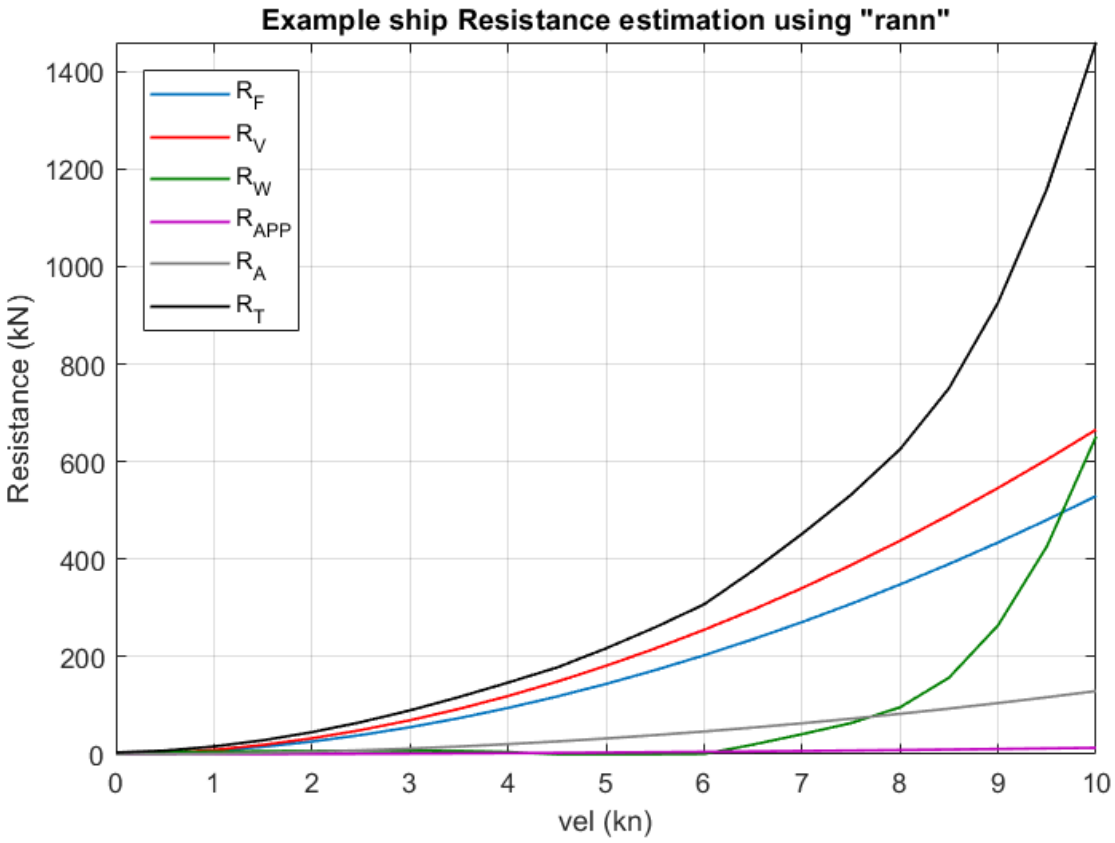

Figure 6.3. Example ship resistance estimation.

Table 6.5. Example ship resistance estimation.

Vel (kn)	R_F (kN)	R_V (kN)	R_W (kN)	R_{APP} (kN)	R_A (kN)	R_T (kN)
0.0	0.0	0.0	0.0	0.0	0.0	3.5
0.5	2.0	2.5	0.1	0.0	0.3	7.4
1.0	7.1	9.0	0.2	0.2	1.3	15.9
1.5	15.2	19.1	0.5	0.3	2.9	28.6
2.0	26.0	32.7	0.9	0.6	5.2	45.3
2.5	39.4	49.5	1.4	0.9	8.1	65.8
3.0	55.4	69.7	2.0	1.3	11.7	89.9
3.5	73.9	92.9	2.7	1.8	15.9	117.3
4.0	94.9	119.3	3.6	2.3	20.7	146.9
4.5	118.3	148.8	4.5	2.8	26.2	177.9
5.0	144.1	181.2	5.6	3.5	32.4	217.1
5.5	172.3	216.7	6.7	4.2	39.2	260.1
6.0	202.9	255.1	8.0	4.9	46.6	307.3
6.5	235.8	296.4	19.7	5.8	54.7	376.6
7.0	270.9	340.7	41.1	6.6	63.5	451.9
7.5	308.4	387.8	63.8	7.6	72.9	532.1
8.0	348.1	437.7	96.2	8.6	82.9	625.4
8.5	390.1	490.5	157.0	9.7	93.6	750.8
9.0	434.3	546.1	264.3	10.8	104.9	926.1
9.5	480.8	604.5	427.0	12.0	116.9	1160.3
10.0	529.4	665.7	651.4	13.2	129.5	1459.8

7 Conclusions and Future work

In this work a computational tool to estimate the different components of mono-hull vessels resistance has been developed. This tool named “rann” (Resistance artificial neural networks) is based on artificial neural networks. It is presented as an alternative to traditional empirical methods based on regression analysis.

It is important to highlight the great advantages of ANN when used to solve the ship resistance problem. These networks are easily retrained with new data from future model tests, they are easy to implement and are able to deal with non-linear problems such as the relationship between the wave resistance and the ship speed.

The ANN has been applied to estimate the main resistance components: the viscous and the wave resistance. The first one has been calculated by means of the form factor.

Other less important components of the resistance have been included in the tool such as the resistance of appendages, tunnel thrusters and the model-ship correlation resistance. These additional components are estimated applying empirical methods defined by Holtrop and Mennen (1982) and the International Towing Tank Conference (Baquero, 2011).

The ANN have been trained using resistance measurements from model test campaigns performed in CEHIPAR. This data base has been pre-processed to obtain full-scale resistance, to add more points regarding the ship speed and to filter the cases per ship type.

Since the behaviour of the hull resistance is different depending on the type of vessel, several networks have been trained for each vessel type considered. The performance of these ANN has been measured by means of the root mean squared error and compared with the Holtrop and Mennen (1978) method, which is one of the most common empirical methods used in the naval architecture.

As the developed tool is intended to be used during the first phases of a ship design, the inputs are simple parameters known in these early stages, such as the beam, draft, or the block coefficient. The output are the different components of the ship resistance obtained as a function of user defined ship speeds.

The results show a good agreement with the data bases. In general, the performance of the developed tool is better than the Holtrop method applied to the same cases defined in the data base. Although, the user must always use it carefully and benchmark the results against other available methods.

The tool “rann" provides a new method to estimate the ship resistance components in early stages of the design. It has been developed for different type of ships:

- Cargo ships
- Warships
- Fishing vessels
- Small crafts.

For other types of ships, such as cruisers or offshore supply vessels, the data base for “cargo ships” may be used.

As future work, it would be interesting to analyse the influence of more hull parameters, such as the bulbous bow or the ship trim. To assess this influence, more preliminary data pre-processing must be done, and more data could be needed.

Another approach would be improving the neural network performance, especially for ranges that are out of the applicable limits, such as low/high ship speeds or very large displacement ships.

Regarding the data base, different “groups of vessels”, or even groups of hull shapes within a group of similar vessels can be applied. For example, filtering a group of ship types per length or number of propellers.

8 References

[1] Aláez Zazurca, J.A. (1972). Resistencia viscosa de buques. Madrid, Spain: Canal de Experiencias Hidrodinámicas del Pardo.

[2] Alvariño, R. Azpíroz, J.J. Meizoso, M. (1997). El Proyecto básico del buque mercante. Madrid, Spain: Fondo Editorial de Ingeniería Naval, Colegio Oficial de Ingenieros Navales.

[3] Baquero, A. (2011). Resistencia al avance del buque mercante. Madrid, Spain: Escuela Técnica Superior de Ingenieros Navales.

[4] Chen, A. & Ye, J. (2009). Research on four-layer back propagation neural network for the computation of ship resistance. In Mechatronics and Automation, 2009. ICMA 2009. International Conference on (pp. 2537-2541). IEEE.

[5] Chen, A. & Ye, J. (2009). Research on the genetic neural network for the computation of ship resistance. In Computational Intelligence and Natural Computing, 2009. CINC'09. International Conference on (Vol. 1, pp. 366-369). IEEE.

[6] Couser, P. Mason, A. Mason, G. Smith, C.R. von Konsky, B. R. (2004). Artificial neural networks for hull resistance prediction.

[7] Froude, W. (1955). Observations and suggestions on the subject of determining by experiment the resistance of ships. The papers of William Froude. London, UK: Royal Institution of Naval Architects, 1810-1879.

[8] Grabowska, K. Szczuko, P. (2015). Ship resistance prediction with artificial neural networks. Signal Processing. The Institute of Electrical and Electronic Engineers.

[9] Hilera González, J.R. Martínez Hernando, V.J. (1995) Redes neuronales artificiales: fundamentos, models y aplicaciones. Madrid, Spain: RA-MA Editorial.

[10] Holtrop, J. Mennen, G.G.J. (1978). A statistical power prediction method. International Shipbulding Progress, 25(290).

[11] Holtrop, J. Mennen, G.G.J. (1982). An approximate prediction method. Maritime Research Institute of Netherlands.

[12] Hou, Y. You, Y. & Liang, X. (2017). Minimum resistance ship hull uncertainty optimization design based on simulation-based design method. Journal of Shanghai Jiaotong University (Science), 22(6), 657-663.

[13] Hudson Beale, M. Hagan, T.M. Demuth, H.B. (2018) Neural Network Toolbox User´s Guide. Matlab R2018a. Massachusetts, USA: The Mathworks, Inc.

[14] INTA-CEHIPAR (2018). http://www.inta.es/opencms/export/sites/default/ICTS-CEHIPAR/es/inicio/

[15] ITTC – Recommended Procedures and Guidelines (2011). Fresh Water and Sea Water Properties. International Towing Tank Conference. 7.5-02-01-03.

[16] ITTC – Recommended Procedures and Guidelines (2014). Example for Uncertainty Analysis of Resistance Test in Toking Tanks. International Towing Tank Conference. 7.5-02-02-02.

[17] Larsson L., Hoyte, R. (2010). Principles of Naval Architecture: Ship Resistance and Flow. The Society of Naval Architects and Marine Engineers.

[18] Margari, V. Kanellopoulou, A. & Zaraphonitis, G. (2018). On the use of Artificial Neural Networks for the calm water resistance prediction of MARAD Systematic Series' hullforms. Ocean Engineering, 165, 528-537

[19] Marón, D. Santos, M. (2017). Aplicación de las redes neuronales para la estimación de la resistencia al avance en buques. Actas de las XXXVIII Jornadas de Automática, 393-400.

[20] Mathworks. MATLAB. (2018). https://es.mathworks.com/

[21] Mason, A. Couser, P. Mason, G. Smith, C. von Konsky, B. (2005). Optimisation of Vessel Resistance using Genetic Algorithms and Artificial Neural Networks.

[22] Molland, A. F. Turnock, S. R. Hudson, D. A. (2011). Ship resistance and propulsion: practical estimation of ship propulsive power. New York, USA: Cambridge University Press.

[23] Ortigosa, I., López, R. García, J. (2009). Prediction of total resistance coefficients using neural networks. Journal of Maritime Research, 6(3), 15-26.

[24] Prpić-Oršić, J. Faltinsen, O. M. (2012). Estimation of ship speed loss and associated CO2 emissions in a seaway. Ocean Engineering, 44, 1-10.

[25] Prohaska, C.W. (1966). A simple method for the evaluation of the form factor and the low speed wave resistance. Proceedings of 11th International Towing Tank Conference, 1966, 65-66.

[26] Radojcic, D. Zgradic, A. Kalajdzic, M. & Simic, A. (2014). Resistance Prediction for Hard Chine Hulls in the Pre-Planing Regime. Polish Maritime Research, 21(2), 9-26.

[27] Sasajima, H. Tanaka, I. (1963). Form effects on viscous resistance and their estimation for full ships. Proceedings of 10th International Towing Tank Conference, 1963, 122.

[28] Schmidhuber, J. (2015). Deep learning in neural networks: An overview. Neural Networks 61, 85-117.

[29] Shiffman, D. (2018). The nature of code. Chapter 10. Neural networks. Downloaded from: https://natureofcode.com/book/chapter-10-neural-networks/

[30] Souto Iglesias, A. (2001). Nuevas herramientas de diseño de formas de buques basadas en códigos de flujo potencial. Doctoral Dissertation. Madrid, Spain: Escuela Técnica Superior de Ingenieros Navales.

[31] International Maritime Organization. www.imo.org

[32] European Comission. (2012). Concerted EU action reduces air pollution from shipping in European coastlines and ports. Brussels, Belgium. Downloaded from: https://ec.europa.eu/info/news/concerted-eu-action-reduces-air-pollution-shipping-european-coastlines-and-ports-2018-apr-12_en

9 Appendix A. An introduction to types of vessels

In this appendix a brief overview of the most typical type of vessels is given.

Bulkcarrier

These are merchant ships specially designed to transport bulk cargo such as grain, coal, ore and cement in cargo holds. They are characterized by being large and full shape vessels (Figure 9.1).

Figure 9.1. Bulkcarrier. Star Polaris.

Container Vessel

They are merchant vessels designed to transport cargo in intermodal containers. Container ship capacity is measured in twenty-foot equivalent units (TEU) (Figure 9.2).

Figure 9.2. Container ship. Edith Maersk.

Tanker

These types of ships are vessels designed to transport and store liquids or gases in bulk. There are several types such as oil tankers, chemical tankers and gas tankers. They are characterized by being large and full shape vessels (Figure 9.3).

Figure 9.3. Crude Oil Tanker. Seamaster.

General Cargo

These types of ships are vessels that carry any cargo, goods or materials from one port to another. They are often equipped with cranes and other mechanisms to load/unload (Figure 9.4).

Figure 9.4.General Cargo vessel. White Miyabi.

RORO

These are ships designed to carry wheeled cargo, such as cars, trucks, semi-trailer trucks, trailers and railroad cars, that are driven on and off the vessel on their own wheels or using a platform vehicle. RORO ships have either built-in or shore-based ramps that allow cargo to be rolled on and off the vessel when in port (Figure 9.5).

Figure 9.5.RORO vessel. Talisman.

Offshore supply vessel

These are vessels specially designed to supply offshore industry. Their functions are logistic support, installations and transportation of goods, tool, equipment and crew to and from oil platforms (Figure 9.6).

Figure 9.6. Offshore Supply vessel. Fortitude.

Warship

They are naval vessels built and intended for naval warfare. They are armed and designed to withstand damage and are in general faster and more manoeuvrable than merchant ships (Figure 9.7).

Figure 9.7. Warship: F-105 Cristobal Colón. Spanish Navy.

Fishing vessel

These ships are used to catch fish at open sea, near shore, lakes or rivers (Figure 9.8).

Figure 9.8. Fishing vessel. Trawler. SCH 22.

Small Craft ship

In this type of ships all small vessels such as yachts have been included (Figure 9.9).

Figure 9.9. Small Craft.

10 Appendix B. Script parse_database flow diagram

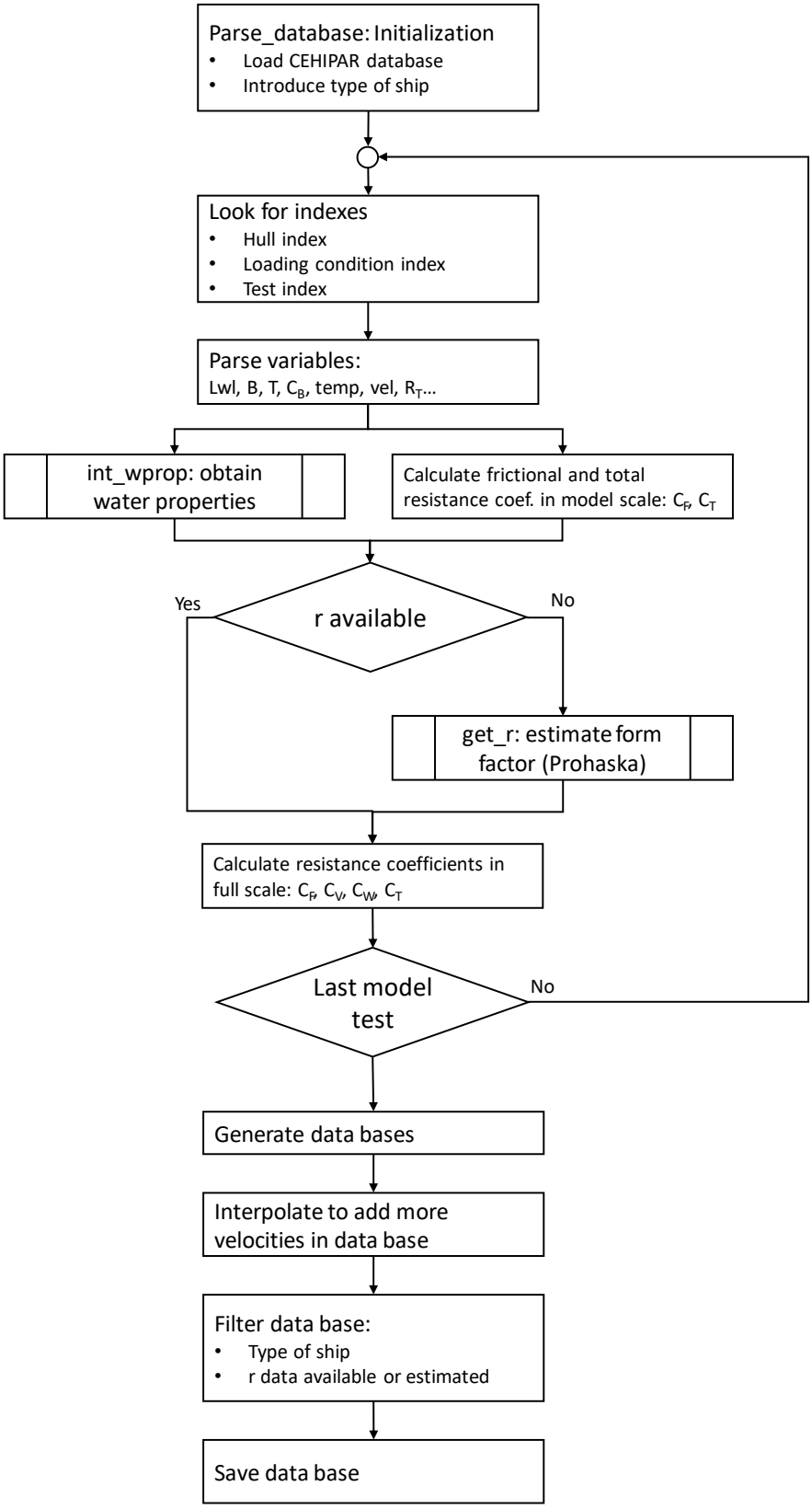

Figure 10.1. Script parse_database flow diagram.

11 Appendix C. Form Factor estimation. Error histograms.

Direct estimation of the form factor

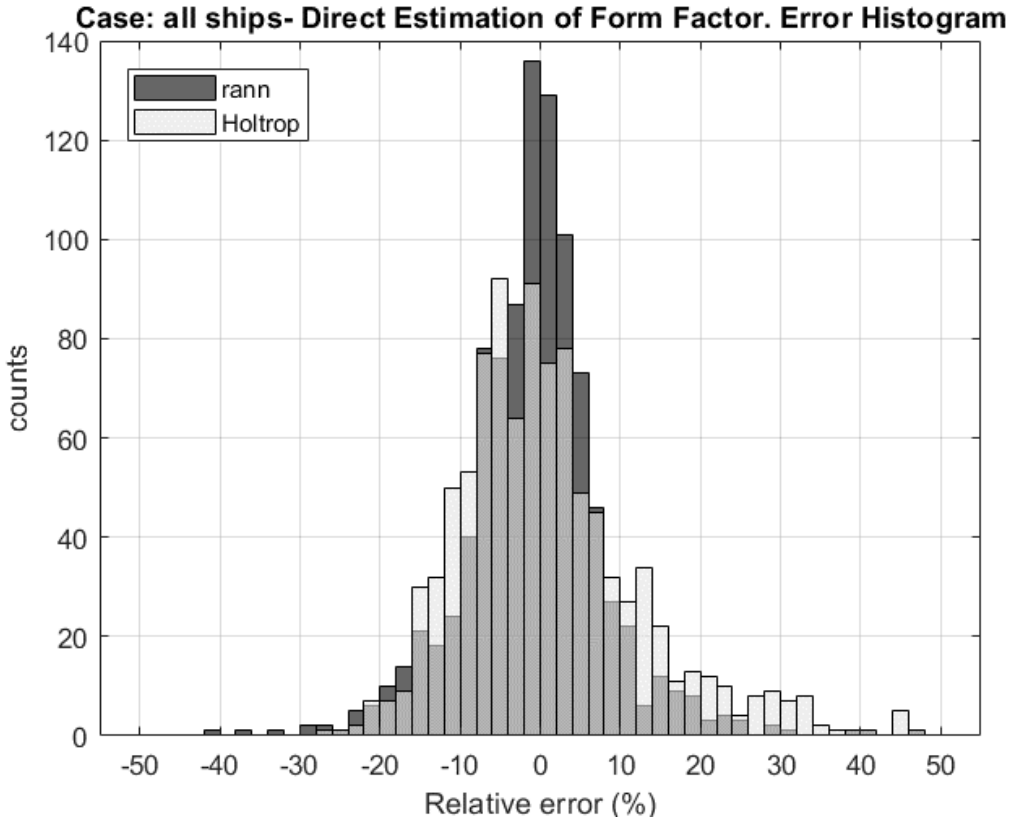

Figure 11.1. Case: all ships. Error histogram. Direct estimation of the form factor.

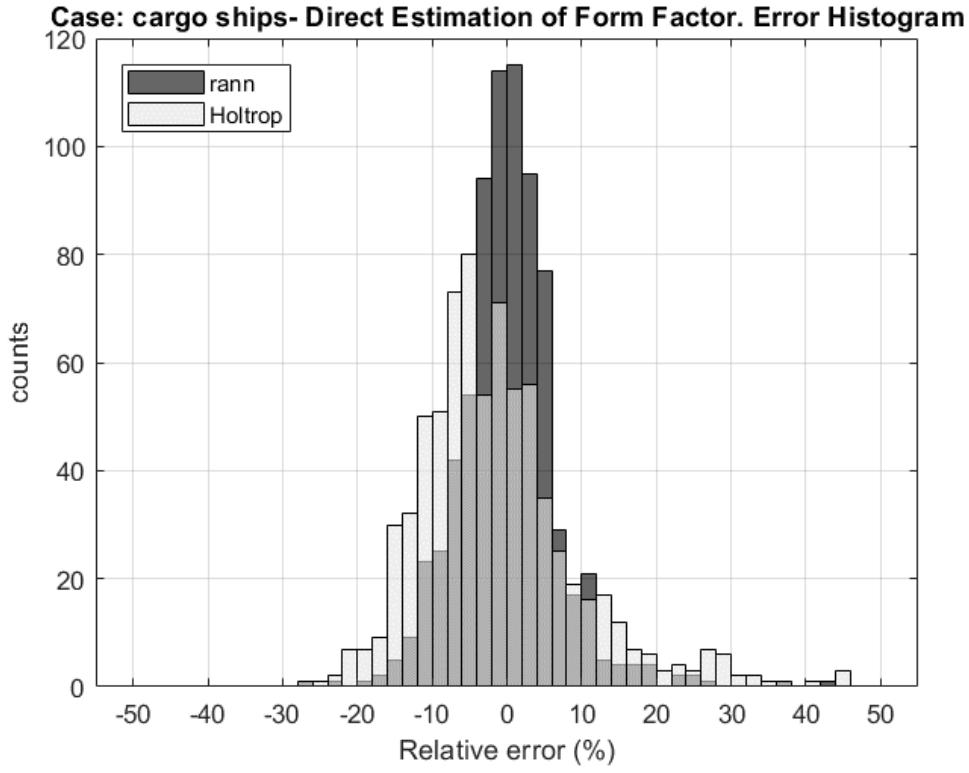

Figure 11.2. Case: cargo ships. Error histogram. Direct estimation of the form factor.

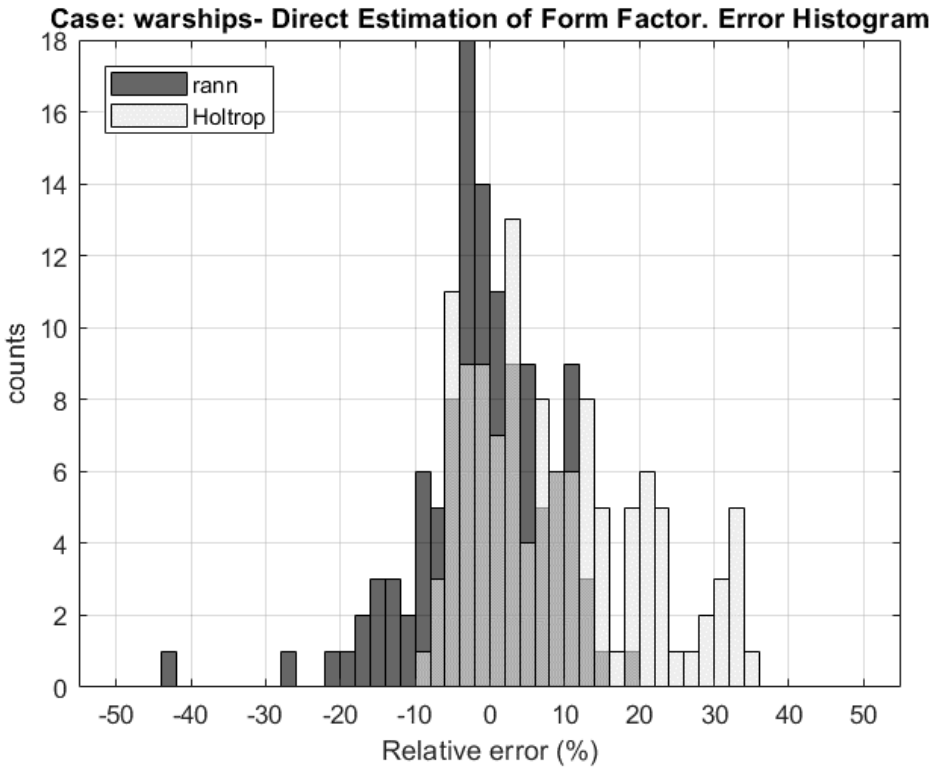

Figure 11.3. Case: warships. Error histogram. Direct estimation of the form factor.

Estimation of the form factor from the viscous resistance

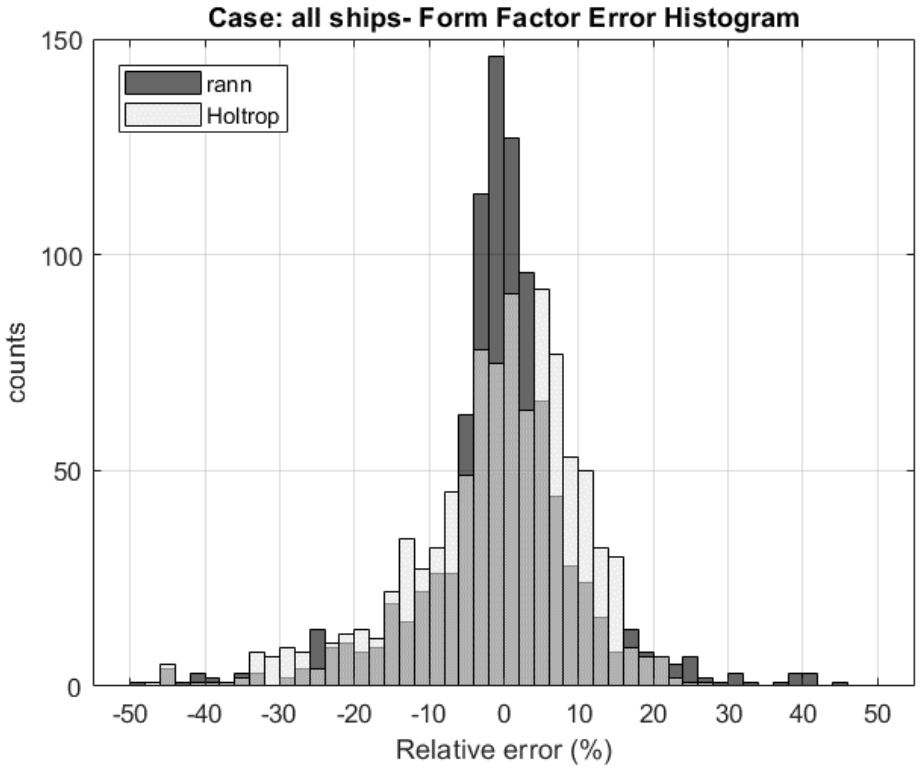

Figure 11.4. Case: all ships. Error histogram. Estimation of the form factor from R_V.

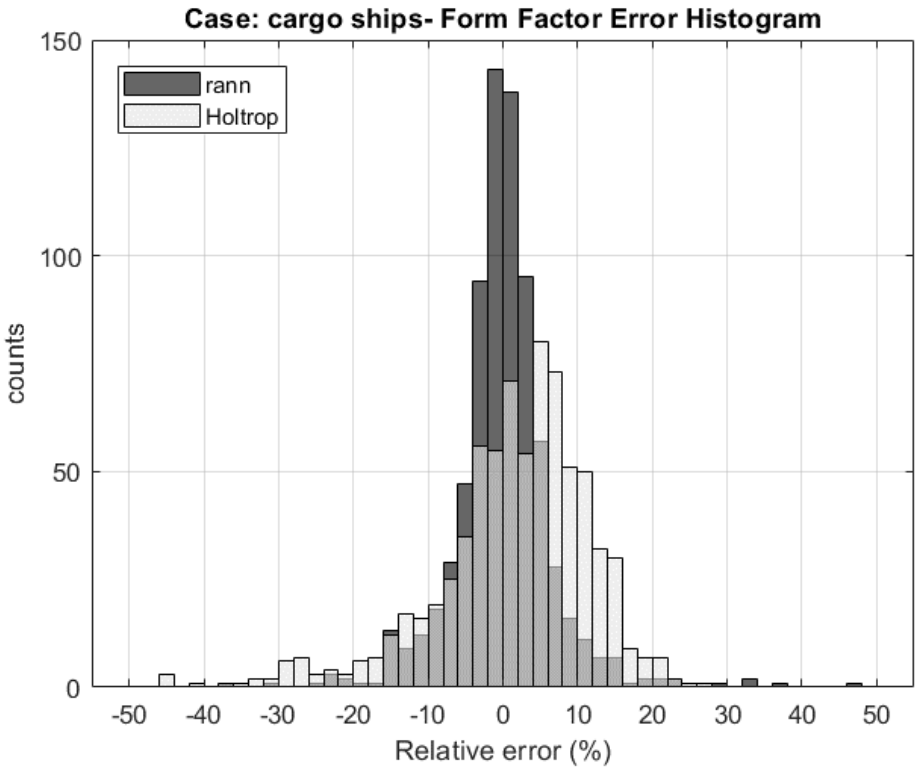

Figure 11.5. Case: cargo ships. Error histogram. Estimation of the form factor from R_V.

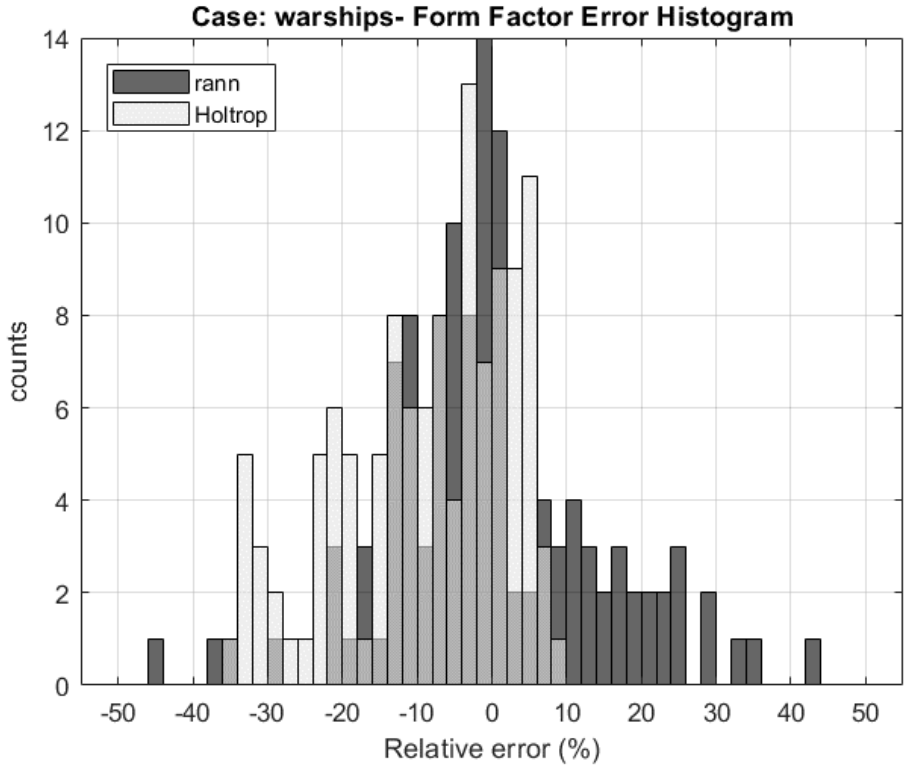

Figure 11.6. Case: warships. Error histogram. Estimation of the form factor from R_V.

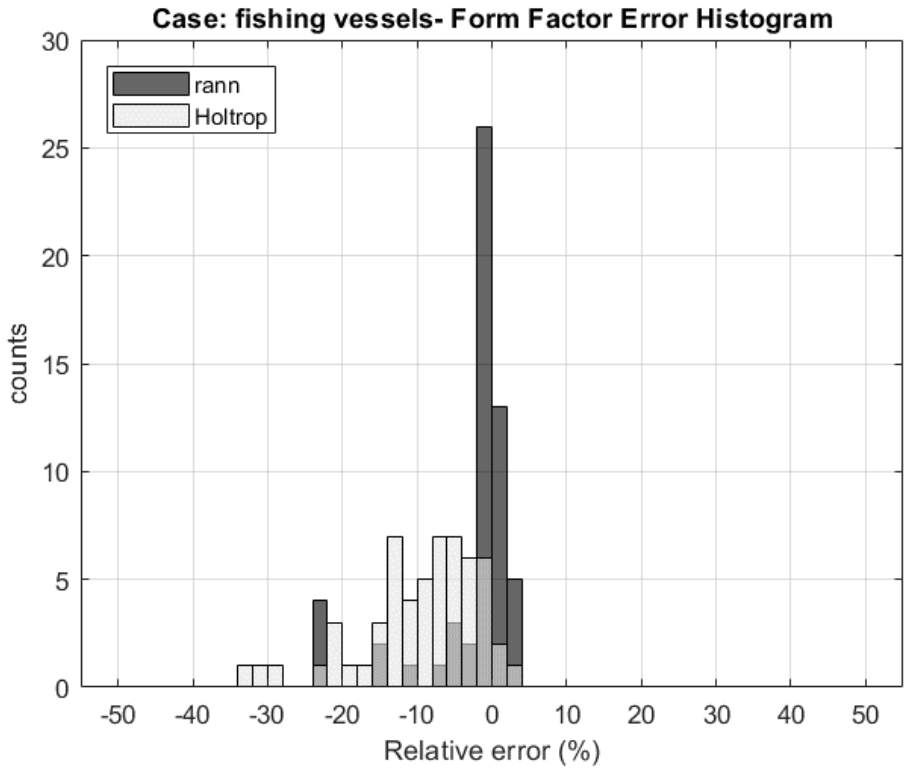

Figure 11.7. Case: fishing vessels. Error histogram. Estimation of the form factor from R_V.

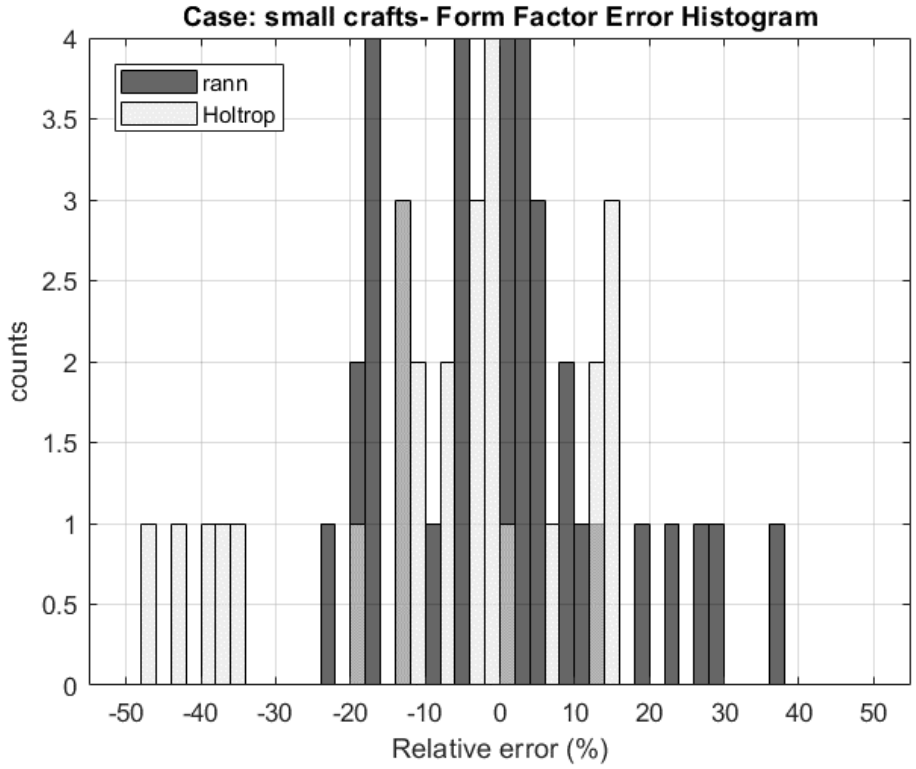

Figure 11.8. Case: small crafts. Error histogram. Estimation of the form factor from R_V.

12 Appendix D. Wave resistance estimation. Error histograms.

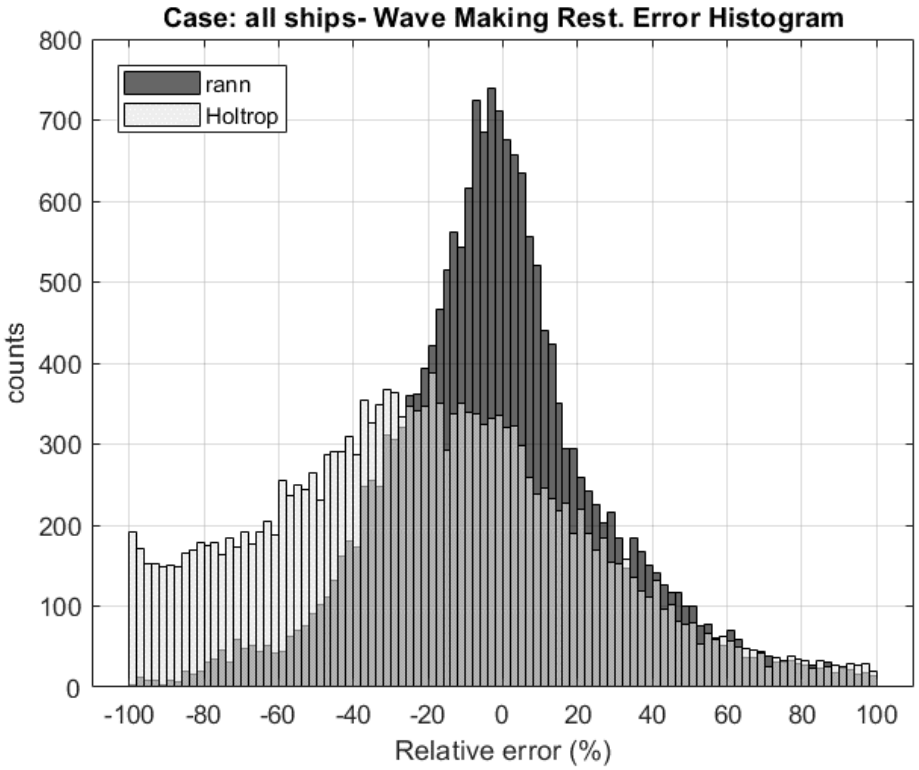

Figure 12.1. Case: all ships. Error histogram. Estimation of the wave resistance.

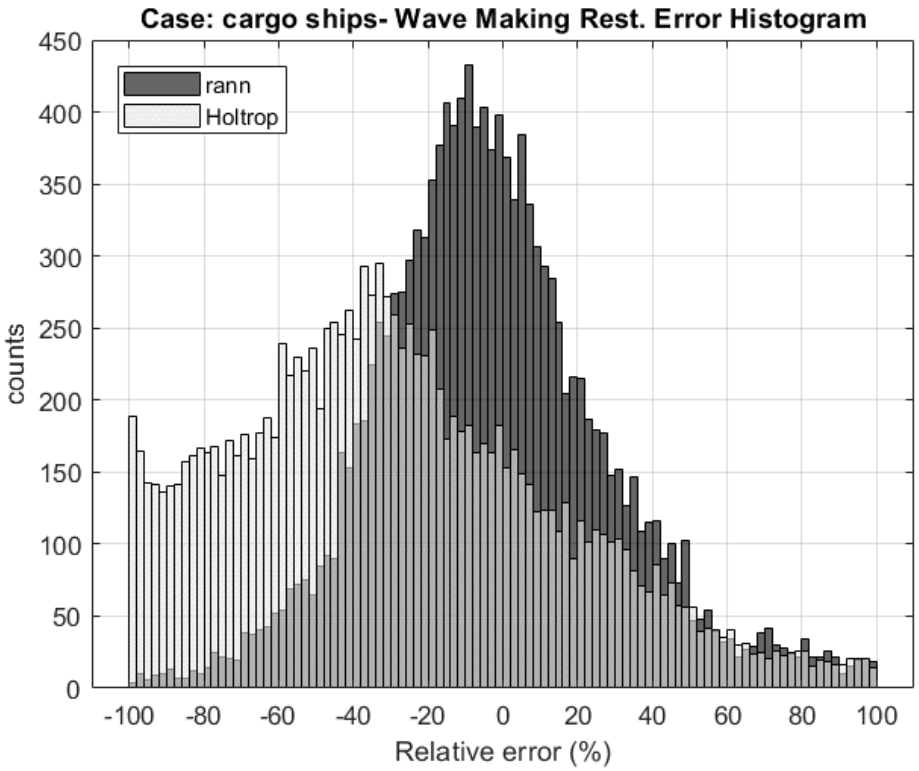

Figure 12.2. Case: cargo ships. Error histogram. Estimation of the wave resistance.

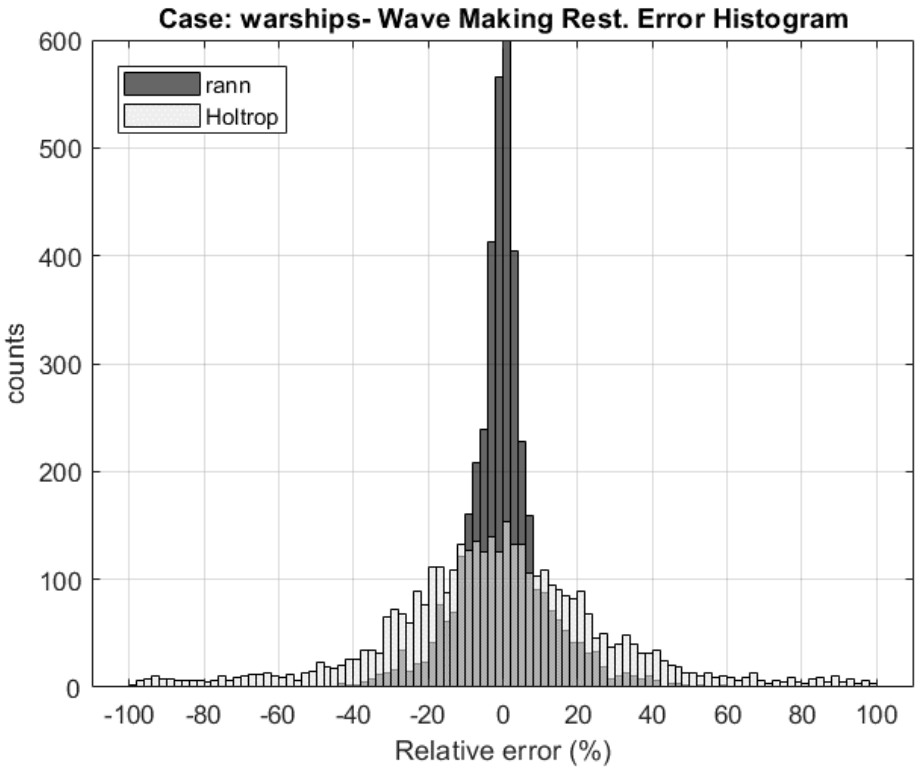

Figure 12.3. Case: warships. Error histogram. Estimation of the wave resistance.

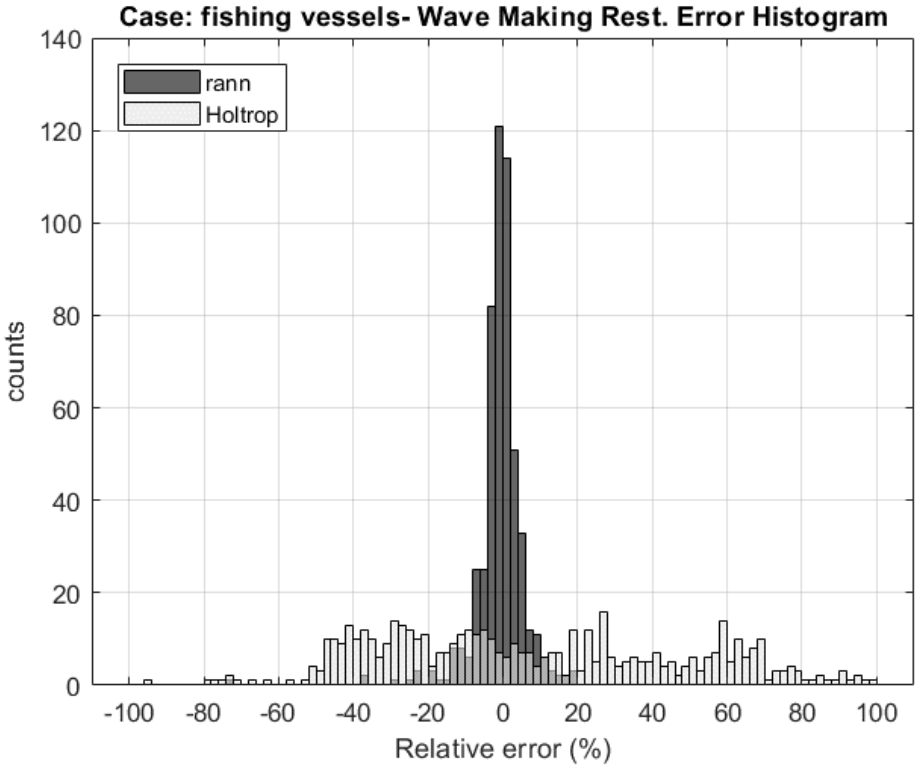

Figure 12.4. Case: fishing vessels. Error histogram. Estimation of the wave resistance.

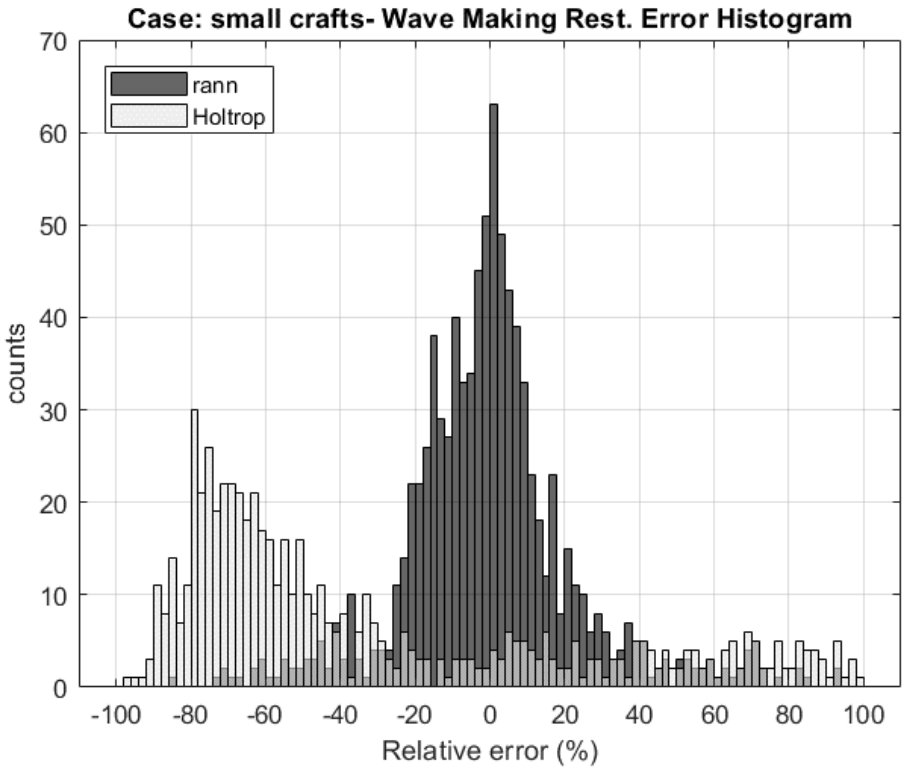

Figure 12.5. Case: small crafts. Error histogram. Estimation of the wave resistance.

13 Appendix E. Total resistance estimation. Error histograms.

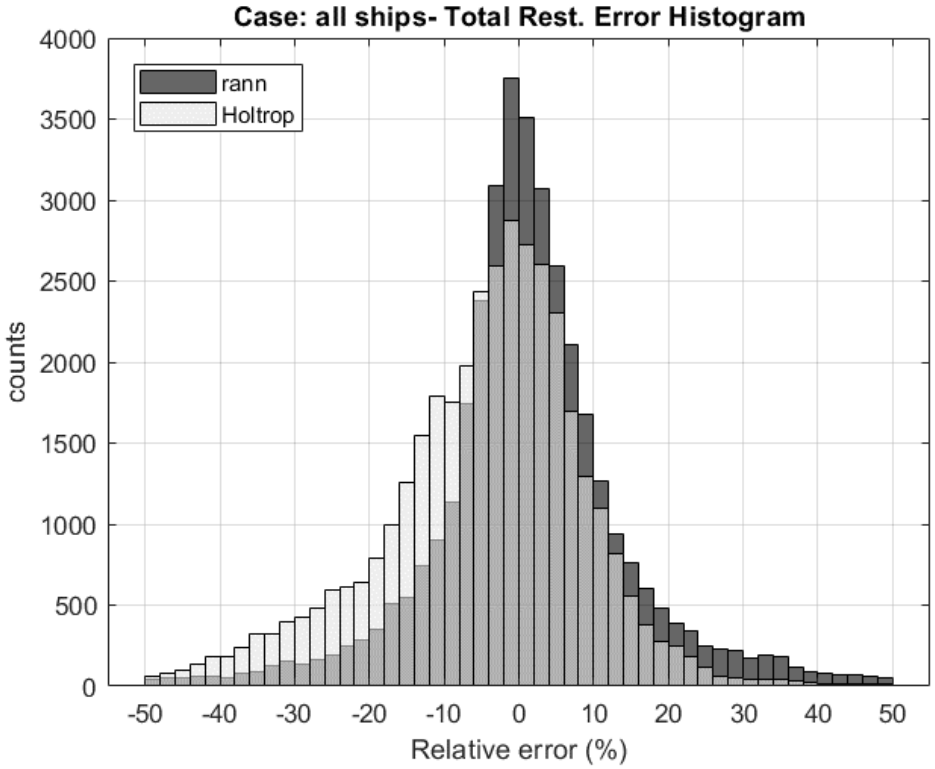

Figure 13.1. Case: all ships. Error histogram. Estimation of the total resistance.

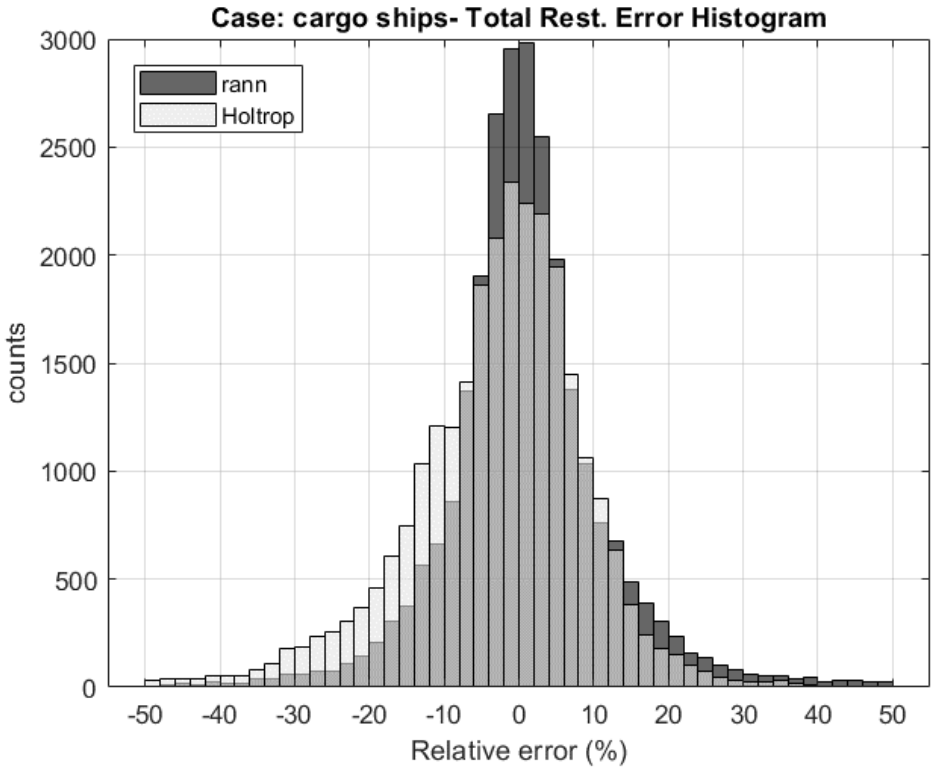

Figure 13.2. Case: cargo ships. Error histogram. Estimation of the total resistance.

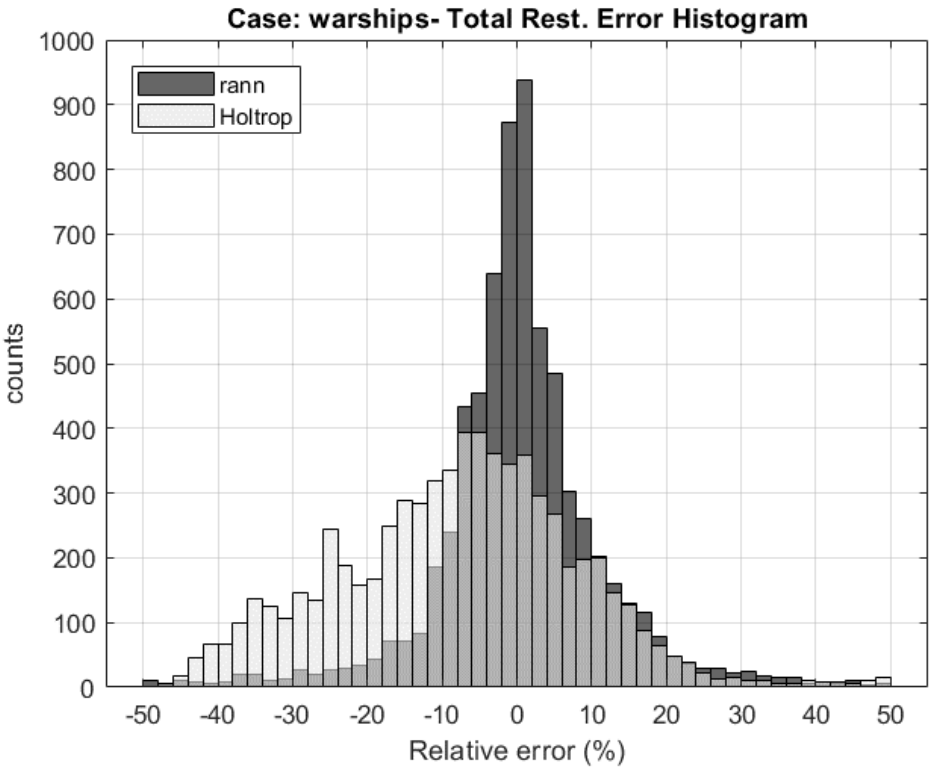

Figure 13.3. Case: warships. Error histogram. Estimation of the total resistance.

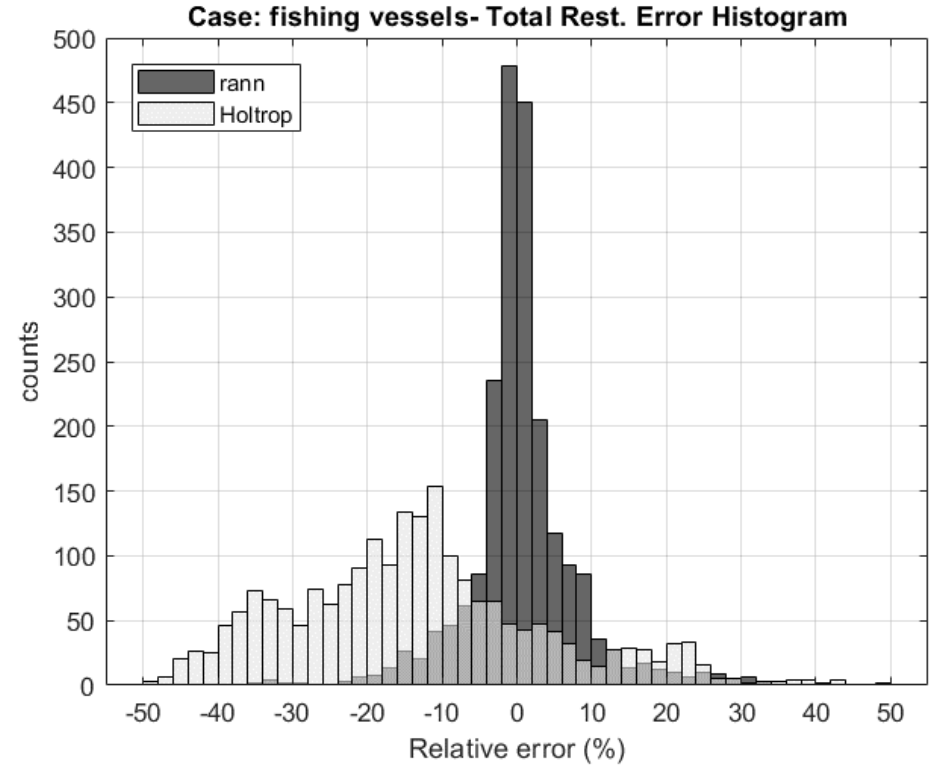

Figure 13.4. Case: fishing vessels. Error histogram. Estimation of the total resistance.

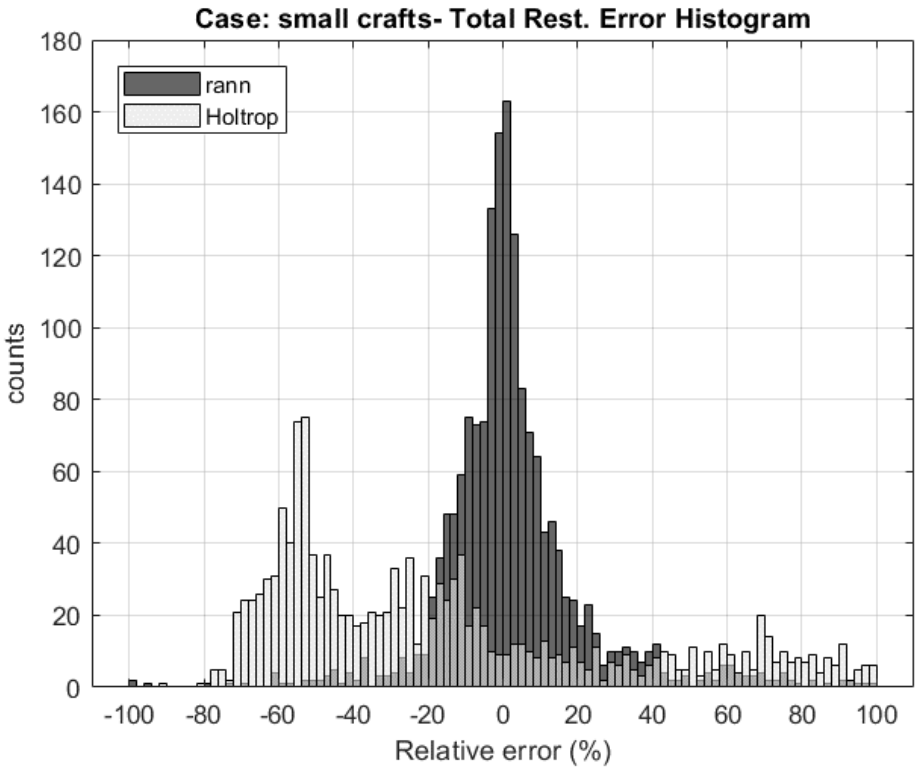

Figure 13.5. Case: small crafts. Error histogram. Estimation of the total resistance.

14 Appendix F. Examples of resistance estimation

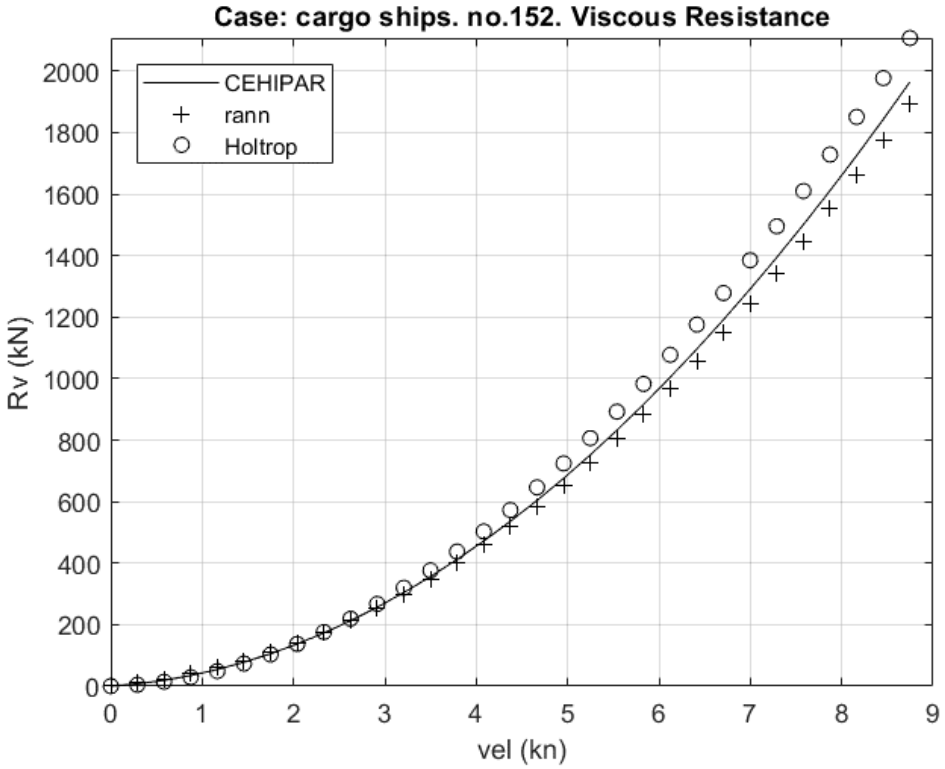

Figure 14.1. Cargo ships data base. Viscous resistance. Case no. 152.

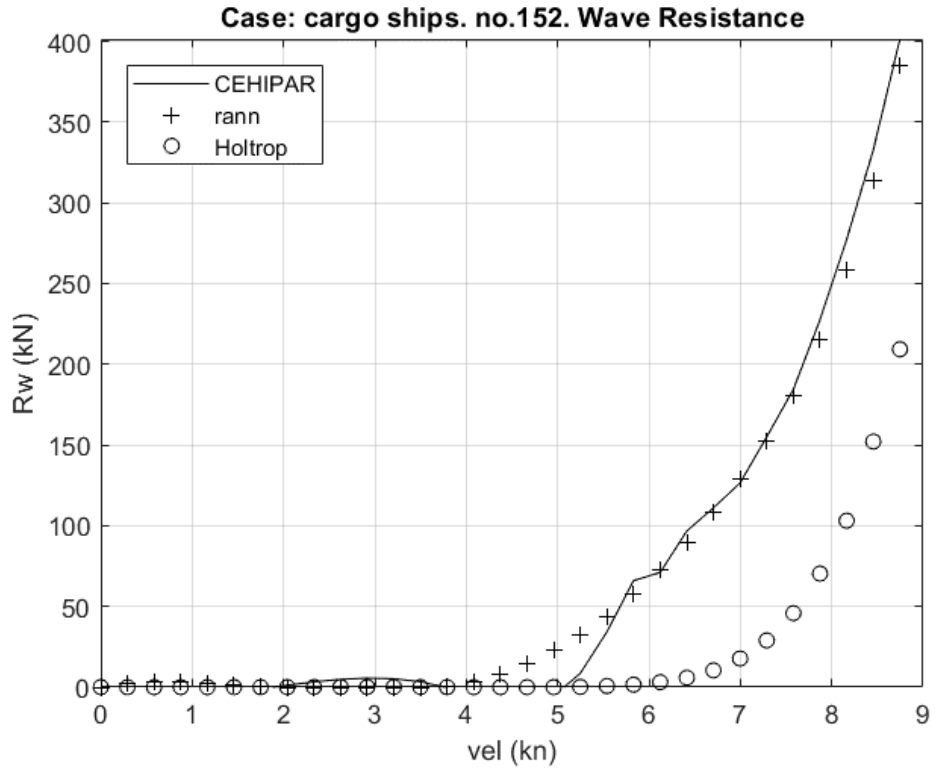

Figure 14.2. Cargo ships data base. Wave resistance. Case no. 152.

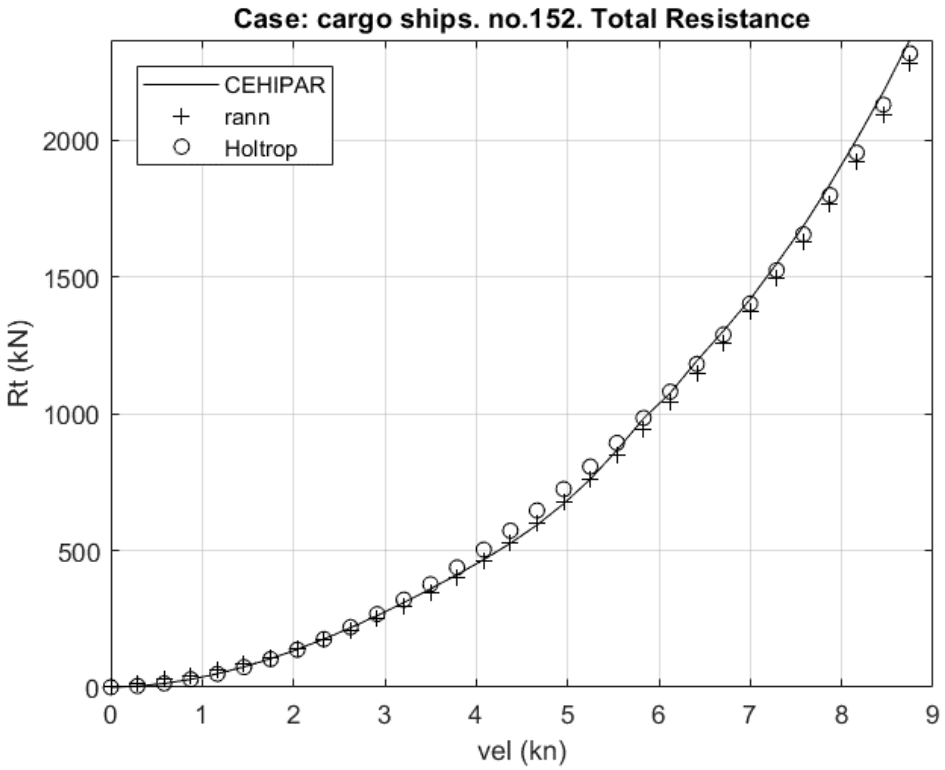

Figure 14.3. Cargo ships data base. Total resistance. Case no. 152.

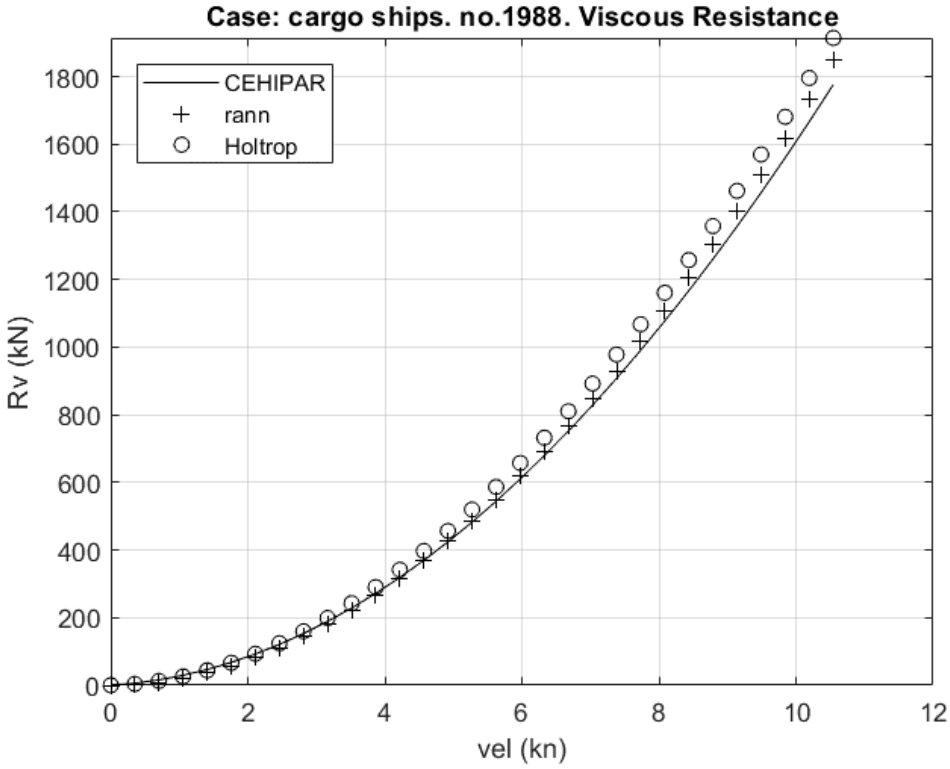

Figure 14.4. Cargo ships data base. Viscous resistance. Case no. 1988.

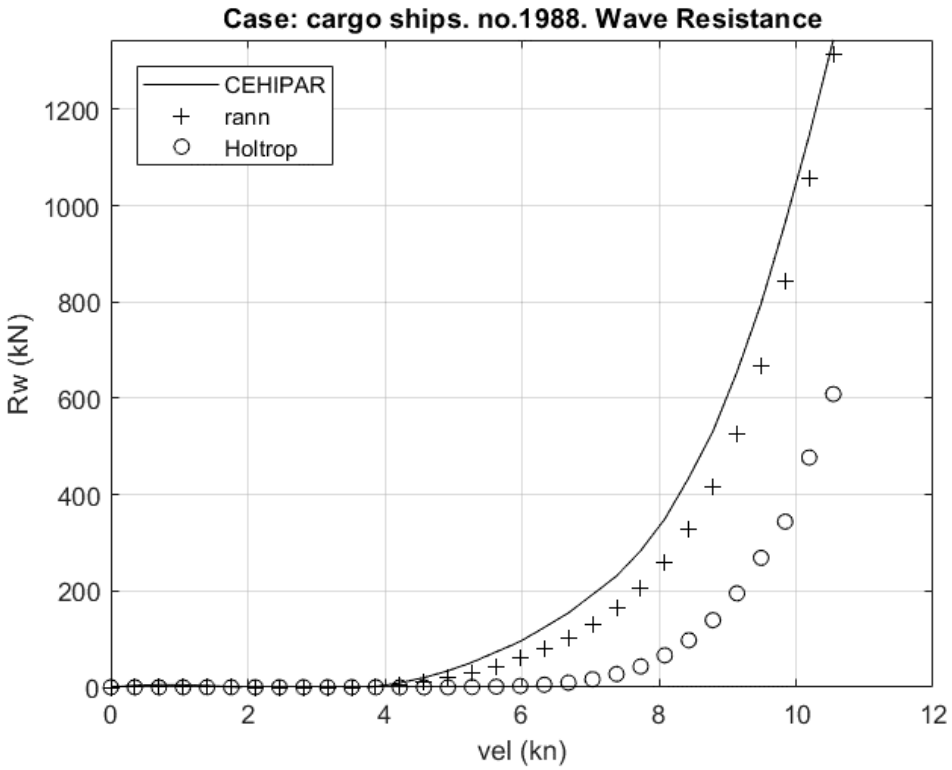

Figure 14.5. Cargo ships data base. Wave resistance. Case no. 1988.

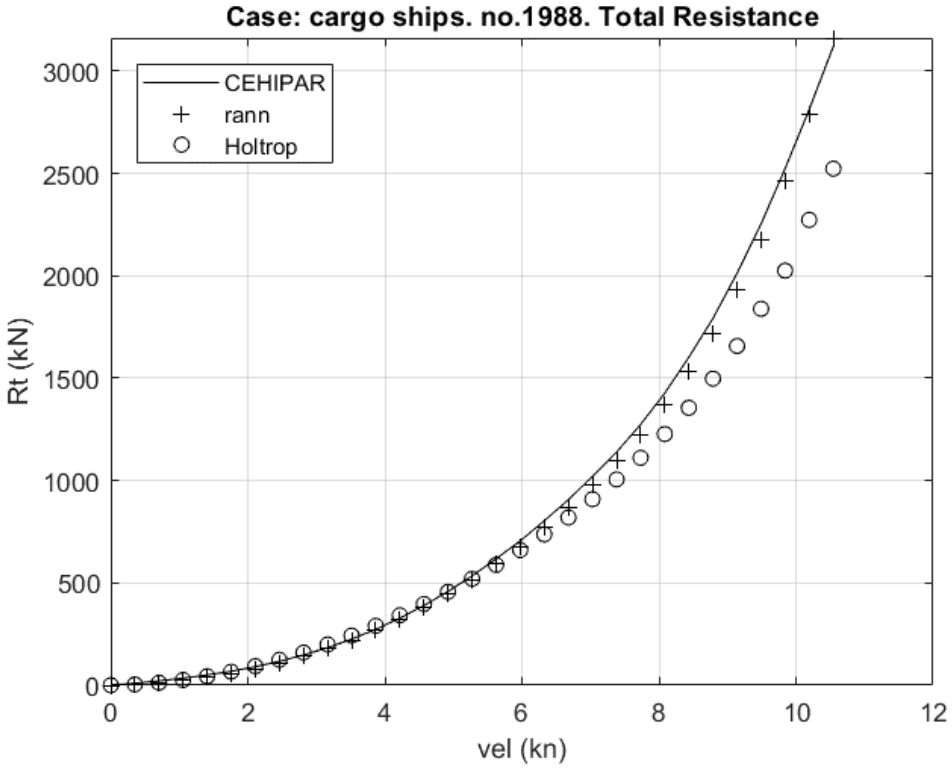

Figure 14.6. Cargo ships data base. Total resistance. Case no. 1988.

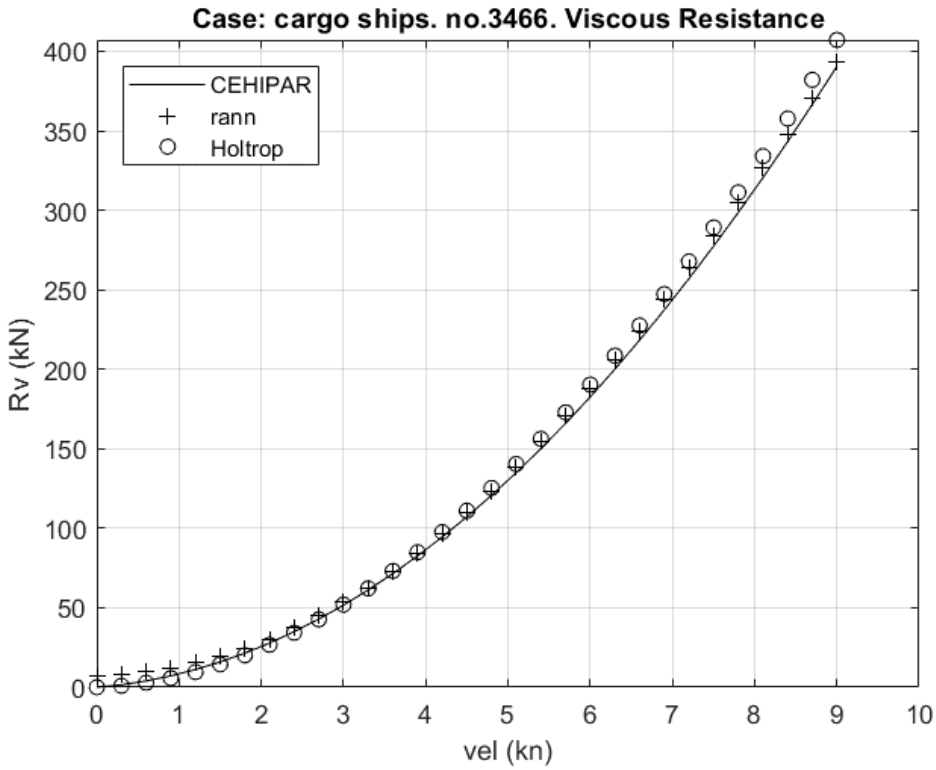

Figure 14.7. Cargo ships data base. Viscous resistance. Case no. 3466.

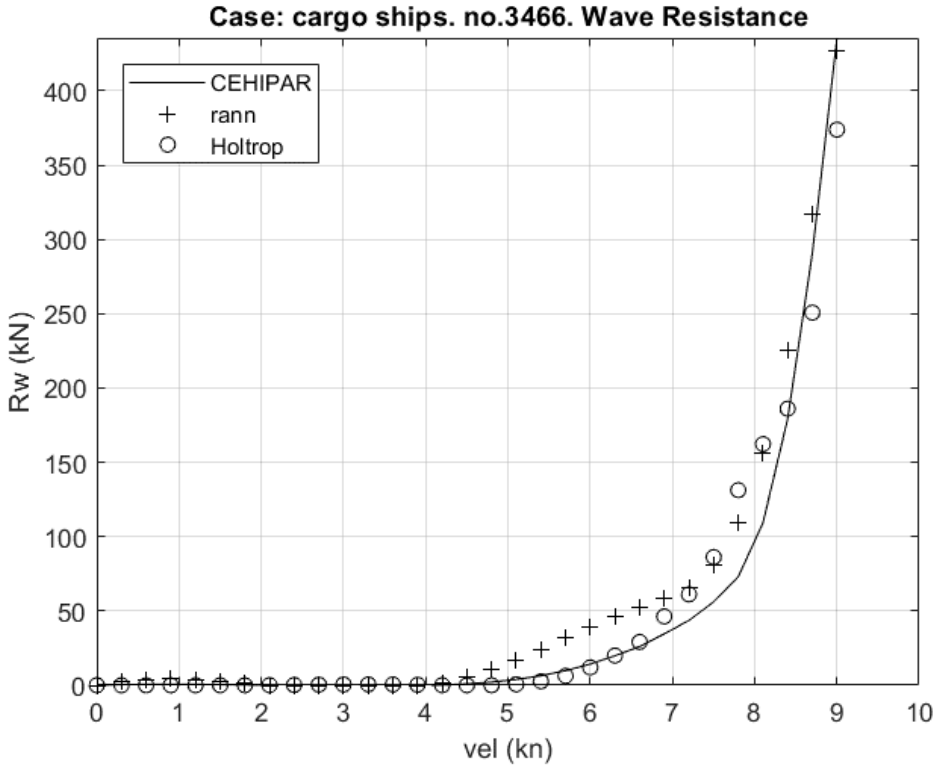

Figure 14.8. Cargo ships data base. Wave resistance. Case no. 3466.

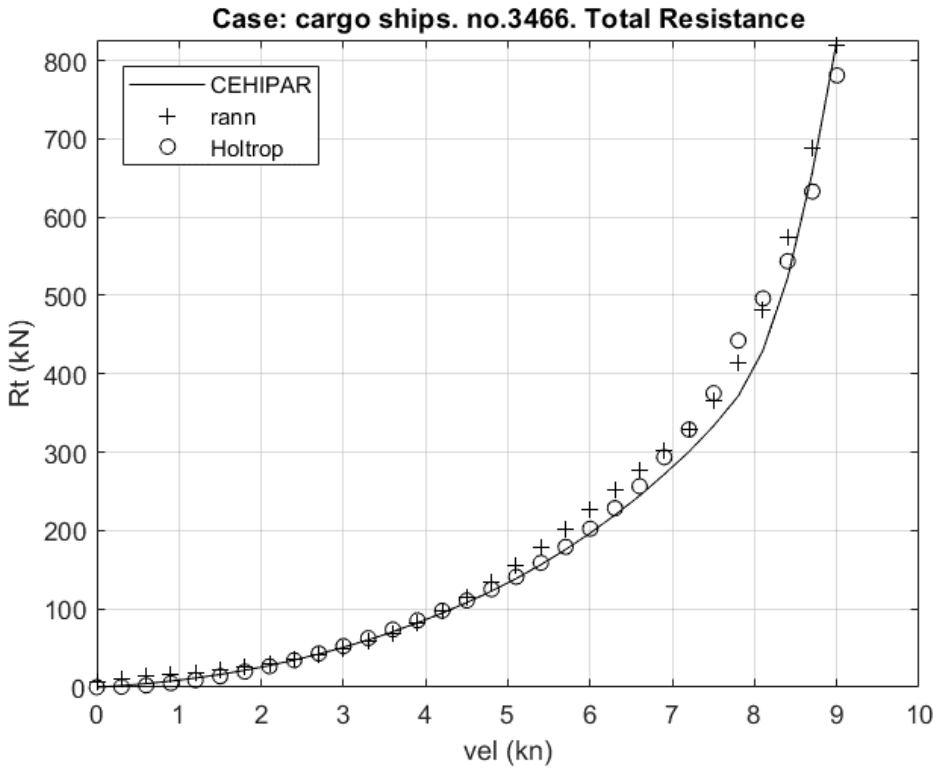

Figure 14.9. Cargo ships data base. Total resistance. Case no. 3466.

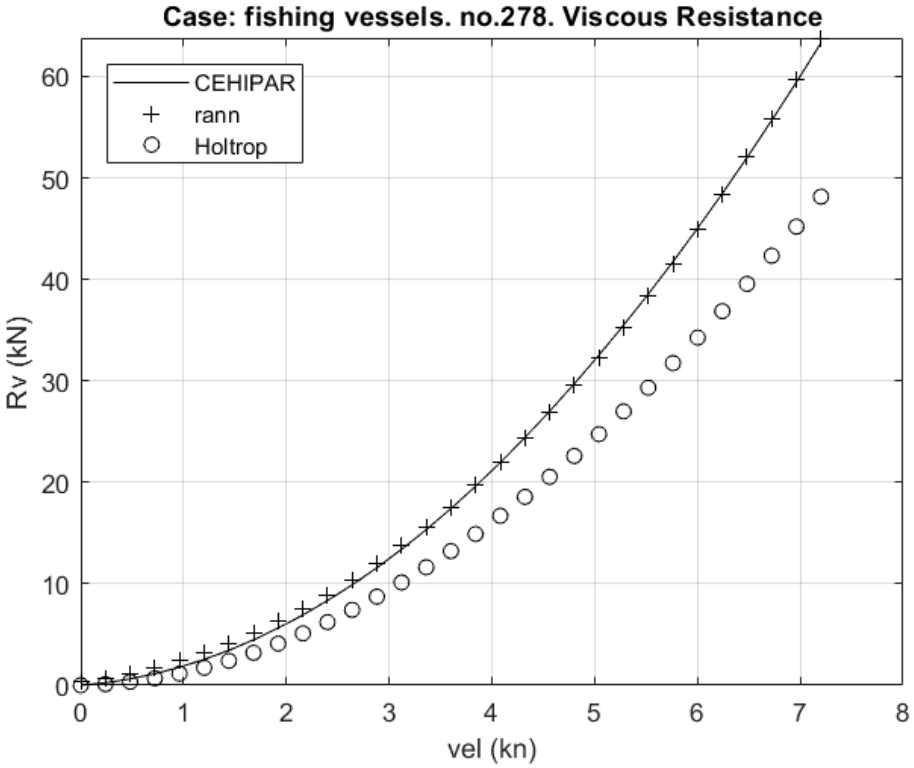

Figure 14.10. Fishing vessels data base. Viscous resistance. Case no. 278.

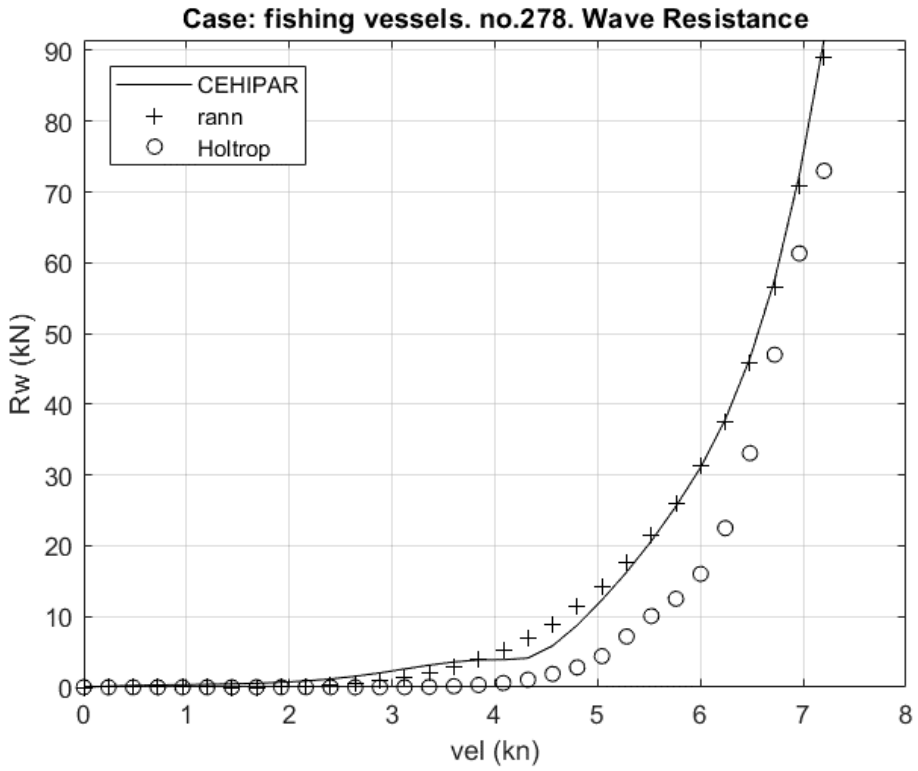

Figure 14.11. Fishing vessels data base. Wave resistance. Case no. 278.

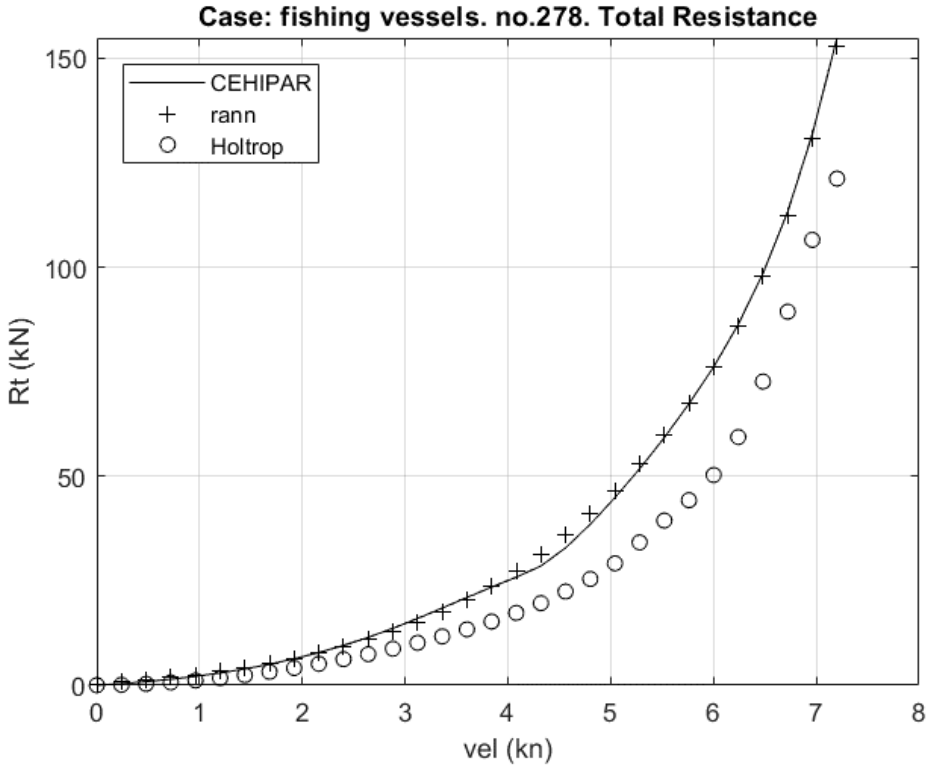

Figure 14.12. Fishing vessels data base. Total resistance. Case no. 278.

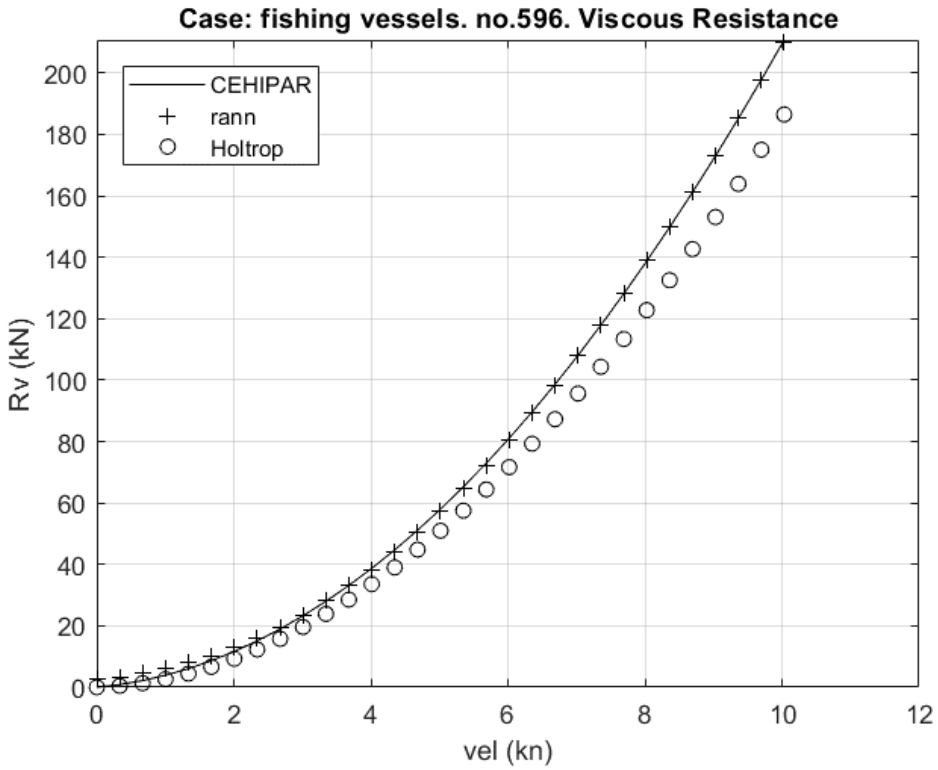

Figure 14.13. Fishing vessels data base. Viscous resistance. Case no. 596.

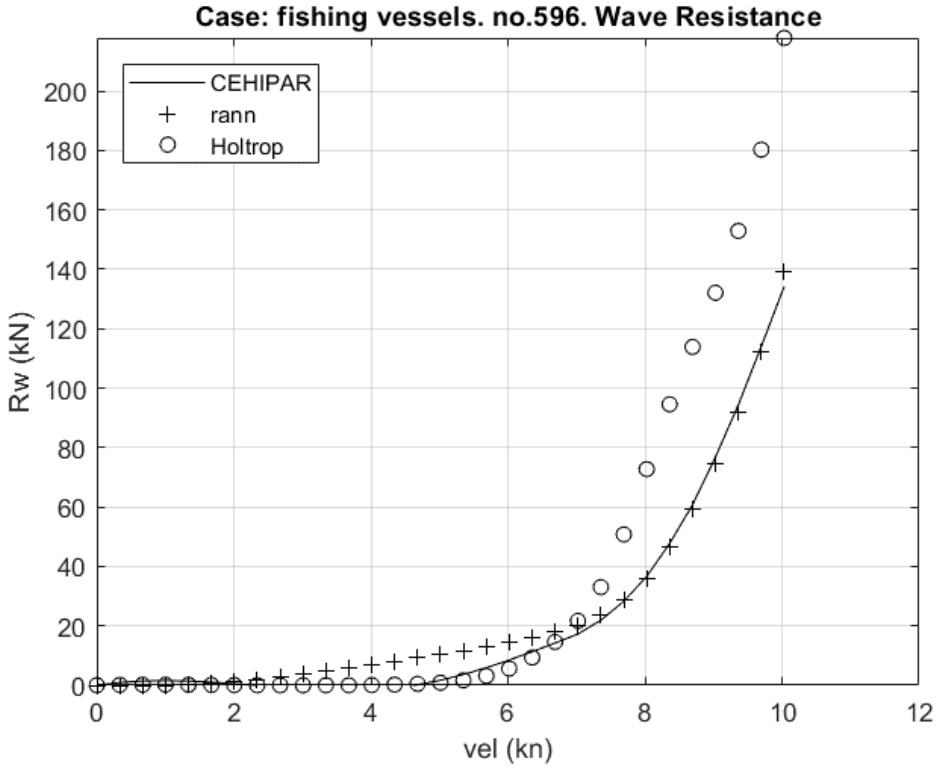

Figure 14.14. Fishing vessels data base. Wave resistance. Case no. 596.

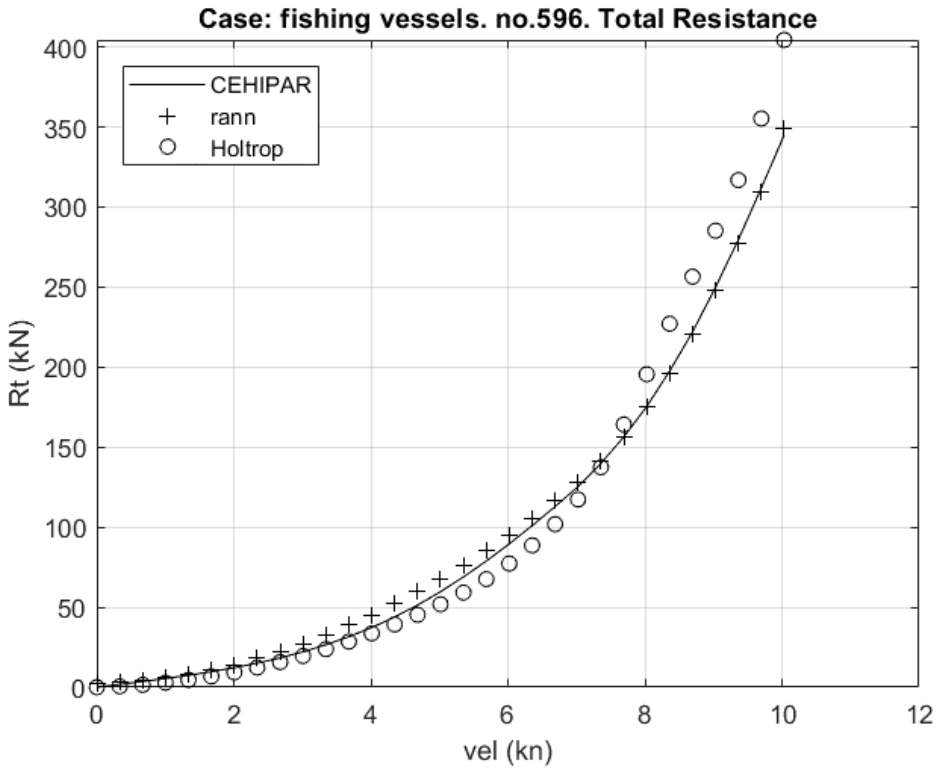

Figure 14.15. Fishing vessels data base. Total resistance. Case no. 596.

Figure 14.16. Small crafts data base. Viscous resistance. Case no. 594.

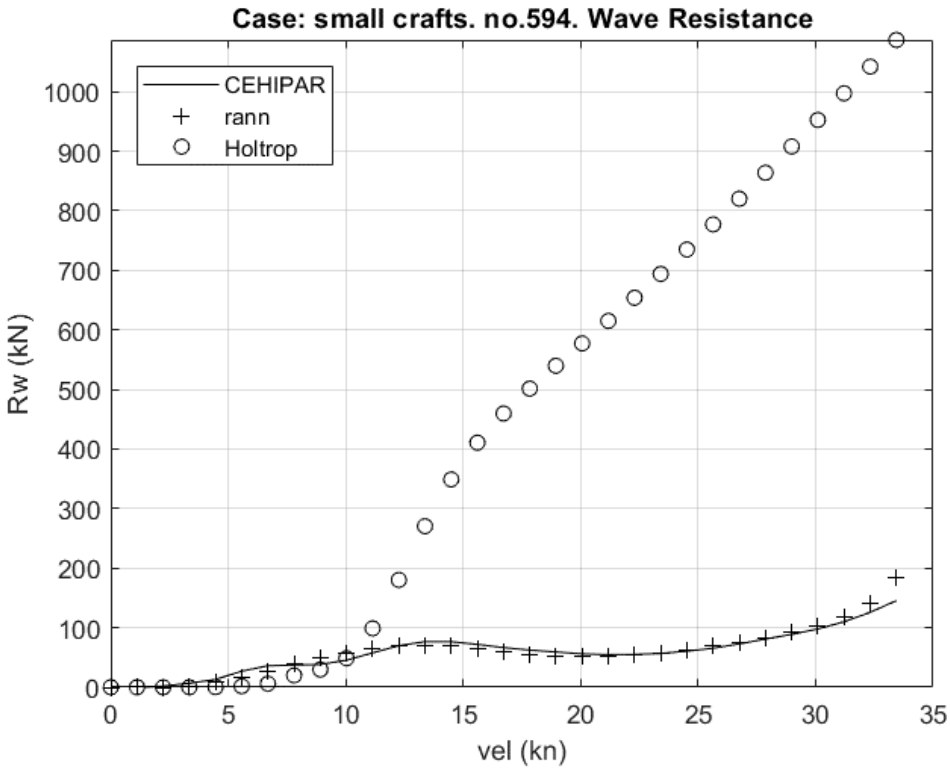

Figure 14.17. Small crafts data base. Wave resistance. Case no. 594.

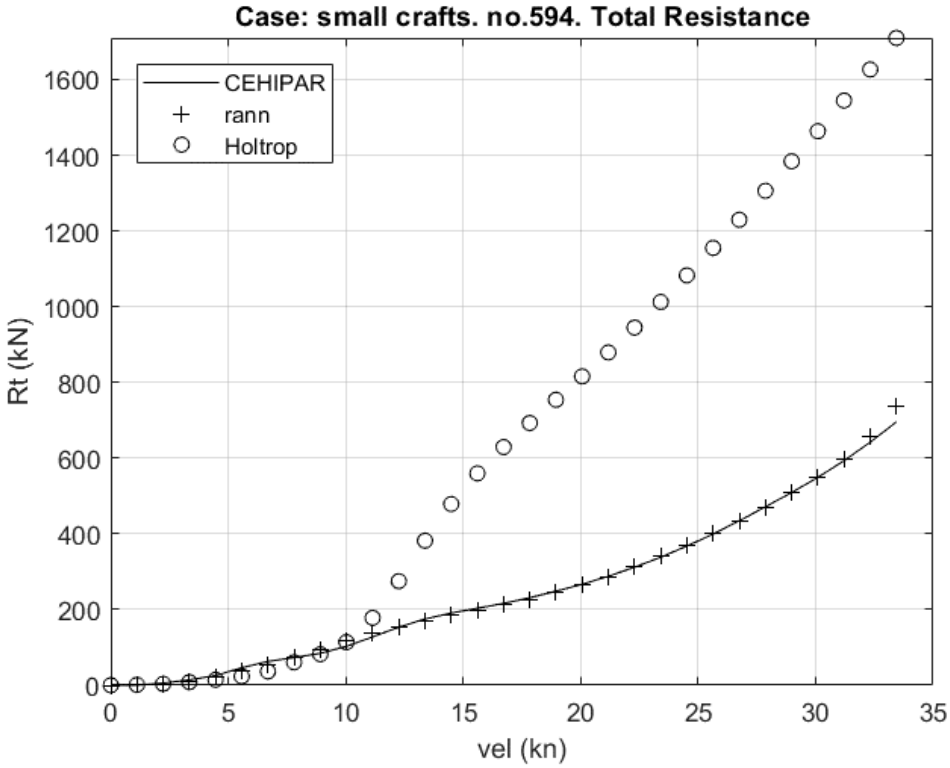

Figure 14.18. Small crafts data base. Total resistance. Case no. 594.

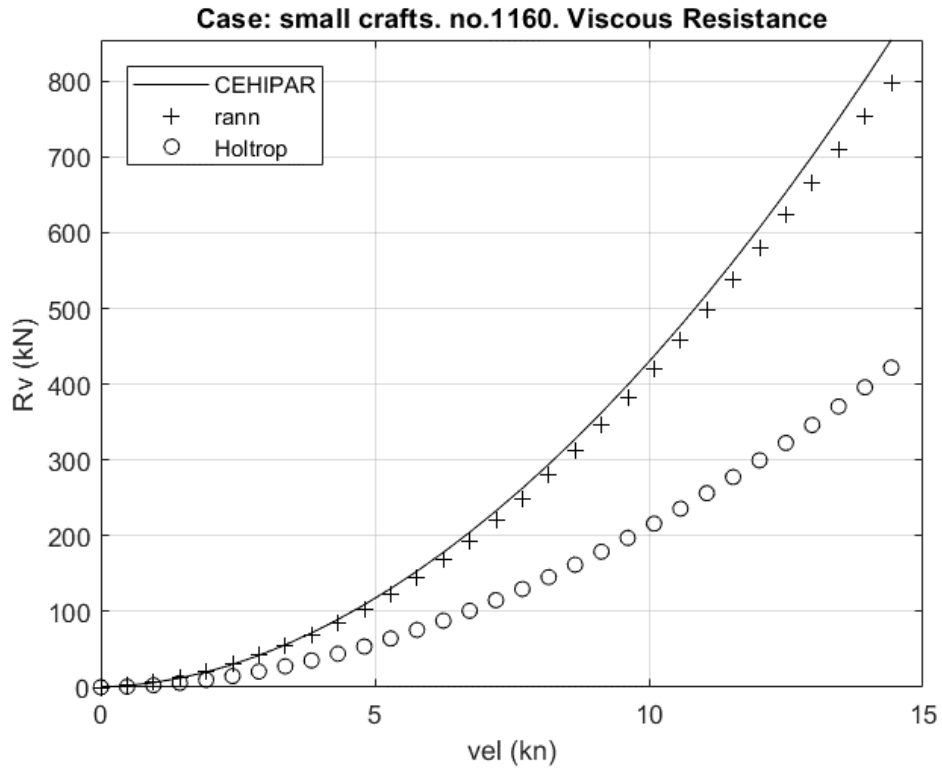

Figure 14.19. Small crafts data base. Viscous resistance. Case no. 1160.

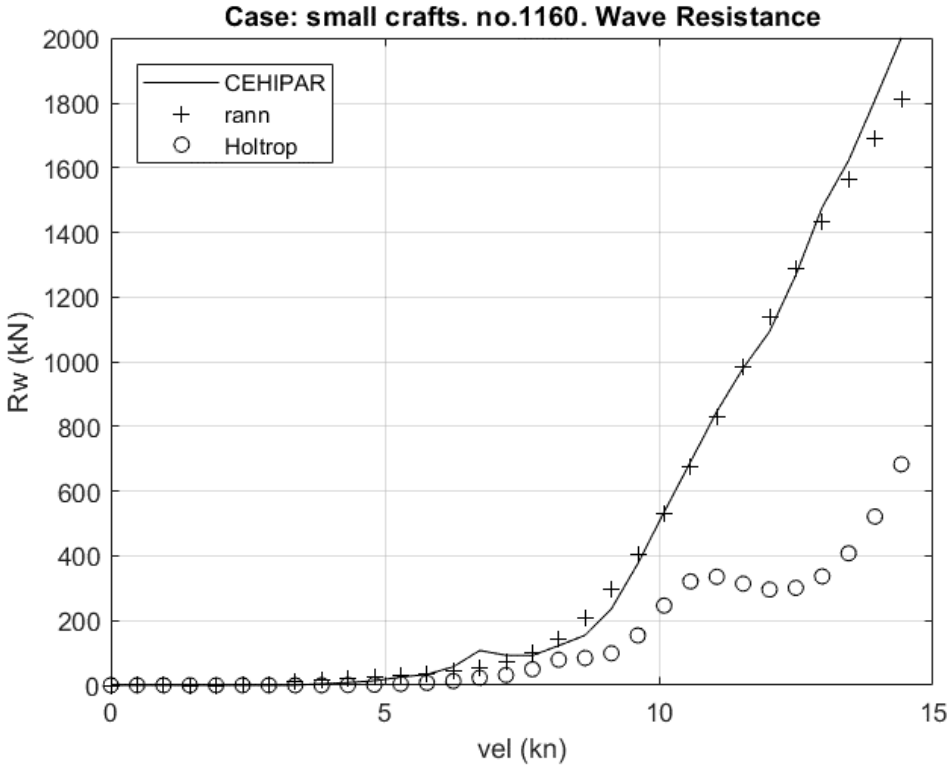

Figure 14.20. Small crafts data base. Wave resistance. Case no. 1160.

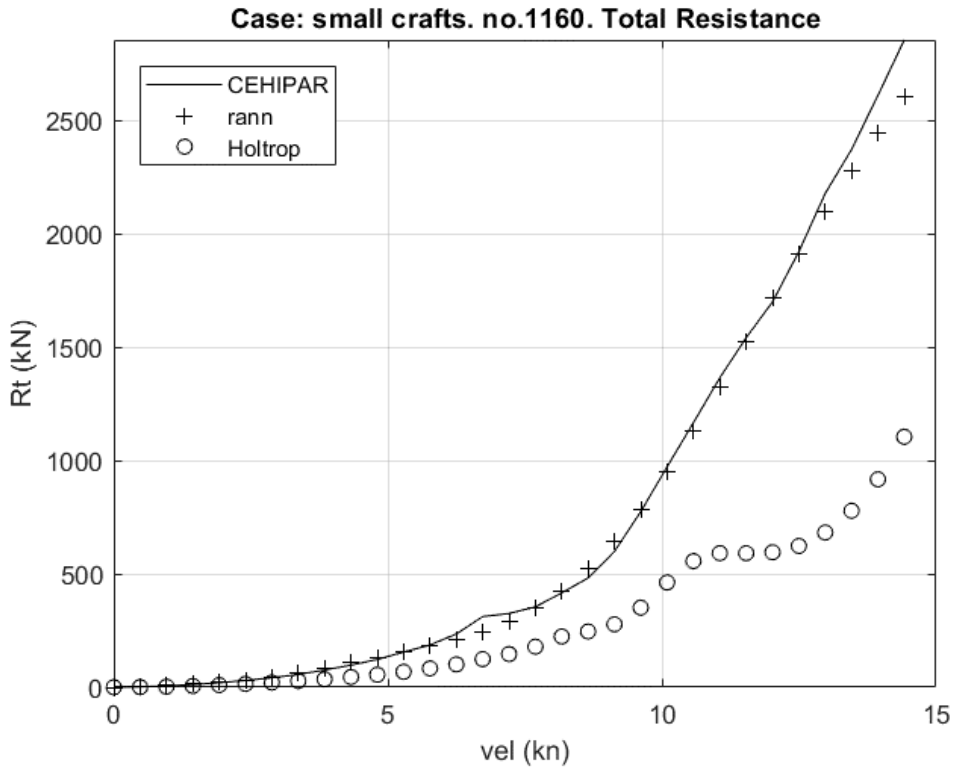

Figure 14.21. Small crafts data base. Total resistance. Case no. 1160.

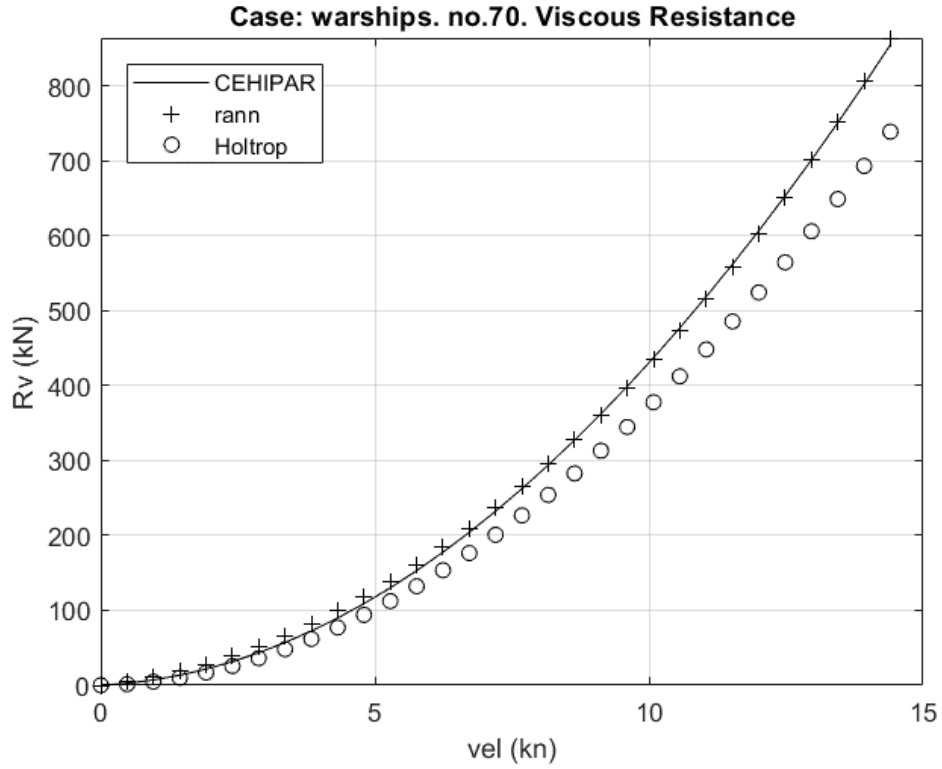

Figure 14.22. Warships data base. Viscous resistance. Case no. 70.

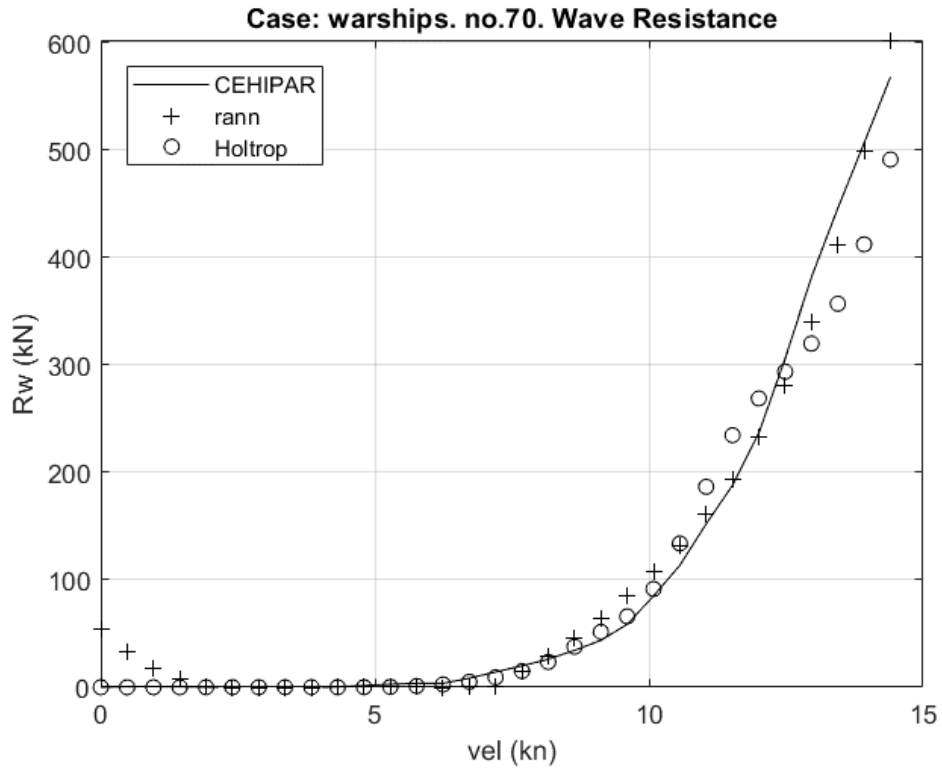

Figure 14.23. Warships data base. Wave resistance. Case no. 70.

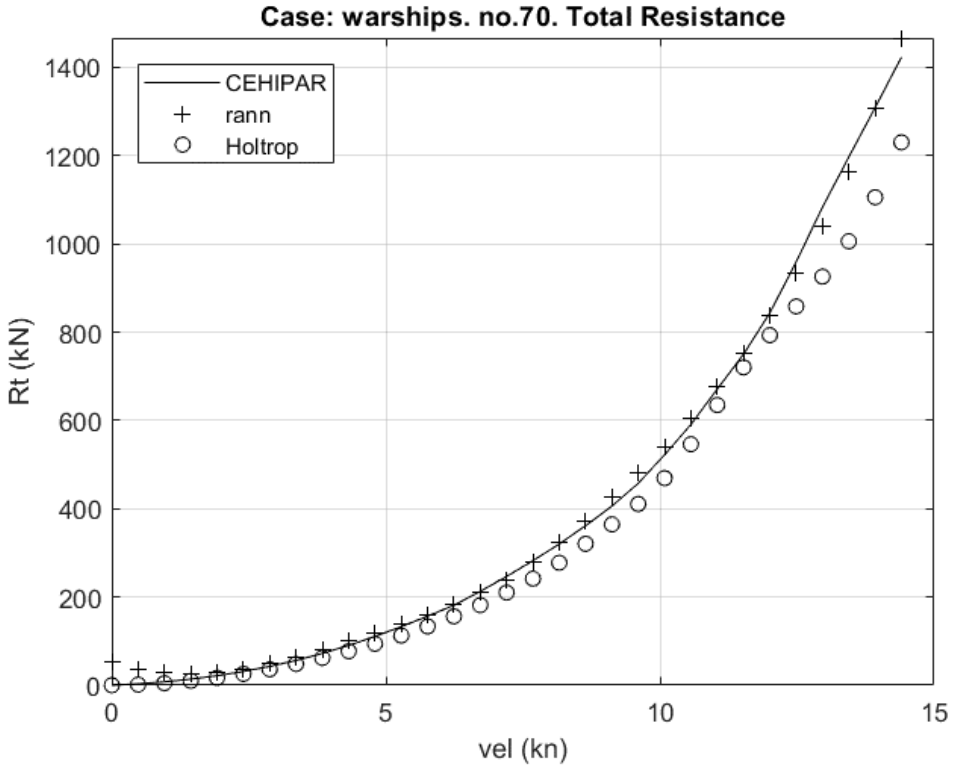

Figure 14.24. Warships data base. Total resistance. Case no. 70.

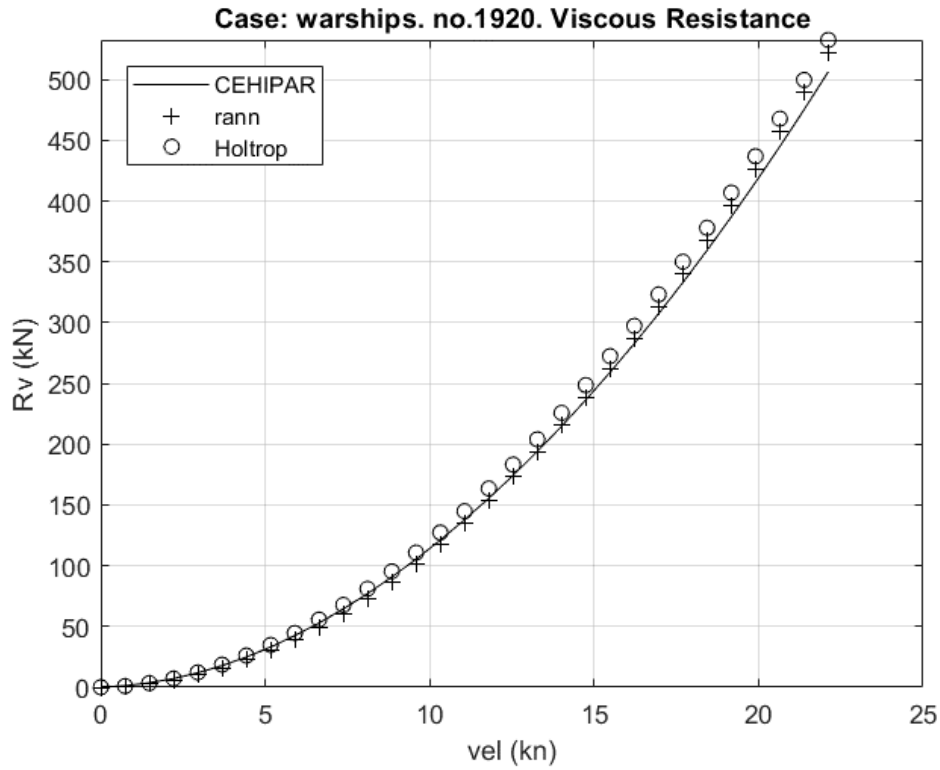

Figure 14.25. Warships data base. Viscous resistance. Case no. 1920.

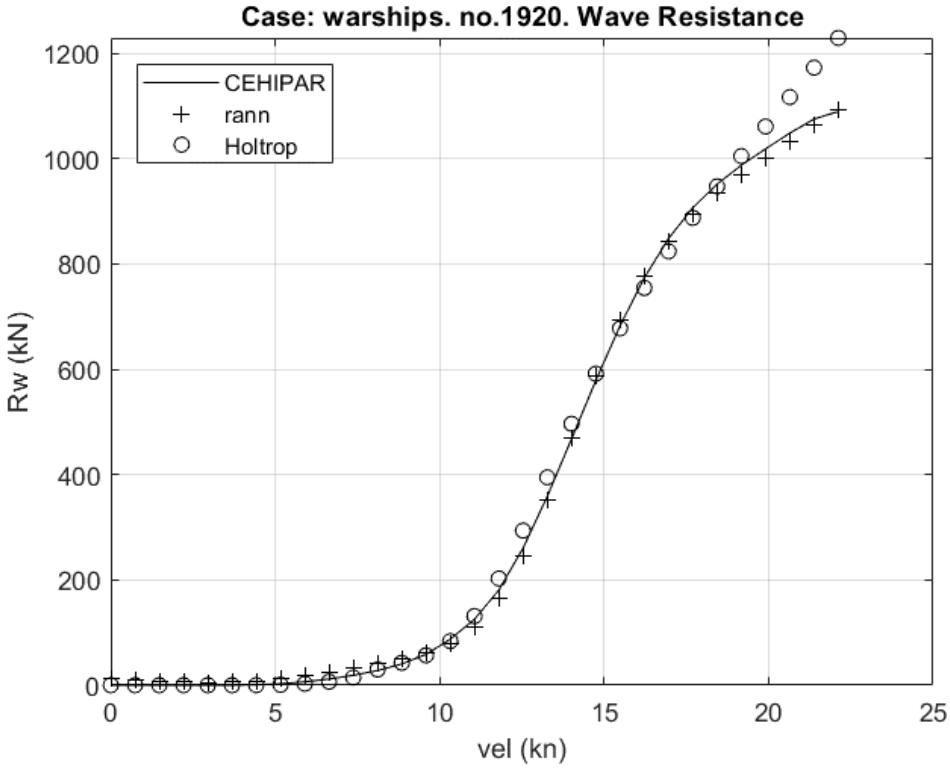

Figure 14.26. Warships data base. Wave resistance. Case no. 1920.

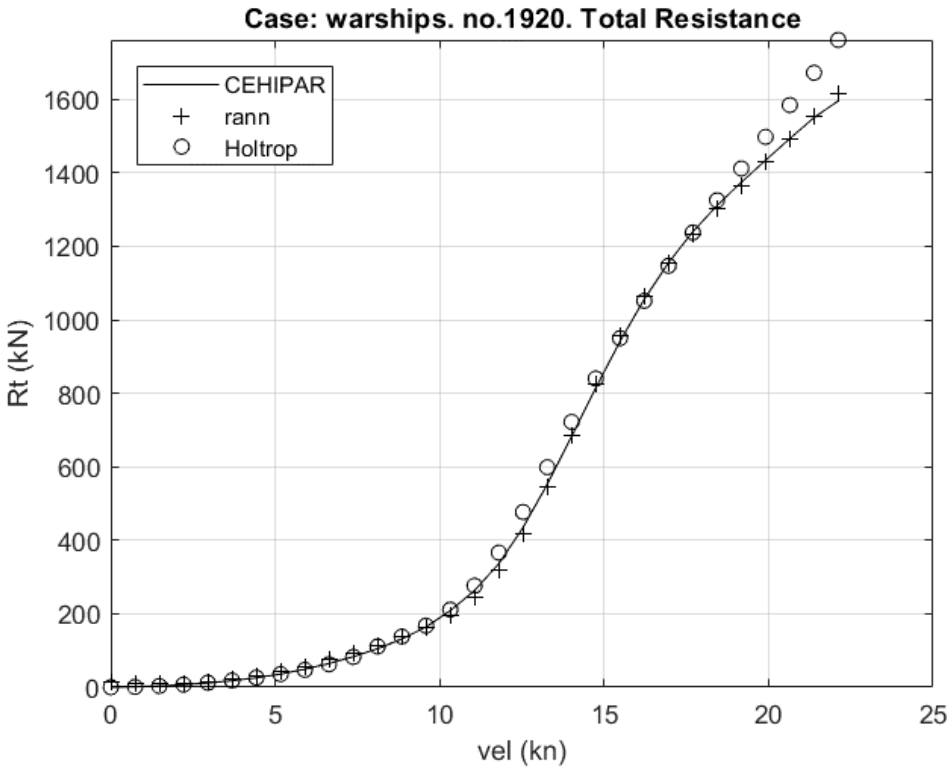

Figure 14.27. Warships data base. Total resistance. Case no. 1920.

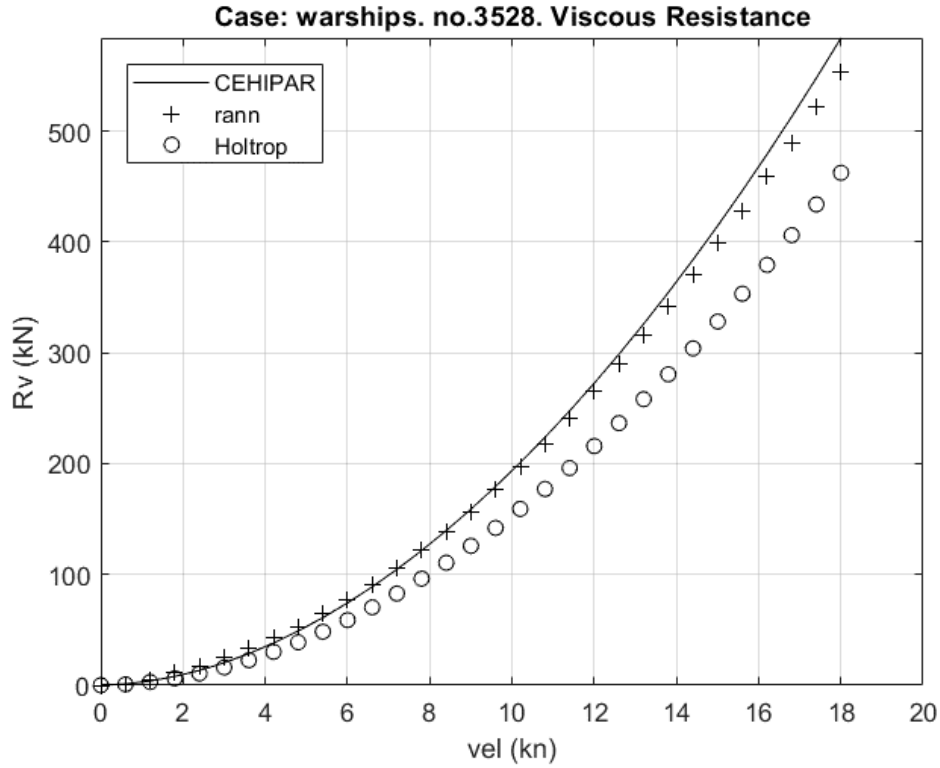

Figure 14.28. Warships data base. Viscous resistance. Case no. 3528.

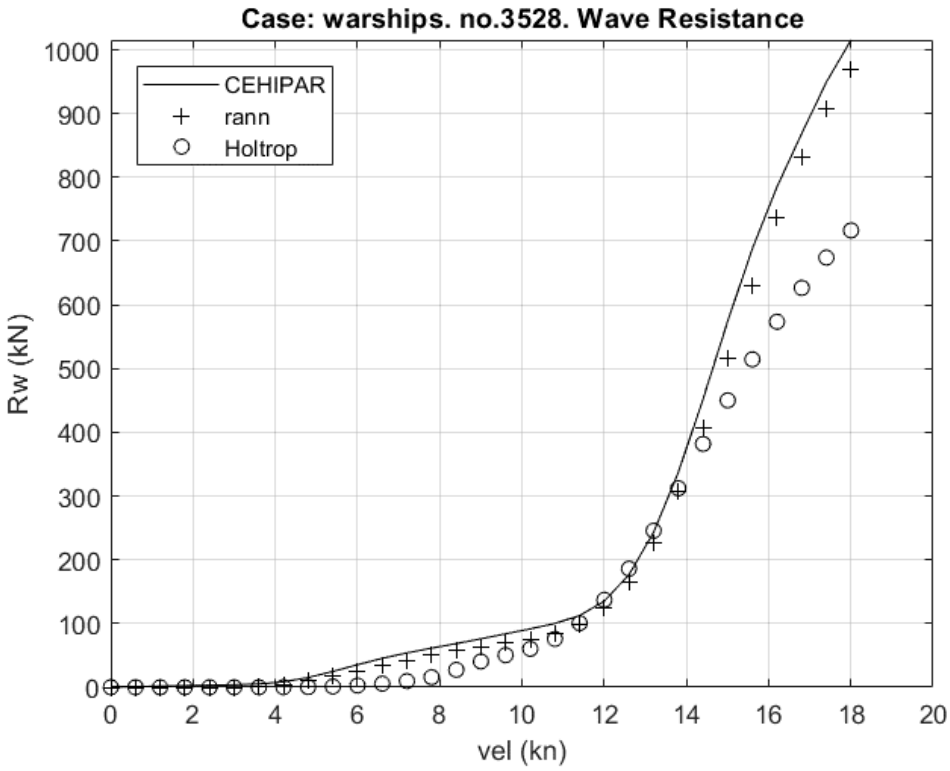

Figure 14.29. Warships data base. Wave resistance. Case no. 3528.

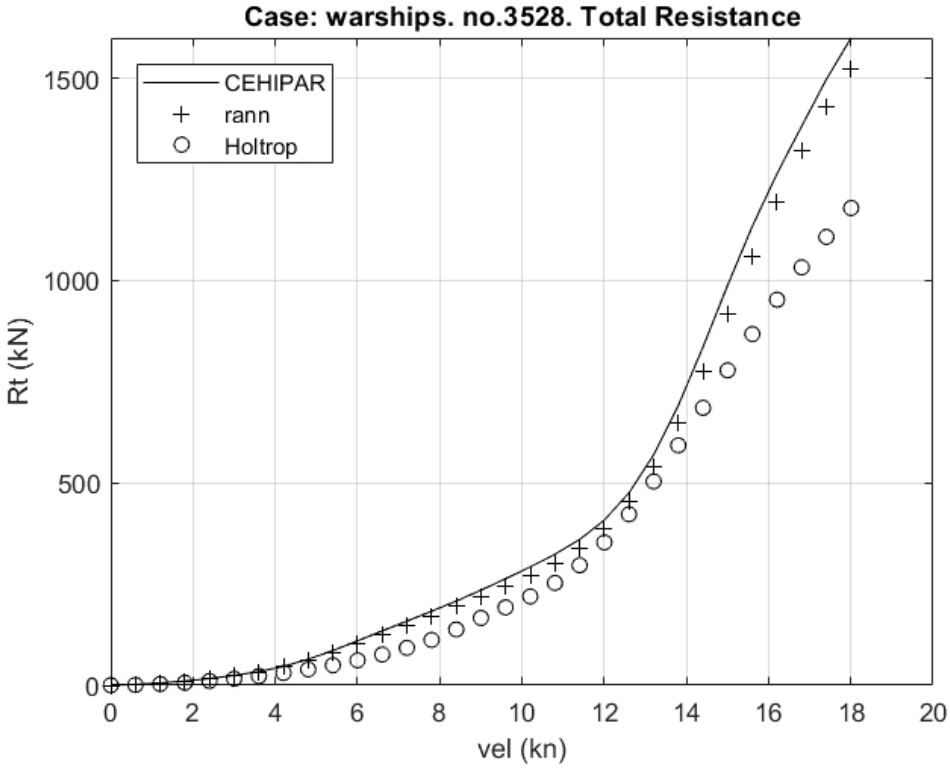

Figure 14.30. Warships data base. Total resistance. Case no. 3528.